THE METABOLIC FATE OF BENZO[A]PYRENE IN VIVO

by

Eric H. Weyand

DISSERTATION submitted to the Faculty of the
Virginia Polytechnic Institute and State University
in partial fulfillment of the requirements for the degree of

DOCTOR OF PHILOSOPHY

IN

BIOCHEMISTRY AND NUTRITION

APPROVED:

_____
D. R. Bevan, chairman

_____ _____
R. E. Ebel M. L. Failla

_____ _____
E. M. Gregory J. B. Meldrum

August, 1986
Blacksburg, Virginia

THE METABOLIC FATE OF BENZO[A]PYRENE IN VIVO

by

Eric H. Weyand

Committee Chairman: David R. Bevan
Biochemistry and Nutrition

(ABSTRACT)

[^{3}H]-B[a]P absorption, distribution, metabolism, excretion and macromolecular binding in male Sprague-Dawley rats were investigated following administration by intratracheal instillation through a cannula. [^{3}H]-radioactivity in various organs was determined at timed intervals between 5 and 360 min. Elimination of radioactivity from lungs was biphasic with half-lives of 5 and 116 min. Radioactivity in liver increased rapidly, reaching a maximum of 21% of the dose within 10 min after instillation and decreasing thereafter, until less than 5% of the dose was detected at 360 min. Radioactivity in intestinal contents accounted for 45% of the dose 360 min after instillation. Carcass accounted for 15-30% of the dose within the time intervals investigated. Toxicokinetic parameters to describe B[a]P disposition following intratracheal administration were similar to those following intravenous injection of B[a]P. HPLC was used to identify various types of metabolites in lungs, liver, and intestinal contents at selected times after B[a]P instillation.

Notably, quinones were at highest concentrations in both lung and liver 5 min after instillation, accounting for 12 and 7% of organic extractable material, respectively. Covalent binding of B[a]P metabolites to DNA, RNA, and protein at 6 hrs after instillation was also quantified for lung and liver. There was extensive binding of metabolites to RNA while much lesser amounts of metabolites were associated with protein and DNA in both organs. Six B[a]P:DNA adducts were detected in lung, while only three such adducts were detected in liver.

Biliary excretion of B[a]P was investigated in Sprague-Dawley rats, Gunn rats, hamsters, and guinea pigs following instillation of [^{3}H]-B[a]P. [^{3}H]-B[a]P was administered at concentrations ranging from 6 ng to 380 μg and biliary radioactivity was monitored for 6 hrs. In addition, tissue distribution of radioactivity was determined. Species differences in biliary excretion of B[a]P and/or metabolites were detected. Rats and guinea pigs, but not hamsters, exhibited differences in biliary excretion of low and high doses of B[a]P. Phase II metabolites of B[a]P in bile were quantified for all species. The majority of these metabolites were glucuronides and thio-ether conjugates. Enterohepatic circulation of B[a]P biliary metabolites was investigated in Sprague-Dawley rats.

DEDICATION

I dedicate this work to my wonderful wife, Mary Ellen and to my loving mother and father, Marjorie E. and Karl J. Weyand.

ACKNOWLEDGMENTS

I thank Dr. David R. Bevan for his support and help during the past four years. I thank the other members of my committee for their time and character building encounters. I also would like to thank the Department of Biochemistry and Nutrition for financial support and faculty members in the department for the use of their supplies, instruments, and time.

Table of Contents

List of Tables

List of Figures

Chapter 1

General Introduction

Polycyclic Aromatic Hydrocarbons

Historical Aspects

Early studies by Pott (1775), Yamayima and Ichikawa (1915), Kennaway (1930), and Cook et al. (1933) were instrumental in establishing that polycyclic aromatic hydrocarbons (PAH) are carcinogenic (1-4). Sir Percival Pott, in 1775, was the first to report a correlation between exposure to chemicals and the development of cancer in humans, noting an increase in the incidence of scrotal cancer among chimney sweeps (1). It was not until 1917 that Yamayima and Ichikawa demonstrated that application of crude coal tar to ears of rabbits would produce skin tumors (2). In 1930 Kennaway obtained similar results when he applied a pure PAH, dibenz[a,h]anthracene, to mouse skin (3). In 1933 Cook et al. (4) determined that benzo[a]pyrene (B[a]P) is a major carcinogenic component of coal tar.

Since these classical observations and experiments, several PAHs have been shown to be very potent carcinogens

in laboratory animals. Consequently, the study of carcinogenic PAHs has become an area of extensive research in hopes of achieving a better understanding of their carcinogenicity.

Source/Exposure

PAHs are a large class of hydrocarbons having three or more fused aromatic rings which contain only carbon. These rings can be fused in a number of linear, angular or cluster arrangements (Figure 1.1.). PAHs are formed as a by-product of incomplete combustion of organic matter and have been found as contaminants in air, water, soil, and food. Some reports estimate that as much as 894 tons of B[a]P are emitted into the air in the United States annually (5). The concentration of B[a]P in drinking water and food has been reported to be as high as 1.2-24 $\mu g/m^3$ and 30-60 $\mu g/kg$, respectively (5).

Exposure to PAHs can be by ingestion, topical absorption, or inhalation. Ingestion may be the route by which most people are exposed to PAHs (6). However, exposure by inhalation may represent the most important route of exposure in relation to lung carcinogenesis (7).

Occupational exposure, such as in coke oven workers, and non-occupational exposure by cigarette smoking represent significant sources of human exposure to PAHs (8,9,10). In addition, particulates from gasoline and diesel engine exhaust contain adsorbed hydrocarbons and thus are major environmental sources of human exposure to PAHs (10).

Figure 1.1. Polycyclic aromatic hydrocarbons commonly found in the environment.

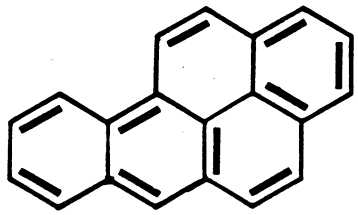

Benzo[a]pyrene

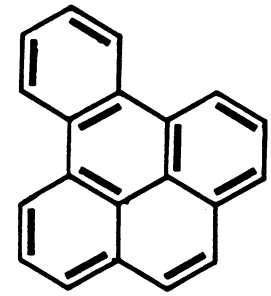

Benzo[e]pyrene

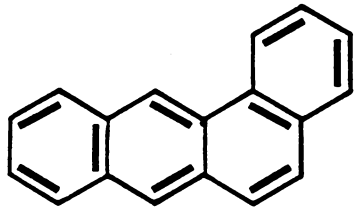

Benzo[a]anthracene

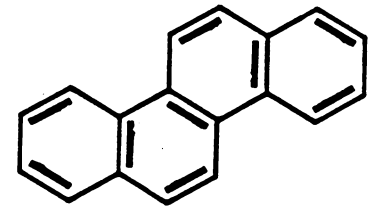

Chrysene

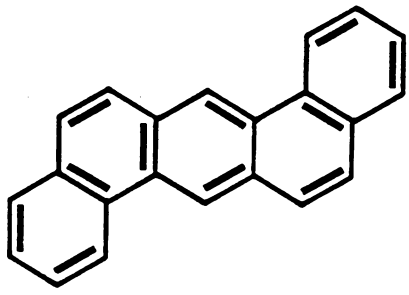

Dibenz(a,h)anthracene

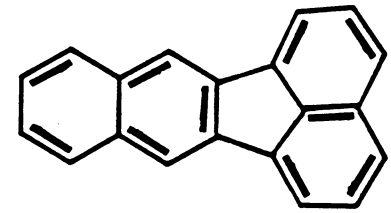

Benzo[k]fluoranthene

Benzo[a]pyrene

General Metabolism

B[a]P has been the most extensively studied PAH because of its early detection as a major carcinogenic component of coal tar, its carcinogenic potency, and its prevalence in the environment. B[a]P must be metabolized to be carcinogenic, and the metabolism of B[a]P has been reviewed periodically (11,12,13).

Phase I and Phase II reactions are involved in metabolism of B[a]P. Phase I metabolism (Figure 1.2.) is an oxidative pathway. Introduction of oxygen into B[a]P generally proceeds via initial formation of arene oxides which either undergo spontaneous rearrangement to phenols or enzymatic conversion to dihydrodiols by epoxide hydrase. The phenols, dihydrodiols, quinones, and arene oxides which are formed initially are regarded as "primary" metabolites. These primary metabolites can undergo another round of oxygenation to a variety of "secondary" metabolites which include dihydrodiol epoxides and tetrols.

Figure 1.2. Benzo[a]pyrene Phase I metabolism

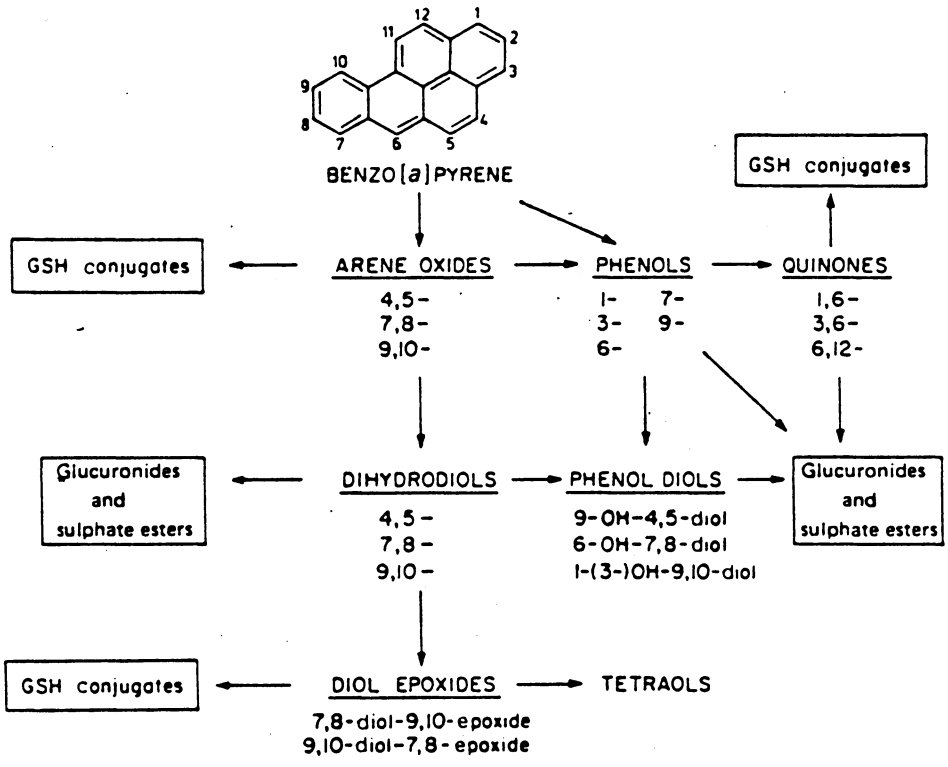
12
1
11
2
10
3
9
4
8
7
6
5
BENZO[a]PYRENE
GSH conjugates
GSH conjugates
ARENE OXIDES
PHENOLS
QUINONES
4,5-
7,8-
9,10-
1- 7-
3- 9-
6-
1,6-
3,6-
6,12-
Glucuronides and sulphate esters
DIHYDRODIOLS
PHENOL DIOLS
Glucuronides and sulphate esters
4,5-
7,8-
9,10-
9-OH-4,5-diol
6-OH-7,8-diol
1-(3-)OH-9,10-diol
GSH conjugates
DIOL EPOXIDES
TETRAOLS
7,8-diol-9,10-epoxide
9,10-diol-7,8-epoxide

Phase I metabolism is catalyzed by a monooxygenase system which consists of cytochromes P-450 (Cyt P-450) and a flavoprotein, NADPH-cytochrome P-450 reductase. Cyt P-450 is a family of hemeproteins first characterized in 1964 by Omura and Sato (14,15). The name "Cyt P-450" refers to an absorption difference spectrum maximum at 450 nm of the carbon monoxide adduct of the reduced hemeprotein. Primarily located in the endoplasmic reticulum of eucaryotic cells, several isoenzymes of Cyt P-450 have been identified (16,17). In addition to being involved in xenobiotic metabolism, Cyt P-450 also catalyzes reactions involved in the biosynthesis of steroid hormones (18).

Phase II metabolism of B[a]P (Figure 1.3.) involves conjugation of Phase I metabolites with glutathione, glucuronic acid or sulfate ions (19). Conjugation, by increasing the polarity of Phase I metabolites, facilitates excretion. Conjugation reactions are catalyzed by glutathione S transferase (GST), glucuronyl transferase (GT), and sulfotransferase (ST), respectively. Most GST and ST are present in the cytosol, while GT is a membrane-bound enzyme located in the endoplasmic reticulum of cells.

The overall purpose of Phase I and Phase II metabolism is to convert nonpolar compounds such as B[a]P to water soluble products that are biologically inactive and readily

excreted. However, both Phase I and Phase II metabolism have also been implicated in the activation of chemicals to more reactive species (20). For example, Phase I metabolism of B[a]P is responsible for forming the B[a]P-7,8-diol-9,10 epoxide metabolite which is a potent carcinogen in laboratory animals. Likewise, the conjugation of glucuronic acid to N-hydroxy-N-arylacetamides results in the activation of these compounds to highly reactive species (21,22).

Much of the available information on B[a]P metabolism has been collected using *in vitro* systems such as tissue homogenates, microsomes, cell cultures and isolated perfused organs. Although these systems have been significant in delineating B[a]P metabolism, they can only approximate events in the intact animal. For example, both B[a]P and aflatoxin B_1 are metabolized to mutagenic metabolites *in vivo*. Similarly, homogenates of liver metabolize both carcinogens to mutagenic metabolites, while only B[a]P is converted to mutagenic forms in isolated hepatocytes (23,24).

Figure 1.3. Examples of Benzo[a]pyrene Phase II metabolites.

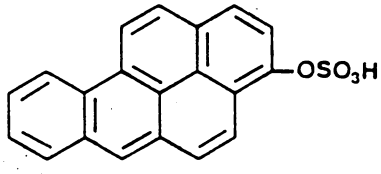

Sulphate ester

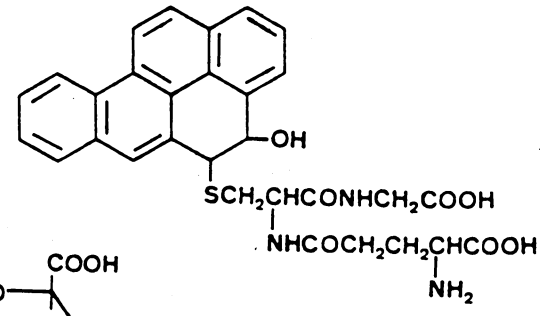

Gluthathione conjugate

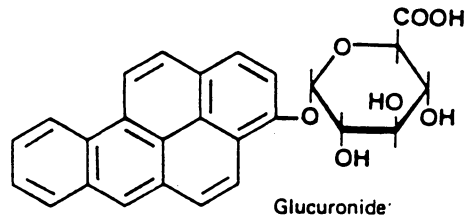

Glucuronide

Carcinogenic Aspects

In general, chemical carcinogens are classified as either genotoxic or epigenetic, and are believed to exert their carcinogenic effect by covalent modification of cellular macromolecule(s). B[a]P has been shown to bind to DNA, RNA, and protein (25). Most studies have concentrated on formation of covalent adducts between B[a]P metabolites and DNA because a good correlation exists between covalent modification of DNA and carcinogenesis (26,27). However, some investigators have been unable to establish a correlation between DNA modification and carcinogenesis and have suggested that a singular event such as DNA modification may not be solely responsible for carcinogenesis (28).

Although several B[a]P metabolites are carcinogenic, the most potent is the B[a]P-7,8-diol-9,10-oxide (B[a]PDE) often referred to as the "ultimate" carcinogenic form of B[a]P (10). Data are consistent with this metabolite being responsible for the majority of DNA modification *in vivo* and in cell culture (29). The major B[a]P:DNA adduct formed is the (+)-anti-B[a]PDE:deoxyguanosine adduct (Figure 1.4), while lesser amounts of (-)-anti-B[a]PDE and syn-B[a]PDE DNA adducts are also formed. B[a]PDEs can also form adducts

with adenine, cytidine, and phosphate residues (30,31). In addition, recent studies have demonstrated that the (±)-anti-B[a]PDE is capable of activating the human c-Ha-ras1 protooncogene *in vitro* (32,33) which is homologues to the Harvey sarcoma virus oncogene, v-Ha-ras. Interestingly, these activated transforming genes have been found in a number of human tumors and may be involved in chemical carcinogenesis (34,35,36).

Figure 1.4 (+)-anti-B[a]PDE:deoxyguanosine adduct.

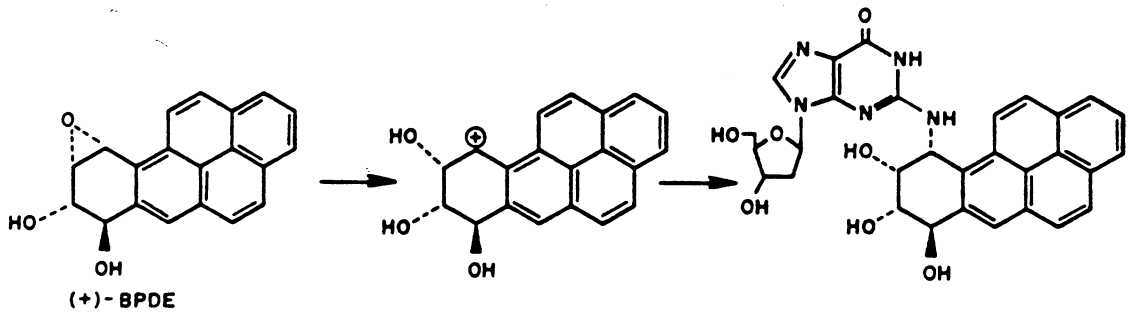
O
HO
OH
(+)-BPDE
HO
HO
OH
O
N
NH
N
N
NH
HO
O
OH
HO
HO
OH

Objectives

The purpose of this study was to provide a comprehensive investigation of B[a]P metabolism *in vivo*. The specific objectives were as follows: (1) to determine the toxicokinetics of absorption, distribution, and excretion of B[a]P in an animal model after intratracheal instillation; (2) to identify the types of metabolites formed and determine the extent of metabolite binding to cellular macromolecules *in vivo*; and, (3) to compare the disposition of B[a]P among different species.

References

1. Pott, P. Chirurgical observations relative to the cancer of the scrotum, 1775, reprinted in Natl. Cancer Inst. Monograph 10:7-13, 1963.

2. Yamagiwa, K., and Ichikawa, K. Experimental studie uber die pathogenese der epithelialgeschwulste. Mitt. Med. Fak., Univ. Tokio 15:295-344, 1915.

3. Kennaway, E. L. and Hieger, I. Carcinogenic substances and their fluorescence spectra. Brit. Med. J., 1:1044-1046, 1930.

4. Cook, J. W., Hewett, C. L., and Hieger, I. The isolation of a cancer-producing hydrocarbon from coal tar. Parts I, II and III. J. Chem. Soc. 295-405, 1933.

5. Zedeck S. M. Polycyclic aromatic hydrocarbons: A review. J. Environ. Pathol. and Toxicol., 3:537-567, 1980.

6. Santodonato, J., Basu, D. and Howard, P. Multimedia exposure and carcinogenic risk assessment for environmental PAH. In: Bjorseth, A. and Dennis, A. (eds.), Polycyclic Aromatic Hydrocarbons: Chemistry and Biological Effects. p435, Ohio, Battelle Press, 1979.

7. International Agency for Research on Cancer. Certain polycyclic aromatic hydrocarbons and heterocyclic compounds. In: IARC Monogr. on the Evaluation of Carcinogenic Risk of Chemicals to Man, Vol. 3. Int. Agency for Cancer Research, Lyon, 1973.

8. Gelboin, H. V. and Ts'o, P. O. P. Polycyclic Hydrocarbons and Cancer. Environment, Chemistry and Metabolim. New York, Academic Press, Vol. 1, 1978.

9. Searle, C. E. (ed.). Chemical Carcinogens. Vol 1 and 2, Washington, ACS Monograph 182, 1984.

10. International Agency for Cancer Research. Polynuclear aromatic compounds. Part 1. Chemical, environmental and experimental data. In: IARC Monogr. on the Evaluation of Carcinogenic Risk of Chemicals to Man, Vol. 32. Int. Agency for Cancer Res., Lyon, 1983.

11. Gelboin, H. V. Benzo(a)pyrene metabolism, activation and carcinogenesis. Role and regulation of mixed-function oxidases and related enzymes. Physiol. Rev., 60:1107-1166, 1980.

12. Pelkonen, O. and Nebert, D. W. Metabolism of polycyclic hydrocarbons. Etiologic role in carcinogenesis. Pharmacol. Reviews, 34:189-221, 1982.

13. DePierre, J. W. and Ernster, L. The metabolism of polycyclic hydrocarbons and its relationship to cancer. Biochim. Biophys. Acta, 473:149-186, 1978.

14. Omura, T. and Sato, R. The carbon monoxide-binding pigment of liver microsomes. I. Evidence for its hemoprotein nature. J. Biol. Chem., 239:2370-2378, 1964.

15. Omura, T. and Sato, R. The carbon monoxide-binding pigment of liver microsomes. II. Solubilization, purification, and properties, J. Biol. Chem., 239:2379-2385, 1964.

16. Johnson, E. F. Multiple forms of cytochrome P-450. Criteria and significance. In: Hodgson, E. H., Bend, J. R., and Philpot, R. M. (eds.), Reviews In Biochemical Toxicology. pp. 1-26, Amsterdam, Elsevier/North-Holland Biomedical press, 1979.

17. Ryan D. E., Thomas, P. E., Koreniowski, D., and Levin, W. Separation and characterization of highly purified forms of liver microsomal cytochrome P-450 from rats treated with polychlorinated biphenyls, phenobarbital, and 3-methylcholanthrene. J. Biol. Chem., 25:1365-1374, 1979.

18. Takemori, S. and Kominami, S. The role of cytochrome P-450 in adrenal steroidogenesis. TIBS, Sept., 393-396, 1984.

19. Gelboin H. V. and Ts'o, P. O. P. (eds.). Polycyclic Aromatic Hydrocarbons and Cancer. Vol. 3, New York, Academic Press, 1981.

20. Mulder, G. J. Detoxication or toxication? Modification of the toxicity of foreign compounds by conjugation in the liver. TIBS 4:86-90, 1979.

21. Irving C. C. Metabolic activation of N-hydroxy compounds by conjugation. Xenobiotica, 1:387-398, 1971.

22. Kadlubar, F. F., Miller, J. A. and Miller, E. C. Hepatic microsomal N-glucuronidation and nucleic acid binding of N-hydroxy arylamines in relation to urinary bladder carcinogenesis. Cancer Res., 37:805-814, 1977.

23. Selkirk, J. K. Divergence of metabolic activation systems for short-term mutagenesis assays. Nature (Lond.), 270:604-607, 1977.

24. Langenbach, B., Freed, H. J., Raveh, D., and Huberman, E. Cell specificity in metabolic activation of aflatoxin B_1 and benzo[a]pyrene to mutagens for mammalian cells. Nature, 276:217-219, 1978.

25. Gelboin, H. V. and Ts'o, P. O. P. (eds.). Polycyclic Hydrocarbons and Cancer. Molecular and Cell Biology. Vol 2, New York, Academic Press, 1978.

26. Brookes, P. and Lawley, P. D. Evidence for the binding of polynuclear aromatic hydrocarbons to the nucleic acids of mouse skin. Relation between carcinogenic power of hydrocarbons and their binding to deoxyribonucleic acid. Nature (Lond.), 202:781-784, 1964.

27. Huberman, E. and Sachs, L. DNA binding and its relationship to carcinogenesis by different polycyclic hydrocarbons. Int. J. Cancer, 19:122-127, 1977.

28. Hecht, S. S., Trushin, N., Castonguay, A. and Rivenson, A. Comparative tumorigenicity and DNA methylation in F344 rats by 4-(methylnitrosamino)-1-(3-pyridyl)-1-butanone and N-nitrosodimethylamine. Cancer Res., 46:498-502, 1986.

29. Cooper, C. S., Grover, P. L. and Sims, P. The metabolism and activation of benzo(a)pyrene. Prog. Drug. Metab., 7:295-396, 1983.

30. Stowers, S. J. and Anderson, M. W. Formation and persistence of benzo(a)pyrene metabolite-DNA adducts. Environ. Hlth. Perspect., 62:31-39, 1985.

31. Jeffrey, A. M. DNA modification by chemical carcinogens. Pharmacol. Ther., 28:237-272, 1985.

32. Marshall, C. J., Vousden, K. H., and Phillips, D. H. Activation of c-Ha-ras-1 proto-oncogene by in vitro modification with a chemical carcinogen, benzo[a]pyrene diol-epoxide. Nature, 310:586-589, 1984.

33. Vousden, K. H., Bos, J. L., Marshall, C. J., and Phillips, D. H. Mutations activating human c-Has-ras1 protooncogene (HRAS1) induced by chemical carcinogens and depurination. Proc. Natl. Acad. Sci., 83:1222-1226, 1986.

34. Land, H., Parada, L. F., and Weinberg, R. A. Cellular oncogenes and multistep carcinogensis. Nature, 222:771-778, 1983.

35. Weinberg, R. A. Oncogenes of human tumor cells. TIBS, April:135-137, 1982.

36. Balmain, A., Ramsden, M., Bowden, G. T., and Smith, J. Activation of the mouse cellular harvey-ras gene in chemically induced benign skin papillomas. Nature, 307:658-660, 1984.

Chapter 2

Benzo[a]pyrene Disposition and Metabolism in Rats Following Intratracheal Administration

Introduction

Benzo[a]pyrene (B[a]P) is a ubiquitous environmental pollutant that poses a significant health risk to humans (1). Exposure to B[a]P may occur via several routes, but inhalation of B[a]P may represent the most important route of exposure in lung carcinogenesis (2).

Carcinogenesis by B[a]P requires metabolism of B[a]P to reactive forms which covalently bind to cellular macromolecules (3). Most studies to characterize B[a]P metabolism have been done *in vitro* using microsomes (4,5), purified enzymes (6), cell culture (7,8) and isolated perfused organs (9,10,11). In the few studies that have considered the fate of B[a]P *in vivo*, most have used routes other than lungs for B[a]P administration and have only partially characterized B[a]P disposition (12,13,14). In early investigations of B[a]P distribution after intratracheal administration, excretion of radiolabel (15) or distribution of radiolabel among various organs (16,17) was determined at various times after administration of

[^{3}H]-B[a]P to rats. More recently, Mitchell characterized distribution of radiolabel (18) and partially characterized metabolism of B[a]P (19) after exposing rats to [^{3}H]-B[a]P by inhalation.

Several studies have investigated the covalent binding of B[a]P metabolites to DNA, RNA, and protein (20,21,22). In addition, B[a]P metabolite:DNA adducts formed have been characterized under a variety of experimental conditions (23,24,25). However, very few studies have investigated the formation of these adducts *in vivo* (26,27,28).

To understand the mechanism of B[a]P carcinogenesis, it will be necessary to characterize more completely the fate of B[a]P *in vivo*. In the present investigation, we report a relatively complete characterization of the disposition of B[a]P and metabolites in rats following intratracheal instillation of [^{3}H]-B[a]P. Based on these data, toxicokinetic parameters were calculated which describe the disposition of B[a]P. Covalent binding of B[a]P metabolites to DNA, RNA, and protein in rat lung and liver were quantified, and types of B[a]P metabolite:deoxyribonucleoside adducts formed in lung and liver were characterized.

Materials and Methods

Chemicals and Biochemicals

[G-^{3}H]-B[a]P (specific activity, 43-80 Ci/mmol) was obtained from Amersham Corp. (Arlington Heights, Ill.) and purified by the method of Van Cantfort et al. (29). B[a]P-9,10-diol, B[a]P-4,5-diol, B[a]P-7,8-diol, B[a]P-1,6-quinone, B[a]P-3,6-quinone, B[a]P-6,12-quinone, 9-OH B[a]P, and 3-OH B[a]P were obtained from IIT Research Institute (Chicago, Ill.). Deoxyribonuclease I (from Bovine Pancreas), ribonuclease A (from Bovine Pancreas), proteinase K (type XI, from Tritirach album), beta-glucuronidase, (ß-glucuronidase, type H-1, from Helix Pomantia), arylsulfatase (type V, from Limpets), D-saccharic acid 1,4-lactone, and tert-butyl hydroperoxide were purchased from Sigma (Sigma Chemical Co., St. Louis, Mo.). Beckman tissue solubilizer (BTS-450) and Ready Solv EP scintillation cocktail were from Beckman (Beckman Instruments Inc., Irvine, Ca.). Silica gel thin-layer chromatography sheets were from Kodak (Eastman Kodak Co., Rochester, N.Y.). [^{14}C]-(+)-anti-B[a]PDE:dGuo adduct was a generous gift from Dr. William Baird (Purdue University).

Distribution Studies

Male Sprague-Dawley rats (Harlan or Va Tech Lab Animal Resources), weighing 200 to 250g, were used. Water and rat chow were provided ad libitum. Animals were fasted 24 hrs prior to each experiment.

Animals were anesthetized with sodium pentobarbital (60 mg kg^{-1}, i.p.) and tracheas were cannulated with polyethylene tubing (PE 240) using the method of Shanker (30). In experiments involving bile collection, bile ducts were cannulated with polyethylene tubing (PE10). Anesthesia was maintained throughout each experiment by administration of additional pentobarbital as required. Body temperatures were monitored and maintained at 37-38°C. In experiments that were longer than 1 hr, animals were given 1 ml of saline hourly by subcutaneous injection to prevent dehydration.

[^{3}H]-B[a]P dissolved in triethylene glycol was administered to rats (1 μg B[a]P kg^{-1} body wt.) at the bronchial bifurcation by injection through the tracheal cannula. Animals were maintained on a steep incline for 5-10 mins following B[a]P administration to allow the dose to

drain into the lungs. Animals were sacrificed by decapitation at selected times ranging from 5 to 360 min after B[a]P administration. Blood (4-5 ml) was collected in tubes containing heparin. Lungs (including trachea and bronchial tree), liver, kidneys, spleen, testes, stomach (including the whole esophagus), heart and thymus, intestinal tract (duodenum to rectum) and intestinal contents (obtained by flushing the intestinal tract with distilled water) were quickly removed, weighed, and placed on ice. Urine was collected from the bladder with a needle and syringe. Excreta voided prior to sacrifice was collected and combined with that obtained after sacrifice. Tissues were minced and homogenized in water using a polytron homogenizer. Duplicate tissue samples of 0.5 ml were solubilized in BTS-450, decolorized with tert-butyl hydroperoxide, and neutralized with glacial acetic acid. Levels of [^{3}H]-radioactivity in samples were determined by liquid scintillation counting in 15 ml of Ready Solv EP. [^{3}H]-radioactivity in urine and bile was measured without addition of solubilizer. Levels of [^{3}H]-radioactivity remaining in the carcass following organ

removal were determined as described for tissues, though the carcass was first digested in 1.5 N NaOH at 50°C for 24 hrs. Correction for quenching was done by the external standardization method. Counting efficiencies ranged from 20 to 40%. Recovery of radioactivity in distribution experiments was greater than 85%. Amounts of radioactivity in replicate tissue, excreta, or carcass samples from a given animal agreed within 10%.

Analysis of B[a]P and B[a]P Metabolites

Amounts of unmetabolized B[a]P in blood were determined following intravenous or intratracheal administration of [^{3}H]-B[a]P as outlined by Wiersma and Roth (11). For intravenous administration, [^{3}H]-B[a]P was suspended in plasma and injected into the tail vein. B[a]P in plasma was determined at selected times after administration. Animals in these experiments received anesthesia and tracheal cannulation treatments identical to those given to animals receiving [^{3}H]-B[a]P by intratracheal administration.

Identification of B[a]P metabolites by HPLC was similar to that reported by Selkirk (31). Aliquots of organ homogenate were combined with an equal volume of cold acetone and extracted 5 times with ethyl acetate (1:1 v/v). The aqueous phase after extraction was combined with an equal volume of BTS-450 and the level of [^{3}H]-radioactivity determined by liquid scintillation counting as previously described. Ethyl acetate extracts were combined for each sample, filtered through a 0.45 μm Millipore filter, and evaporated to dryness under a stream of nitrogen. Samples were stored under nitrogen at -90°C and analyzed the following day. Prior to analysis, sample residues were dissolved in methanol. A Perkin Elmer series 400 HPLC

equipped with a 5 μm C-18 reverse phase column (Vydac) was used for separation of B[a]P metabolites. A 40 min linear gradient from 60% methanol:40% H_2O to 100% methanol with a flow rate of 1 ml min^{-1} was used. Column temperature was 35°C. The effluent was monitored at 254 nm and fractions were collected at 0.5 min intervals. Ready Solv EP (5 ml) was added to each fraction and the elution profile of [^{3}H]-radioactivity was determined by liquid scintillation counting. Radioactive metabolites were identified by retention times corresponding to authentic metabolite standards of B[a]P.

Conjugates of B[a]P were identified using the method of MacLeod et al. (32) with slight modifications (Appendix A). Aliquots of samples were combined with four volumes of ethanol and placed in the cold for 3 hrs. Precipitated material was pelleted by centrifugation and the supernatant fraction was removed and evaporated to dryness under a stream of nitrogen. Residues were dissolved in 1 ml of 0.2 M acetate buffer (pH 5), with β-glucuronidase (4000 Fishman units) or aryl sulfatase (20 Fishman units) which included 60 mM D-saccharic acid 1,4-lactone. Samples without enzymes served as controls. Sample tubes were flushed with nitrogen, sealed, and incubated at 37°C in a water bath with gentle agitation for 24 hrs. After incubation the samples

were combined with four volumes of ethanol and placed in the cold for 3 hrs. Precipitated material was pelleted by centrifugation and the supernatant was removed and concentrated to a small volume under a stream of nitrogen. Aliquots of samples were chromatographed on silica gel thin-layer chromatography sheets with ethyl acetate/methanol/water/formic acid (100:25:20:1) (32). After development of the chromatogram, sample lanes were divided into 0.5 cm sections, placed into scintillation vials and counted by liquid scintillation to determine the migration profile of [^{3}H]-radioactivity in each lane. B[a]P glucuronic acid and sulfate conjugates were identified by sensitivity to ß-glucuronidase and sulfatase hydrolysis, respectively. Material resistant to enzyme hydrolysis was considered to be thio-ether conjugates of B[a]P metabolites. Non-conjugated metabolites and unmetabolized B[a]P migrated at the solvent front.

Enterohepatic Circulation

[^{3}H]-B[a]P biliary metabolites were collected from rats with cannulated bile ducts over a 6 hr time interval following [^{3}H]-B[a]P administration (1 μg kg^{-1} body wt.). Aliquots of bile were incubated with both β-glucuronidase (4000 Fishman units ml^{-1}) and aryl sulfatase (20 Fishman units ml^{-1}) for 24 hrs at 37°C. Bile containing B[a]P metabolites (5-6 μCi/3ml) which was treated as described above or not treated with enzymes was infused into the duodenum of rats with cannulated bile ducts. Cannulas also were implanted in the trachea of these animals. Immediately after infusion, bile was collected at 10 min intervals over a 6 hr time period. Animals were sacrificed after 6 hrs and distribution of [^{3}H]-radioactivity was determined as described in the previous section.

Toxicokinetic Analysis

Data representing B[a]P concentrations in blood as a function of time after administration for intravenously and intratracheally administered [^{3}H]-B[a]P were analyzed by the Simulation, Analysis and Modeling (SAAM) computer program

(33). Data fit best to a three-term exponential represented by the following general equation: $C(t) = \Sigma C_i e^{-\lambda_i t}$. Values for C_i and λ_i were estimated using SAAM while area under the curve (AUC), volume of distribution (V_d) and clearance (Cl) were calculated as follows (34):

$$AUC = \Sigma\ C_i/\lambda_i$$

$$V_d = \frac{Dose \cdot \Sigma\ (C_i/\lambda_i^2)}{(C_i/\lambda_i)^2}$$

$$Cl = Dose/AUC$$

The systemic availability of B[a]P administered intratracheally was calculated from the following equation:

$$F_{it} = \frac{AUC_{it} \cdot Dose_{iv} \cdot \lambda_{z,it}}{AUC_{iv} \cdot Dose_{it} \cdot \lambda_{z,iv}}$$

where $\lambda_{z,it}$ and $\lambda_{z,iv}$ represent the terminal elimination rates for B[a]P following intratracheal and intravenous administration, respectively.

Isolation of DNA, RNA and Protein

[^{3}H]-B[a]P (1 mCi/animal) corresponding to a dose of 5 µg B[a]P was administered by intratracheal instillation. After 6 hr, DNA, RNA, and protein were isolated from lung and liver. The isolation procedure reported by Diamond et al. (35) and subsequently by Kuroki et al. (22) was used with slight modifications. Organs were homogenized using a tissuemizer at low speed in 10 vols per gram tissue, of 10 mM Tris buffer containing 0.15 M NaCl, 10 mM EDTA, and 1% SDS (pH 8). After homogenization, an equal volume of phenol:m-cresol:8-hydroxyquinoline:water (500/70/0.5/55 by wt.) was added and the mixture was stirred at room temperature for 30 min. The mixture was then centrifuged at 12,000xg for 30 min after which the upper aqueous phase was removed along with the protein interphase. These phases were combined with 0.5 volumes of the phenol mixture. The phases were again separated by centrifugation and the aqueous phase without protein was removed. DNA was precipitated from the aqueous phase by adding 2 volumes of 95% ethanol containing 2% potassium acetate. The precipitated DNA was removed by centrifugation and/or spooled out onto a glass rod and dissolved in 10 mM Tris (pH 7). The solution of DNA was incubated at 37°C with 50 µg/ml

RNase which had been treated at 80°C for 10 min to inactivate DNase. The sample was then incubated with 50 μg/ml proteinase K for 30 min at 37°C. The solution of DNA was deproteinized with chloroform:isoamyl alcohol (24:1 v/v), precipitated by adding 2 volumes of 95% ethanol, and redissolved in 10 mM Tris (pH 7). After another repetition of RNase and proteinase K treatment, the DNA was precipitated with 100% ethanol, washed with ether and redissolved in 10 mM $MgCl_2$, 10 mM Tris (pH 7). Glycogen was removed from samples by centrifugation at 100,000 xg for 60 min.

The aqueous phase remaining after DNA removal was placed in a freezer overnight to precipitate RNA. RNA was pelleted by centrifugation at 2,500 rpm for 30 min and dissolved in 10 mM Tris (pH 7). The solution of RNA was treated with DNase (50 μg/ml) followed by proteinase K (50 μg/ml) for 30 min each at 37°C. The RNA solution was deproteinized with chloroform:isoamyl alcohol (24:1) and RNA reprecipitated with 2 vol 95% ethanol/2% potassium acetate at -20°C overnight. RNA was dissolved and reprecipitated with 95% ethanol/2% potassium acetate at -20°C overnight. Finally, RNA was dissolved in 10 mM $MgCl_2$, 10 mM Tris (pH 7). The intermediate and phenol layers following the removal of the aqueous phase were combined and protein was

precipitated by addition of 3 volumes of cold methanol. Protein was washed 3 times with methanol and once with ether. Residual ether was evaporated under nitrogen and protein was dissolved in a small volume of 1 N NaOH.

DNA and RNA were quantitated using the fluorometric assay (36) and orcinol assay (37), respectively. A_{260}/A_{280} ratios ranged from 1.8-2.0. Protein was determined by the procedure of Lowry et al. (38) with bovine serum albumin as a standard. [^{3}H]-radioactivity associated with DNA, RNA, and protein was determined by liquid scintillation counting.

HPLC Analysis of B[a]P:DNA Adducts

DNA isolated from lung and liver was enzymatically degraded to deoxyribonucleosides following the procedure of Baird et al. (39). After hydrolysis, B[a]P:deoxyribonucleosides were concentrated using Sep-pak C_{18} cartridges, and B[a]P-modified deoxyribonucleosides that contained cis-vicinal hydroxyl groups were separated from the other B[a]P:deoxyribonucleoside adducts by chromatography on a column of {N-[N'-m-(dihydroxyboryl)phenyl]succinamyl}amino ethyl cellulose (boronate) as described previously by Baird et al. (30).

The synthesis and characterization of boronate columns are described in Appendix B.

The B[a]P:deoxyribonucleoside adducts from 3 animals were pooled and chromatographed by HPLC using a 5 μm C_{18} reverse-phase column (Vydac). The column was eluted with 42/58 percent MeOH/H_2O for 15 min, then for 30 min with a linear gradient of 42/58 to 50/50 MeOH/H_2O, followed by a 10 min linear gradient of 50/50 to 55/45 MeOH/H_2O, then for 20 min at 55/45 followed by a 20 min linear gradient of 55 to 100% MeOH. Eluent was collected in minivials at 0.5 min intervals for 100 min. [^{3}H]-radioactivity was determined by liquid scintillation counting. An aliquot of [^{14}C]-(+)-anti-B[a]PDE:dGuo marker was added as a standard to selected samples prior to HPLC analysis.

Results

[^{3}H] Distribution Following Intratracheal Administration of [^{3}H]-B[a]P

Radioactivity in various organs of rats was determined at intervals following [^{3}H]-B[a]P instillation. Largest amounts were detected in lungs, liver, intestines, intestinal contents, and carcass (Figures 2.1.-2.3.). Elimination of radioactivity from lungs was determined to be biphasic by nonlinear regression analysis, with data fitting the equation $C(t) = C_1 e^{-\lambda 1 t} + C_2 e^{-\lambda 2 t}$. Half-lives of 5 min and 116 min were calculated for the rapid and slow phases of elimination, respectively. Radioactivity in the liver increased rapidly, reaching a maximum of 20% of the injected dose within 10 min after [^{3}H]-B[a]P administration after which levels of radioactivity slowly declined (Figure 2.2.). Radioactivity in intestines and intestinal contents increased throughout the period of observation (Figure 2.3.). Radioactivity in carcass increased rapidly and declined slowly thereafter.

Figure 2.1. Clearance of [^{3}H]-radioactivity from lung following intratracheal administration of [^{3}H]-B[a]P (1 $\mu g\ kg^{-1}$). The amount of [^{3}H]-radioactivity in lung was determined as described in "Materials and Methods". Results are expressed as percent of dose (mean ± S.E., for 3 animals at each time point).

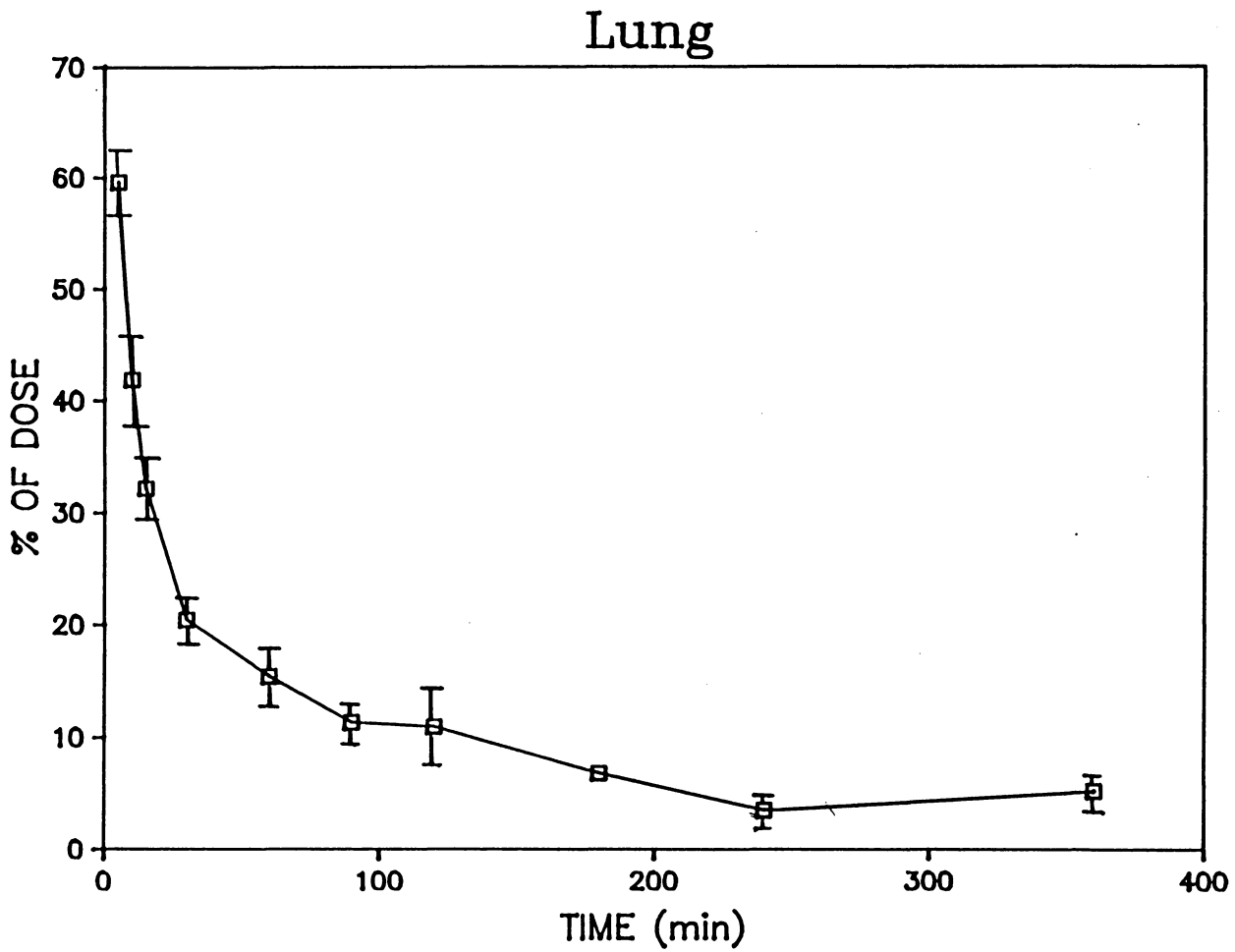
Lung
70
60
50
40
30
20
10
0
% OF DOSE
0
100
200
300
400
TIME (min)

Figure 2.2. Disposition of [^{3}H]-radioactivity in liver and carcass following intratracheal administration of [^{3}H]-B[a]P (1 μg kg^{-1}). The amount of [^{3}H]-radioactivity in the organs was determined as described in "Material and Methods". Results are expressed as the percent of dose (mean ± S.E., for 3 animals at each time point).

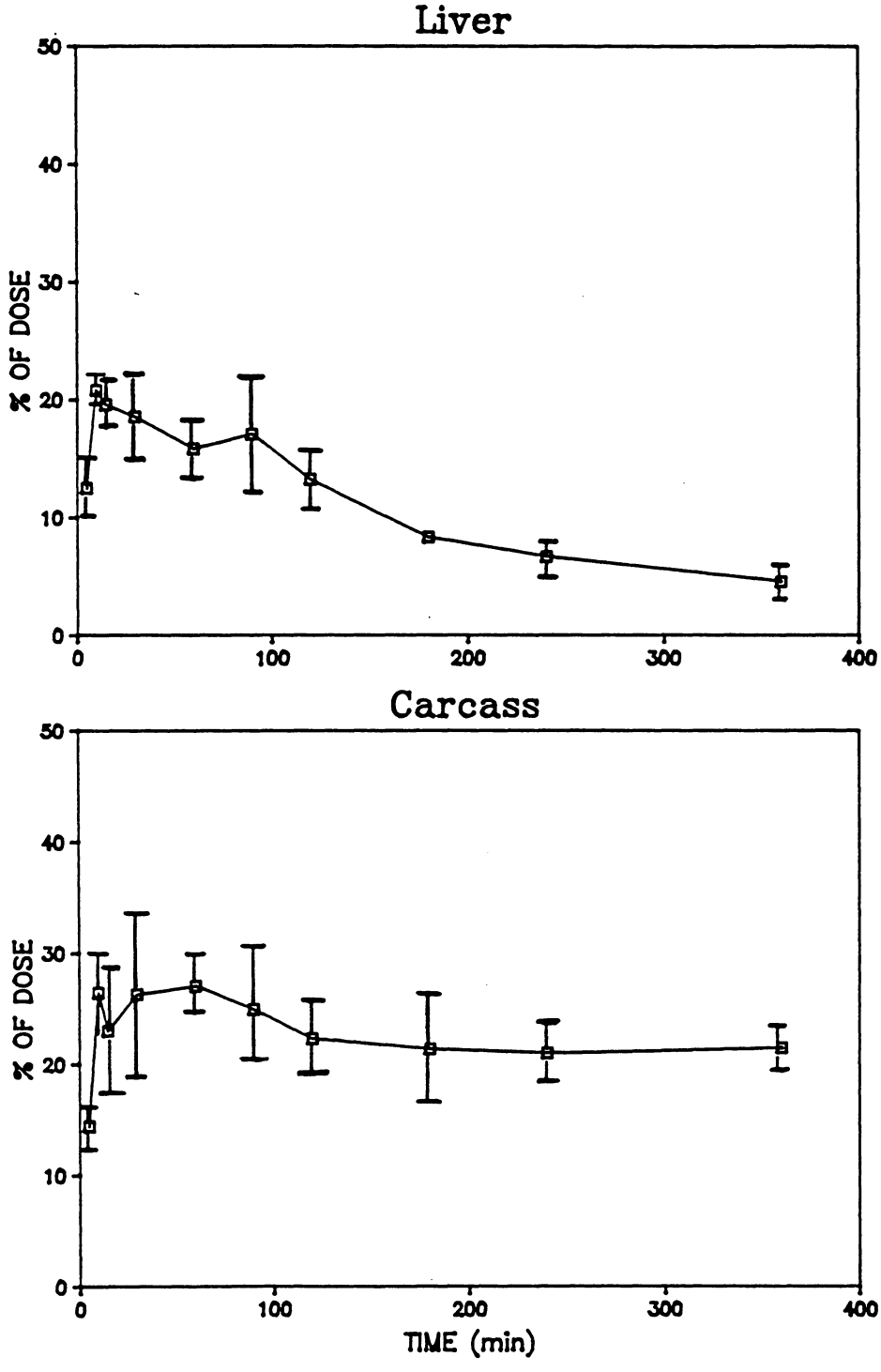
Liver
% OF DOSE
0
10
20
30
40
50
0
100
200
300
400
Carcass
% OF DOSE
0
10
20
30
40
50
0
100
200
300
400
TIME (min)

Figure 2.3. Disposition of [^{3}H]-radioactivity in intestines and intestinal contents following intratracheal administration of [^{3}H]-B[a]P (1 $\mu g\ kg^{-1}$). The amount of [^{3}H]-radioactivity in the organs was determined as described in "Material and Methods". Results are expressed as the percent of dose (mean ± S.E., for 3 animals at each time point).

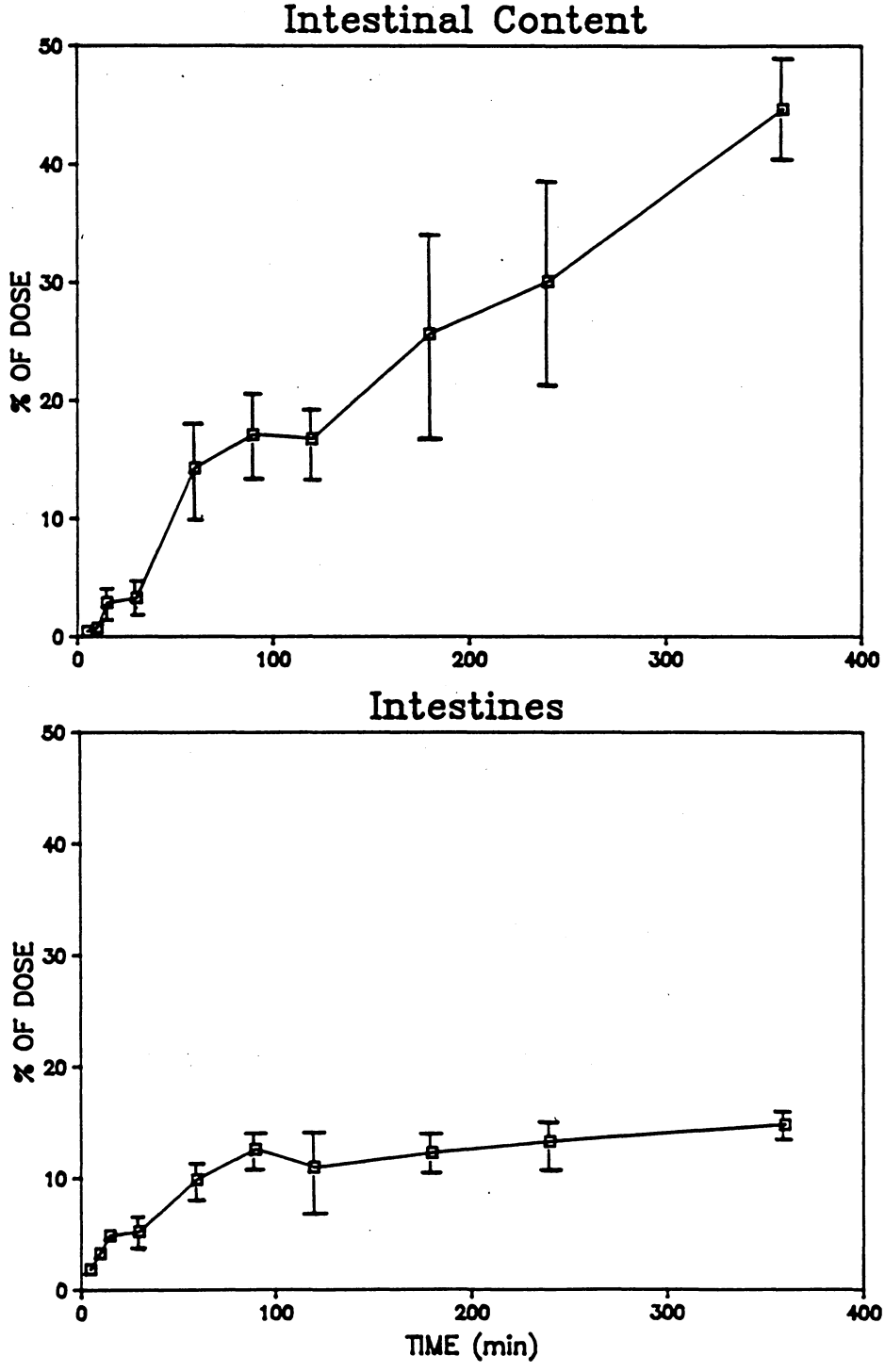
Intestinal Content
% OF DOSE
0
10
20
30
40
50
0
100
200
300
400
Intestines
% OF DOSE
0
10
20
30
40
50
0
100
200
300
400
TIME (min)

Maximum amounts of radioactivity were associated with carcass 90 min after administration of [^{3}H]-B[a]P, and 22% of injected dose remained at 360 min (Figure 2.2.). Lesser amounts of radioactivity were associated with other organs (Table 2.1.). It is unlikely that radioactivity in the stomach resulted from swallowing some of the administered dose for two reasons. First, the radioactivity in stomach increased very gradually, and second, the tracheal cannula was left in place throughout the experiments. In addition, under experimental conditions in which intestines were ligated prior to B[a]P instillation, only 0.5% of the dose was detected in stomach after 6 hrs (data not shown). The material in the stomach is probably the result of regurgitation of bile from the duodenum. Kidneys consistently accounted for about 2% of the injected dose at all times post injection while testes, spleen, and heart/thymus each accounted for less than 1% of the injected dose. Excretion of radioactivity in urine accounted for a very small fraction of the administered dose.

Table 2.1.

Disposition of [^{3}H]-radioactivity following intratracheal administration of [^{3}H]-B[a]P

[^{3}H]-B[a]P was administered by intratracheal instillation through a tracheal cannula and amounts of radioactivity in tissues were determined as described in "Materials and Methods". The results are expressed as percent of dose (mean ± S.E., for 3 animals at each time point).

	Time (min)									
tissue	5	10	15	30	60	90	120	180	240	360
Kidney	1.1 ± 0.4	1.9 ± 0.4	1.9 ± 0.2	1.4 ± 0.3	2.2 ± 0.2	2.4 ± 0.2	2.0 ± 0.2	1.8 ± 0.2	1.7 ± 0.2	2.0 ± 0.4
Stomach	0.3 ± 0.05	0.7 ± 0.2	0.7 ± 0.2	1.2 ± 0.1	4.6 ± 1.9	3.7 ± 1.7	6.9 ± 0.03	5.0 ± 1.2	4.0 ± 0.8	5.8 ± 0.2
Testes	0.4 ± 0.04	0.5 ± 0.05	0.7 ± 0.1	0.6 ± 0.1	1.1 ± 0.06	1.3 ± 0.3	1.1 ± 0.05	0.8 ± 0.1	0.9 ± 0.08	0.8 ± 0.08
Spleen	0.5 ± 0.03	0.3 ± 0.07	0.4 ± 0.03	0.2 ± 0.01	0.3 ± 0.01	0.2 ± 0.03	0.2 ± 0.01	0.2 ± 0.02	0.1 ± 0.02	0.2 ± 0.05
Heart/thymus	0.9 ± 0.2	1.6 ± 0.8	0.8 ± 0.1	0.5 ± 0.1	0.5 ± 0.03	0.5 ± 0.02	0.6 ± 0.1	0.5 ± 0.08	0.4 ± 0.04	0.4 ± 0.03
Urine	N.D.[a]	0.01 ± 0.01	0.2 ± 0.2	0.1 ± 0.06	0.3 ± 0.05	0.8 ± 0.3	1.1 ± 0.4	1.2 ± 0.5	1.6 ± 0.3	2.2 ± 0.6
Blood	3.9 ± 1.0	3.0 ± 1.0	3.8 ± 1.0	1.6 ± 0.4	1.6 ± 0.3	2.1 ± 0.4	1.9 ± 0.3	1.1 ± 0.2	0.8 ± 0.4	1.7 ± 0.3

[a] N.D. - no radioactivity detected

Amounts of radiolabel in blood also were very small. To allow calculation of toxicokinetic parameters, amounts of unmetabolized B[a]P in blood were determined (Figure 2.4.). Also shown in Figure 2.4. is elimination of [^{3}H]-B[a]P from blood following intravenous administration from which toxicokinetic parameters were calculated (Table 2.2.).

Figure 2.4. Clearance of [^{3}H]-B[a]P from blood when [^{3}H]-B[a]P (1μg kg^{-1}) was administered by intratracheal instillation (□ --□) or intravenous injection (▲—▲). Blood samples were analyzed for unmetabolized B[a]P concentration at time intervals between 5 and 360 min after [^{3}H]-B[a]P administration as described in "Materials and Methods". Amounts of unmetabolized B[a]P are expressed as percent of dose per ml of blood. Data for intravenously injected B[a]P represent the mean of 3 determinations at each time point while data for intratracheally injected B[a]P represent the mean B[a]P concentration for 2 to 3 animals at each time point.

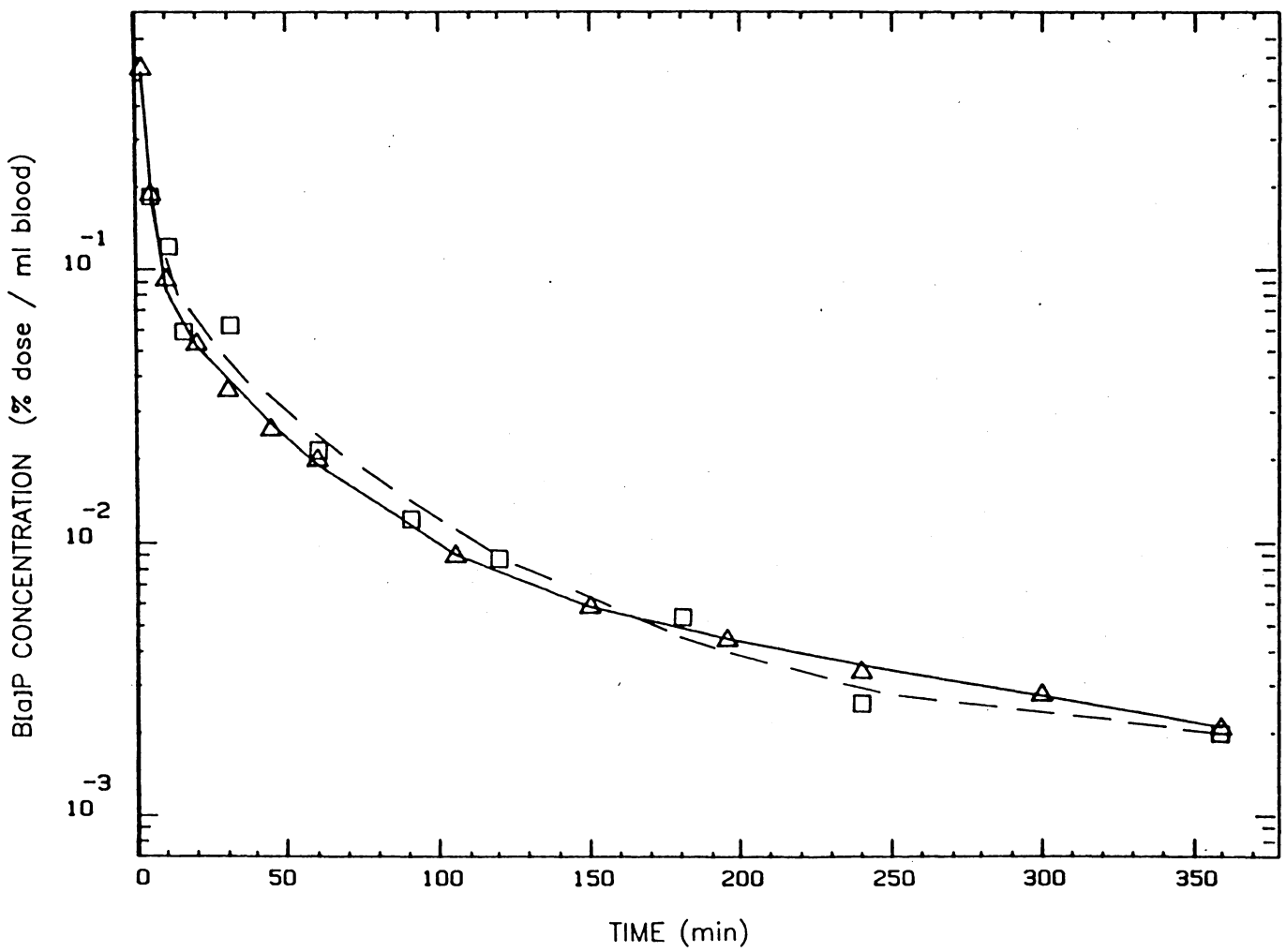
BIaJP CONCENTRATION (% dose / ml blood)
10^-1
10^-2
10^-3
0
50
100
150
200
250
300
350
TIME (min)

Table 2.2.

Toxicokinetic parameters
describing B[a]P disposition following
intravenous and intratracheal administration

Anesthetized rats with cannulas inserted in tracheas were given [^{3}H]-B[a]P (1 μg kg^{-1}) dissolved in plasma by intravenous injection. Blood samples were taken between 2 and 360 min after [^{3}H]-B[a]P administration and B[a]P concentrations were determined. Likewise, B[a]P concentrations in blood samples collected from animals given [^{3}H]-B[a]P (1 μg kg^{-1}) dissolved in triethylene glycol by intratracheal injection were also determined and kinetic parameters were calculated as described in "Materials and Methods".

	Route of Administration	
	Intravenous[A]	Intratracheal
λ_1 (min^{-1})	0.45 ± 0.048	0.16
λ_2 (min^{-1})	0.031 ± 0.00019	0.022
λ_3 (min^{-1})	0.0039 ± 0.00051	0.0025
Vd (l)	1.29 ± 0.18	2.2
Cl (ml/min)	13.73 ± 0.23	15.3
AUC (% dose/min/ml blood)	7.30 ± 0.12	6.52
Systemic availability	---	0.57

[A]Results are mean ± S.E. for 3 animals.

B[a]P Metabolites in Lung, Liver, and Intestinal Contents

Metabolites in lung, liver, and intestinal contents were determined at selected time points following administration of [^{3}H]-B[a]P. Amounts of metabolites which were soluble in the ethyl acetate and aqueous phases were determined as were profiles of B[a]P metabolites in organic phases. Amounts of both organic- and aqueous-soluble metabolites in lungs declined with time, and the relative amount of metabolites in the aqueous phases increased substantially by 360 min (Table 2.3.). By 5 min after administration of [^{3}H]-B[a]P, the B[a]P metabolites present in greatest amounts in the organic phase from lungs were conjugates and/or polyhydroxylated metabolites and quinones. The percentages of total metabolites that were B[a]P dihydrodiols, phenols, and conjugates and/or polyhydroxylated metabolites at 360 min were considerably higher than at 5 min though molar amounts of metabolites were less.

A shift in the ratio of metabolites in organic versus aqueous phases also was seen in liver, with organic-soluble metabolites predominating at 5 min and aqueous-soluble metabolites predominating at 360 min (Table 2.4.). Amounts

of each metabolite in the organic phase relative to the total organic-extractable material increased with time with a corresponding decrease in the amount of unmetabolized B[a]P. In intestinal contents, metabolites soluble in the aqueous phase predominated at 60 and 360 min (Table 2.5.). Of material in the organic phase, about 24% was associated with conjugates and/or polyhydroxylated metabolites at 60 and 360 min. Nonconjugated metabolites and small amounts of unmetabolized B[a]P also were detected in intestinal contents.

Table 2.3.

Benzo[a]pyrene metabolites in rat lung

Metabolites were isolated from tissues of animals used in distribution studies (Table 2.1. and Figure 2.1.). Results for organic and aqueous metabolites shown in the upper part of the Table are expressed as percent of injected dose. Metabolites soluble in the organic phase are shown in the lower part of the table and results are expressed as percent of total organic-soluble metabolites (mean ± S.E., for 3 animals at each time point). Numbers in parentheses represent pmoles of each metabolite.

Metabolites	5 min	60 min	360 min
Total	59.6 ± 2.57 (508)	15.4 ± 2.61 (143)	3.99 ± 0.48 (51.3)
Organic	47.7 ± 1.46 (408)	11.0 ± 1.85 (103)	2.16 ± 0.35 (29.3)
Aqueous	11.9 ± 3.25 (99.8)	4.37 ± 0.81 (40.6)	1.83 ± 0.68 (22.1)
conjugates and/or polyhydroxylated metabolites	4.23 ± 0.76 (17.2)	12.5 ± 3.88 (12.8)	16.3 ± 4.57 (4.76)
9,10-diol	1.83 ± 0.23 (7.46)	2.63 ± 0.36 (2.70)	4.95 ± 1.12 (1.45)
4,5-diol	0.89 ± 0.21 (3.63)	1.09 ± 0.28 (1.12)	2.60 ± 0.53 (0.76)
7,8-diol	1.12 ± 0.06 (4.57)	1.57 ± 0.12 (1.61)	3.11 ± 0.69 (0.91)
1,6-quinone	4.01 ± 2.39 (16.4)	2.04 ± 0.41 (2.10)	2.99 ± 0.17 (0.87)
3,6-quinone	5.03 ± 1.53 (20.5)	4.35 ± 1.01 (4.47)	4.09 ± 0.92 (1.20)
6,12-quinone	2.68 ± 1.03 (10.9)	3.59 ± 1.54 (3.69)	2.23 ± 0.28 (0.65)
9-OH	0.90 ± 0.11 (3.67)	1.94 ± 0.83 (1.99)	2.26 ± 0.63 (0.66)
3-OH	1.15 ± 0.18 (4.69)	1.95 ± 0.25 (2.00)	4.59 ± 0.74 (1.34)
B[a]P	67.4 ± 8.38 (274)	47.1 ± 5.20 (48.4)	20.0 ± 4.04 (5.84)

Table 2.4.

Benzo[a]pyrene metabolites in rat liver

Metabolites were isolated from tissues of animals used in distribution studies (Table 2.1. and Figure 2.2.). Results for organic and aqueous metabolites shown in the upper part of the Table are expressed as percent of injected dose. Metabolites soluble in the organic phase are shown in the lower part of the table and results are expressed as percent of total organic-soluble metabolites (mean ± S.E., for 3 animals at each time point). Numbers in parentheses represent pmoles of each metabolite.

Metabolites	5 min	60 min	360 min
Total	12.5 ± 2.42 (106)	15.8 ± 2.32 (147)	4.57 ± 0.99 (40.3)
Organic	10.9 ± 2.18 (93.1)	8.68 ± 1.43 (80.8)	1.80 ± 0.32 (16.0)
Aqueous	1.56 ± 0.32 (13.3)	7.15 ± 1.55 (66.6)	2.67 ± 0.63 (23.7)
conjugates and/or polyhydroxylated metabolites	2.93 ± 0.47 (2.71)	12.5 ± 0.28 (10.1)	23.8 ± 2.37 (3.74)
9,10-diol	1.35 ± 0.24 (1.26)	4.42 ± 0.63 (3.57)	6.81 ± 1.40 (1.09)
4,5-diol	0.96 ± 0.04 (0.89)	1.99 ± 0.73 (1.61)	3.50 ± 0.48 (0.56)
7,8-diol	1.02 ± 0.01 (0.95)	1.28 ± 0.38 (1.03)	2.65 ± 0.46 (0.42)
1,6-quinone	2.47 ± 0.94 (2.30)	2.84 ± 1.04 (2.29)	5.61 ± 1.50 (0.90)
3,6-quinone	2.13 ± 0.08 (1.98)	3.70 ± 0.68 (2.99)	7.15 ± 1.81 (1.14)
6,12-quinone	2.27 ± 0.82 (2.11)	4.41 ± 1.28 (3.56)	7.35 ± 1.77 (1.17)
9-OH	0.71 ± 0.14 (0.66)	1.34 ± 0.17 (1.08)	2.51 ± 0.15 (0.40)
3-OH	0.99 ± 0.18 (0.92)	1.35 ± 0.20 (1.09)	2.95 ± 0.33 (0.47)
B[a]P	79.0 ± 0.99 (73.5)	54.4 ± 6.29 (43.9)	15.7 ± 4.34 (2.51)

Table 2.5.

Benzo[a]pyrene metabolites in rat intestinal contents

Metabolites were isolated from tissues of animals used in distribution studies (Table 2.1. and Figure 2.3.). Results for organic and aqueous metabolites shown in the upper part of the Table are expressed as percent of injected dose. Metabolites soluble in the organic phase are shown in the lower part of the table and results are expressed as percent of total organic-soluble metabolites (mean ± S.E., for 3 animals at each time point). Numbers in parentheses represent pmoles of each metabolite.

Metabolites	60 min	360 min
Total	14.3 ± 4.10 (133)	44.7 ± 6.78 (442)
Organic	5.51 ± 1.66 (51.3)	18.2 ± 1.43 (180)
Aqueous	8.75 ± 2.45 (81.4)	26.5 ± 2.80 (262)
conjugates and/or polyhydroxylated metabolites	23.4 ± 1.20 (12.0)	24.1 ± 1.55 (43.3)
9,10-diol	9.76 ± 1.10 (5.00)	7.75 ± 0.46 (13.9)
4,5-diol	6.75 ± 1.15 (3.46)	8.43 ± 1.51 (15.2)
7,8-diol	5.96 ± 2.52 (3.06)	5.73 ± 1.02 (10.3)
1,6-quinone	8.73 ± 2.07 (4.48)	7.13 ± 2.00 (12.8)
3,6-quinone	9.61 ± 2.40 (4.93)	7.85 ± 1.33 (14.1)
6,12-quinone	3.93 ± 1.21 (2.02)	7.10 ± 1.55 (12.8)
9-OH	2.20 ± 0.46 (1.13)	2.24 ± 0.33 (4.02)
3-OH	4.96 ± 1.51 (2.54)	4.66 ± 1.28 (8.37)
B[a]P	2.17 ± 0.36 (1.11)	1.55 ± 0.12 (2.79)

Distribution and Metabolism of B[a]P in Animals With and Without Biliary Cannulas

[^{3}H]-B[a]P was administered to animals with biliary cannulas and distribution of radioactivity and identity of metabolites which were excreted were compared with those in animals without biliary cannulas.

Distribution of radioactivity among organs was similar in animals without and with biliary cannulas (Table 2.6.). However, in animals with cannulas, radioactivity in bile, intestines, and intestinal contents accounted for about 77% of the injected dose while intestines and intestinal contents in animals without a cannula accounted for only about 58% of the injected dose. In addition, consistently lower amounts of radiolabel were detected in the stomach of animals with biliary cannulas.

Conjugates of B[a]P metabolites were identified in intestinal contents and bile 6 hrs after [^{3}H]-B[a]P administration (Table 2.7.). When results are considered as percent of dose, amounts of thioether conjugates and glucuronides in intestinal contents were significantly lower ($p<0.05$) than amounts of these conjugates in bile.

Table 2.6.

Disposition of [^{3}H]-radioactivity
in animals without and with biliary cannulas

[^{3}H]-B[a]P was administered (1 $\mu g\ kg^{-1}$) to animals without and with a biliary cannula. Tissue levels of [^{3}H]-radioactivity were determined 6 hours after [^{3}H]-B[a]P administration as detailed in "Materials and Methods". Results are expressed as percent of dose (mean ± S.E., for 3 animals/experiment).

ORGANS	WITHOUT	WITH
lung	4.4 ± 0.8	4.0 ± 0.3
liver	4.5 ± 0.7	6.7 ± 0.5
intestines	13.0 ± 1.4	2.7 ± 0.3
intestinal contents	44.7 ± 3.8	0.3 ± 0.1
stomach	5.4 ± 0.4	0.4 ± <0.1
kidney	1.8 ± 0.3	2.4 ± 0.4
testes	0.8 ± 0.1	1.4 ± 0.1
spleen	0.2 ± 0.1	0.1 ± <0.1
heart/thymus	0.3 ± <0.1	0.4 ± 0.1
urine	1.7 ± 0.7	2.3 ± 0.7
blood	1.8 ± 0.2	1.9 ± 0.5
carcass	19.4 ± 2.3	15.5 ± 0.6
bile	---	74.1 ± 2.1

Table 2.7.

B[a]P metabolites in bile and intestinal contents 6 hrs after [^{3}H]-B[a]P administration

[^{3}H]-B[a]P was administered (1 μg kg^{-1}) at the site of the bronchial bifurcation by injection through a tracheal cannula. Aliquots of bile (from animals with a biliary cannula) and intestinal contents (from animals without a biliary cannula) were analyzed for thio-ether, glucuronic acid, and sulfate conjugates and non-conjugated metabolites as detailed in "Materials and Methods". Results are expressed as percent of dose for each metabolite in bile and intestinal contents (mean ± S.E., for 3 animals/experiment). Numbers in parentheses give the amount of each metabolite as a percent of total metabolites in bile and intestinal contents.

Metabolites	Intestinal Contents	Bile
thio-ether conjugates	27.7 ± 2.1 (62.9)	45.5 ± 3.0 (61.0)
glucuronides	4.0 ± 0.7 (9.4)	13.6 ± 0.6 (18.4)
sulfate conjugates	2.7 ± 0.8 (6.5)	3.1 ± 0.4 (4.3)
non-conjugated	10.4 ± 1.7 (23.2)	12.1 ± 1.3 (16.3)

Enterohepatic circulation of B[a]P metabolites

Bile was collected from rats via cannulas following intratracheal instillation of [^{3}H]-B[a]P. A portion of the bile was treated with ß-glucuronidase and arylsulfatase. Samples of bile with and without enzyme treatment were infused intraduodenally into animals which contained biliary cannulas and the amount of [^{3}H]-radioactivity excreted in bile was monitored for 6 hrs after which tissue disposition of radioactivity was determined.

Differences in the biliary excretion of radioactivity following infusion of treated and non-treated bile were detected (Figure 2.5). Metabolites treated with enzymes were absorbed and excreted in bile more rapidly than those in non-treated bile. When enzyme-treated bile was infused, almost 21% of the dose was absorbed with nearly 15% appearing in bile in 6 hrs. When bile which was not treated with enzymes was infused, only about 7% of the dose was absorbed with less than 4% appearing in bile.

Table 2.8.

Disposition of [^{3}H]-radioactivity in animals via enterohepatic circulation

[^{3}H]-B[a]P biliary metabolites were infused into the duodenum of rats with cannulated bile ducts. Tissue levels of [^{3}H]-radioactivity were determined 6 hours after infusion as detailed in "Materials and Methods". Results are expressed as percent of dose (mean ± S.E., for 3 animals/experiment).

ORGANS	NON-TREATED	TREATED[A]
lung	0.038 ± 0.011	0.152 ± 0.032
liver	0.351 ± 0.351	0.556 ± 0.104
gi tract	92.6 ± 0.904	79.2 ± 2.87
kidney	0.175 ± 0.070	0.214 ± 0.033
testes	0.054 ± 0.006	0.064 ± 0.001
spleen	0.015 ± 0.005	0.018 ± 0.004
heart/thymus	0.065 ± 0.019	0.073 ± 0.018
urine	0.023 ± 0.009	0.139 ± 0.053
blood	0.475 ± 0.417	1.08 ± 0.255
carcass	2.45 ± 1.12	3.61 ± 0.726
bile	3.73 ± 1.14	14.9 ± 2.23

[A]Biliary metabolites treated with ß-glucuronidase and aryl sulfatase.

Figure 2.5. Biliary excretion of [^{3}H]-radioactivity from rats following intraduodenal instillation of bile containing [^{3}H]-B[a]P metabolites. Bile was collected from rats following intratracheal instillation of [^{3}H]-B[a]P (1 μg kg^{-1}). A portion of the bile was treated with β-glucuronidase and arylsulfatase and a portion was not treated. Aliquots of enzyme-treated (□—□) and non-treated (X---X) bile were infused intraduodenally into rats with cannulated bile ducts and amounts of [^{3}H]-radioactivity excreted in bile were measured. The rate of excretion (% dose/fraction) is depicted in the upper part of the Fig. and cumulative excretion is shown in the lower part. Results are expressed as percent of infused dose (mean ± S.E., for 3 animals).

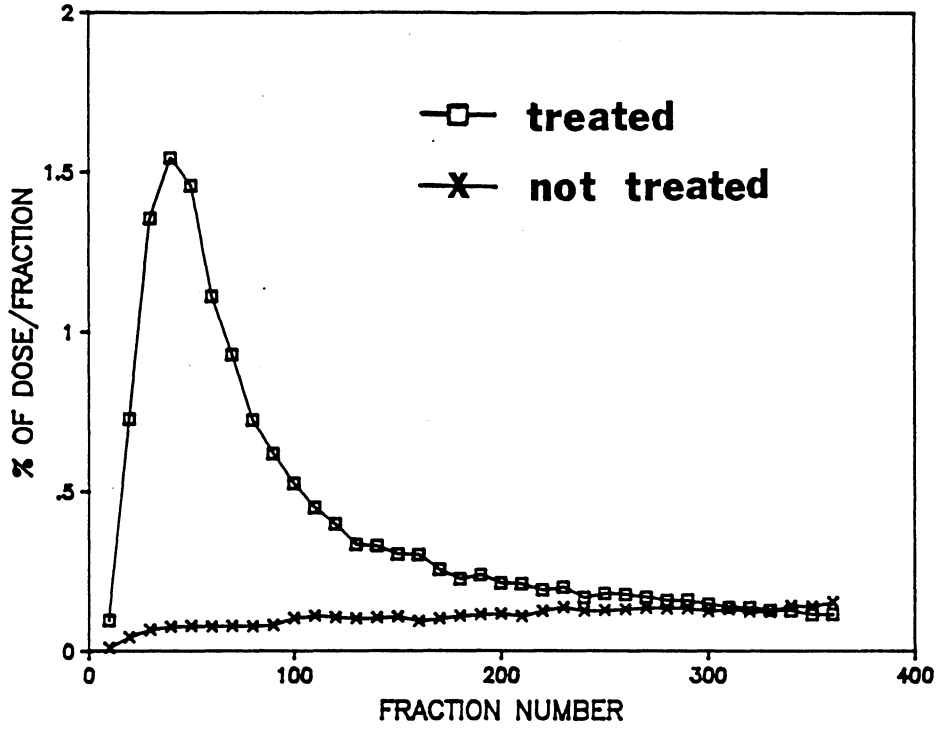
treated
not treated
% OF DOSE/FRACTION
FRACTION NUMBER
0
.5
1
1.5
2
0
100
200
300
400

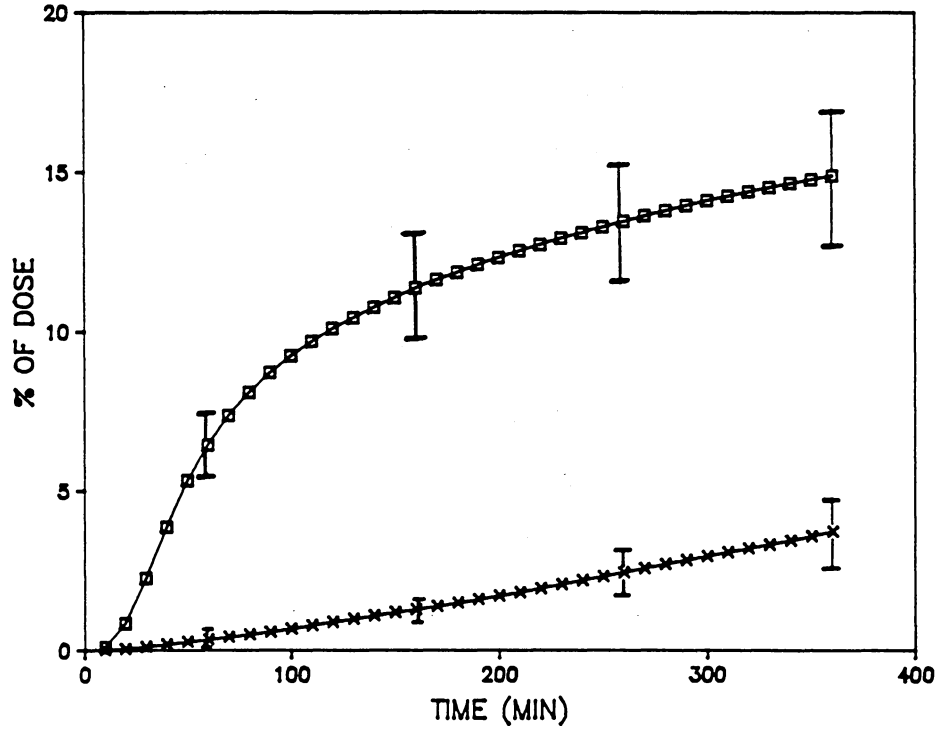
% OF DOSE
TIME (MIN)
0
5
10
15
20
0
100
200
300
400

Covalent Binding of B[a]P Metabolites to DNA, RNA, and Protein

Covalent binding of B[a]P metabolites to DNA, RNA, and protein in lung and liver 6 hrs after [^{3}H]-B[a]P administration was determined (Table 2.9.). In both lung and liver, amounts of radioactivity covalently bound decreased in the order RNA > protein > DNA, when results were expressed on the basis of mass of each macromolecule. For DNA and RNA, but not protein, binding in liver exceeded that in lung.

Analysis of DNA adducts was performed using boronate chromatography followed by HPLC. Adducts derived from metabolites which do not contain cis-vicinal hydroxyl groups elute from the boronate column in 1M morpholine. Those containing cis-vicinal hydroxyl groups elute in 1M morpholine containing 10% sorbitol. The percent of adducts containing cis-vicinal hydroxyl groups was 64% in lung and 9% in liver. Six different adducts were present in DNA isolated from lung (Figure 2.6.). The elution position of the (+)-anti-B[a]PDE:dGuo adduct is denoted by

the arrow and corresponds to peak IV. Fewer adducts were formed in liver, though it is apparent that the (+)-anti-B[a]PDE:dGuo was present (Figure 2.7.). Peaks I, II, III, V, Va, and VI are unidentified due to a lack of standards. Amounts of each of the adducts are given in Table 2.10.

Table 2.9.

Covalent binding
of [^{3}H]-B[a]P to DNA, RNA,
and protein in lung and liver of rats

[^{3}H]-B[a]P (1 mCi/animal) was administered by intratracheal instillation through a tracheal cannula and amounts of radioactivity bound to DNA, RNA, and protein were determined as described in "Materials and Methods". The results are expressed as fmoles B[a]P/mg macromolecule (mean ± S.E., for 3 animals per determination except for DNA data which represents the mean of 4-5 animals).

	Specific activity (fmole/mg)		
Tissue	Protein	RNA	DNA
lung	243 ± 9.28	2663 ± 668	13.3 ± 0.73
liver	120 ± 19.4	11429 ± 2740	32.7 ± 8.3

Figure 2.6. HPLC profile of B[a]P:deoxyribonucleoside adducts isolated from rat lungs. [^{3}H]-B[a]P (1 mCi/animal) was administered to rats by injection through a tracheal cannula. After 6 hr, DNA was isolated and hydrolyzed. B[a]P:deoxyribonucleosides were subjected to boronate chromatography followed by HPLC as described in "Materials and Methods". The upper half (A) of the figure is the HPLC profile of adducts which were eluted from the boronate column in 1M morpholine, and the lower half (B) is that for adducts eluted in 1M morpholine/10% sorbitol. The arrow indicates the elution position of [^{14}C]-(+)-anti-B[a]PDE:dGuo adduct marker.

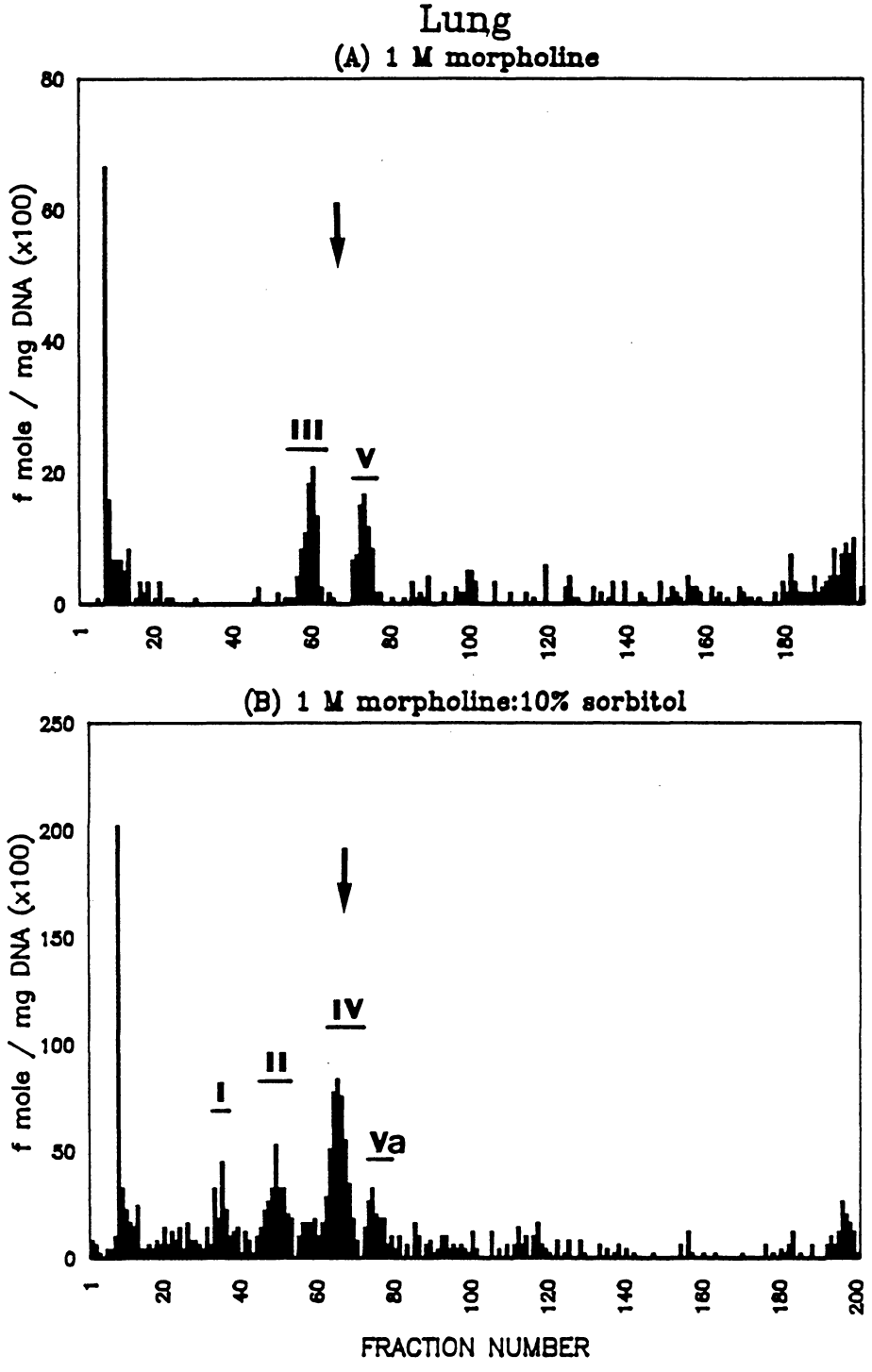
Lung
(A) 1 M morpholine
f mole / mg DNA (x100)
80
60
40
20
0
III
V
1
20
40
60
80
100
120
140
160
180
(B) 1 M morpholine:10% sorbitol
f mole / mg DNA (x100)
250
200
150
100
50
0
IV
II
I
Va
1
20
40
60
80
100
120
140
160
180
200
FRACTION NUMBER

Figure 2.7. HPLC profile of B[a]P:deoxyribonucleoside adducts isolated from rat liver. [^{3}H]-B[a]P (1 mCi/animal) was administered to rats by injection through a tracheal cannula. After 6 hr, DNA was isolated and hydrolyzed. B[a]P:deoxyribonucleosides were subjected to boronate chromatography followed by HPLC as described in "Materials and Methods". The upper half (A) of the figure is the HPLC profile of adducts which were eluted from the boronate column in 1M morpholine, and the lower half (B) is that for adducts eluted in 1M morpholine/10% sorbitol. The arrow indicates the elution position of [^{14}C]-(+)-anti-B[a]PDE:dGuo adduct marker.

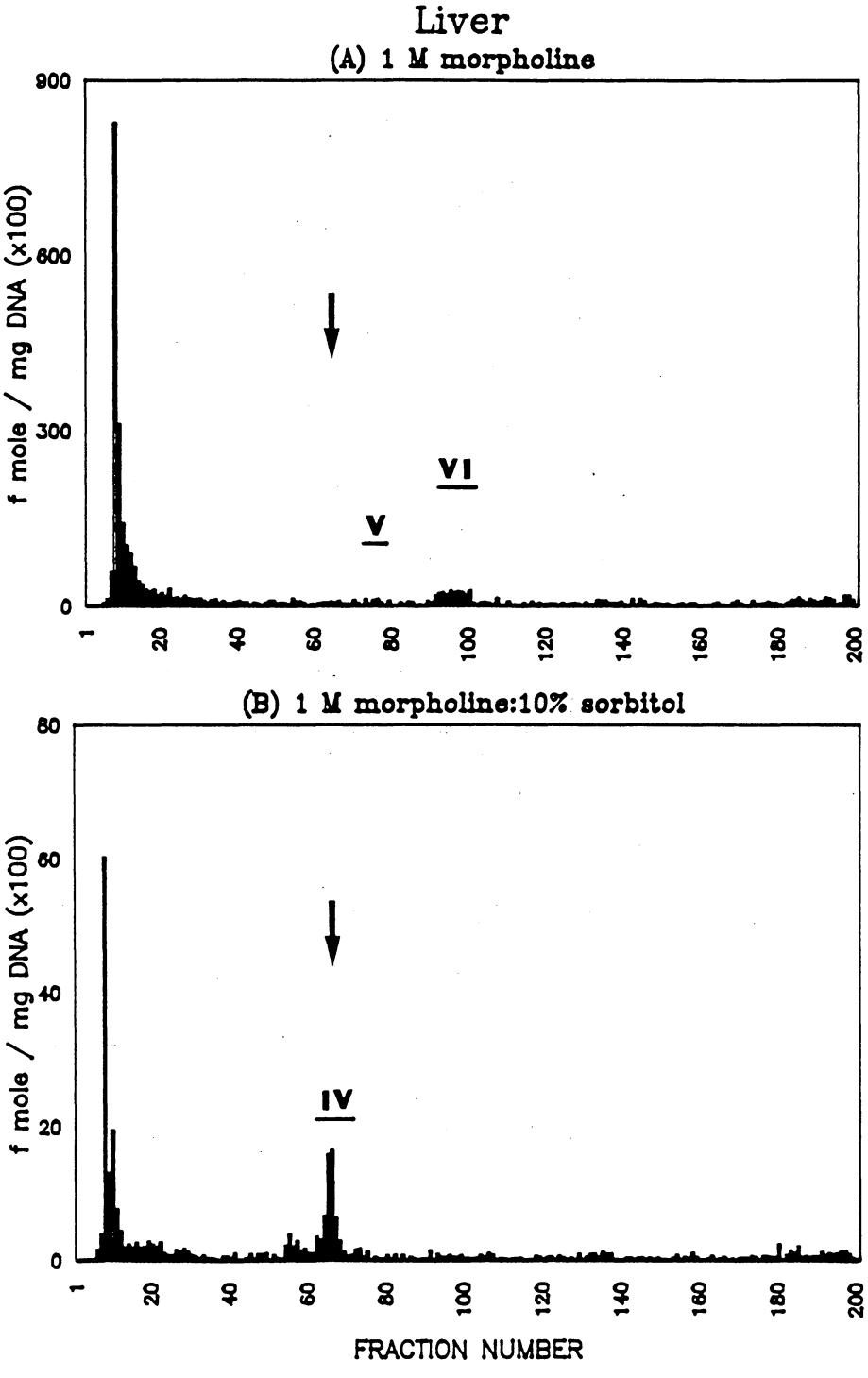
Liver
(A) 1 M morpholine
900
600
300
0
f mole / mg DNA (x100)
VI
V
1
20
40
60
80
100
120
140
160
180
200
(B) 1 M morpholine:10% sorbitol
80
60
40
20
0
f mole / mg DNA (x100)
IV
1
20
40
60
80
100
120
140
160
180
200
FRACTION NUMBER

Table 2.10

In vivo formation of B[a]P:DNA adducts in lung and liver of rats

[^{3}H]-B[a]P (1 mCi/animal) was administered to rats by injection through a tracheal cannula. The DNA was isolated and hydrolyzed, and the B[a]P:deoxyribonucleosides were subjected to boronate chromatography followed by HPLC as described in "Materials and Methods". Line (A) represents B[a]P:deoxyribonucleoside adducts separated by HPLC which had been eluted from the boronate column in 1 M morpholine fractions; line (B) represents those adducts separated by HPLC which had been eluted from the boronate column in 1 M morpholine/10% sorbitol. Adduct IV corresponds to the elution position of [^{14}C]-(+)-anti-B[a]PDE:dGuo adduct marker.

		Specific activity (fmole/mg DNA)						
Organ		I[A]	II	III	IV	V	Va	VI
lung	(A)	n.d.[B]	n.d.	0.78	n.d.	0.69	n.d.	n.d.
	(B)	0.72	1.12	n.d.	1.87	n.d.	0.60	n.d.
liver	(A)	n.d.	n.d.	n.d.	n.d.	0.43	n.d.	2.46
	(B)	n.d.	n.d.	n.d.	0.57	n.d.	n.d.	n.d.

[A]Peaks I-VI are defined by the chromatograms in Figures 6 and 7.
[B]Not detectable.

Discussion

The fate of B[a]P *in vivo* after intratracheal administration was studied. Previous investigators have only partially characterized the disposition of B[a]P *in vivo*. For example, Kotin et al. (17) studied the effect of vehicle on distribution of B[a]P in rats and mice following subcutaneous, intravenous, or intratracheal administration. When triethylene glycol was used as vehicle for intratracheal instillation of [^{14}C]-B[a]P, they observed 18% of administered radioactivity in lungs, 44% in intestines, and 17% in feces 4 hrs after [^{3}H]-B[a]P administration. Amounts of radiolabel reported by Kotin et al. to be in association with intestine are much higher than we observed and may result from a less thorough washing of the intestines than we employed. Another notable difference between our results and those of Kotin et al. is in amounts of radioactivity located in carcass. Kotin and coworkers did not report any radioactivity in carcass while we observed 15-30% of administered dose in carcass between 5 and 360 min after administration.

Pylev et al. (40) studied the rate of elimination of B[a]P from lungs of hamsters after intratracheal instillation in a vehicle containing amino acids, peptides,

and Tween 80. After 3 hrs, 46% of the administered dose remained in lungs, and after 6 hrs, 23%. These values are considerably higher than we observed and may result from the much higher dose (5 mg) used by Pylev et al. Other investigators also have observed relatively slow elimination of B[a]P from hamster lungs when high (0.5-3 mg) doses of B[a]P were administered intratracheally (41,42). However, these differences in rates of elimination of B[a]P from lungs also may derive from species differences because we have observed slower elimination of B[a]P from lungs of hamsters than from lungs of rats at doses as low as 130 ng. Species differences in B[a]P metabolism are addressed in more detail in Chapter 3. Elimination of intratracheally instilled B[a]P from rat lungs in our study was similar to that of Dehnen and Verbucheln (43) who instilled a 46 ng dose of B[a]P. Medinsky and Kampcik (44) studied the pulmonary retention of B[a]P in rats as influenced by the amount instilled and obtained results comparable to those reported here.

A concern when using intratracheal instillation of a solution of B[a]P is whether or not the clearance of B[a]P from lungs is similar to that when B[a]P is inhaled, as would occur in most human exposures. Comparison of our results with those in which B[a]P was administered by

inhalation indicates similar clearance rates from lungs. For example, Mitchell (18) and Sun et al. (45) investigated the disposition of B[a]P in rats following inhalation exposures. It is difficult to make direct comparisons of their results with ours because their zero time point was 0.5 hr after termination of exposures which lasted 0.5 to 1 hr. Thus, considerable distribution of B[a]P would have occurred prior to their observations. However, it is apparent from their data that elimination of the majority of B[a]P from lungs was rapid, with considerable quantities of radiolabel becoming associated with the intestinal tract. Amounts of radiolabel in carcass or feces were not reported. Other studies have examined rates of elimination of PAH other than B[a]P from lungs of rats following inhalation exposure and found rates of elimination to be similar to that of B[a]P (46,47). In addition, Bond et al. (48) correlated partition coefficients of several PAH with their rates of lung clearance following intratracheal instillation of solutions of these PAH. A general conclusion from that study was that PAH were cleared from lungs at similar rates when administered by intratracheal instillation or inhalation.

Calculation of toxicokinetic parameters to describe disposition of B[a]P following intratracheal administration

has not previously been reported. Wiersma and Roth (49) have determined these parameters following intravenous and arterial administration of B[a]P in control and 3-methylcholanthrene-pretreated rats. These investigators did not report results from i.v. administration in control animals. However, our data from i.v. administration are comparable to those of Wiersma and Roth. Differences which exist may result from our using animals which were anesthetized during our experiments. Systemic availability of unmetabolized B[a]P following intratracheal instillation was less than that following intravenous administration. This reduction may result from differences in distribution of B[a]P when the site of administration is different and/or from metabolism of B[a]P by enzymes in lungs. In fact, Wiersma and Roth (11,49) used isolated perfused organs to demonstrate that lungs make a significant contribution to metabolism of B[a]P.

We also have presented a detailed analysis of metabolites observed in lung, liver, and intestinal contents at selected times after intratracheal administration of B[a]P. Lung was chosen for analysis of metabolites because it is the organ through which B[a]P was administered, it is a target organ for B[a]P carcinogenesis, and it is capable of metabolizing B[a]P. Liver was chosen because of its high

intrinsic capacity to metabolize B[a]P, and intestinal contents was chosen because the majority of B[a]P metabolites are excreted via this route. Profiles of metabolites were generally as would be expected. That is, amounts of aqueous-soluble metabolites relative to organic-soluble metabolites increased with time, and relative amounts of conjugates and/or polyhydroxylated metabolites in the organic phase also increased with time. Interestingly, metabolites found in greatest amounts at 5 min after B[a]P administration were quinones. We realize that the metabolites observed were not necessarily generated in the organs in which they were detected.

Extensive studies of metabolism of B[a]P in vivo have not previously been reported, though more limited analyses have been performed. For example, Mitchell (18) studied metabolism of B[a]P in rats following 0.5 hr inhalation exposures. Animals were sacrificed at 0.5, 6, and 24 hrs after termination of exposure, and amounts of organic extractable versus non-extractable and covalently bound radioactivity in lung, liver, and kidney were determined. In addition, profiles of organic extractable metabolites in lung, liver, and kidneys at the 0.5 hr time point were reported. Shifts in the ratio of organic extractable to nonextractable radioactivity were similar to ours, and

Mitchell also observed large amounts of quinones in the organic extract.

Other investigators have considered excretion of B[a]P metabolites in bile (50). Chipman et al. (51) administered B[a]P to rats intravenously and determined the rate of excretion of radiolabel in bile. In addition, these investigators partially characterized metabolites which appeared in bile. They observed that 59% of the administered dose was excreted in bile in 6 hrs with less than 3% of the dose being excreted in urine. That Chipman et al. observed a smaller fraction of the dose being excreted in 6 hrs than we did may result from the higher dose (approx. 150 μg) which they used. Their analyses of conjugated metabolites were performed somewhat differently than ours, but in general the results were similar. Boroujerdi et al. (28) administered 60 μg B[a]P to rats intravenously and observed excretion of 68% of the dose in bile in 6 hrs, a value which is very close to that obtained in our investigations. They reported slightly greater amounts of glucuronides and sulfate conjugates and slightly smaller amounts of conjugates which were resistant to β-glucuronidase and arylsulfatase than were observed in studies reported in this dissertation. Comparison of these studies with ours indicates that mode of administration

(intratracheal vs. intravenous) does not have a major effect on the excretion of B[a]P in bile.

Our results provide evidence for enterohepatic circulation of B[a]P metabolites. In 6 hrs 53% of the administered dose was excreted into intestines and intestinal contents of animals lacking a biliary cannula. In animals containing a biliary cannula, 74% of the administered dose was excreted over the same period of time (Table 2.6.). In addition, treatment of bile with ß-glucuronidase and arylsulfatase prior to intraduodenal administration increased the amount of radioactivity absorbed (Table 2.8.). Analysis of conjugates (Table 2.7.) reveals essentially no difference in amounts of sulfate conjugates excreted from animals with and without biliary cannulas. However, lower percentages of total dose were excreted as glucuronide and thio-ether conjugates in intestinal contents of animals without a biliary cannula than in bile of animals with a biliary cannula. Many investigators have reported the presence of ß-glucuronidase in intestinal microflora which can cleave glucuronic acid from glucuronides of B[a]P metabolites (52,53). Evidence also exists for the presence of cysteine conjugate ß-lyase activity in intestinal microflora (54,55). A recent study by Elmhirst et al. (56) reported that glutathione and

glucuronic acid conjugates of B[a]P-4,5-epoxide both undergo enterohepatic circulation. In the case of glucuronides, hydrolysis in intestines forming the B[a]P-4,5-diol aglycone occurs prior to enterohepatic circulation. Absorption of glutathione conjugates from intestines is much slower than glucuronides and hydrolysis may not be a prerequisite for enterohepatic circulation of glutathione conjugates.

A recent study by Morse et al. (20) investigated the effect of route of administration and strain differences on B[a]P disposition and macromolecular binding in Sencar and BALB/c mice. Binding was examined in skin, liver, lung, and stomach at 6 and 48 hrs after oral or topical administration of B[a]P. A direct comparison of our results to those of Morse et al. is not possible since we used a dose of 5 μg kg^{-1} and they used 50 mg kg^{-1}. However, a qualitative comparison can be made. At 6 hrs after oral administration, the extent of binding in liver and lung was RNA > protein > DNA. In addition, the amount bound to RNA and protein was 2-3 times greater in liver than lung which is comparable to what we observed.

B[a]P macromolecular binding *in vivo* is different from that observed using *in vitro* systems. Kuroki et al. (22) using cultured embryonic cells reported highest amounts of *B[a]P metabolite binding to protein while Foth et al. (21)*

using isolated perfused lung reported that RNA and protein were similar in the amount of covalently bound B[a]P.

B[a]P:DNA adducts have been identified *in vivo* (26,27,28) and *in vitro* (20,21,22). In our studies 6, adduct peaks were detected in lung with 14% (1.87 fmole mg^{-1}) of the total DNA binding in lung being detected as the (+)-anti-B[a]PDE:dGuo adduct. Three adduct peaks were detected in liver with only 2% (0.57 fmole mg^{-1}) of total binding being detected as the (+)-anti-B[a]PDE:dGuo adduct. In lung and liver 64% (8.5 fmole mg^{-1}) and 89% (29.1 fmole mg^{-1}) of radioactivity bound to DNA eluted in the breakthrough peak during HPLC analysis, respectively. This material may represent modified DNA which was not hydrolysed to nucleosides. The formation of more B[a]P:DNA adducts in lung than in liver has been previously observed. Boroujerdi et al. (28) using rats observed 4 adduct peaks in lung and 1 adduct peak in liver 1 hr following an i.v. administration of B[a]P. A direct comparison of all adducts detected in our study to those observed by Boroujerdi et al. is not possible because of differences in the way adducts were isolated and identified. However, they reported 2 fmole mg^{-1} of the (+)-anti-B[a]PDE:dGuo adduct in rat lung which is similar to our value.

In a more recent study, Adriaenssens et al. (57)

investigated the effect of aspirin and indomethacin on B[a]P adduct formation in lungs, liver, and forestomach of mice. In control experiments after a 60 μg B[a]P dose, 4 adduct peaks were observed in lung while only 2 were detected in liver. In addition, the amount of (+)-anti-B[a]PDE:dGuo adduct in lung was greater than the amount in liver.

References

1. International Agency for Research on Cancer. Certain polycyclic aromatic hydrocarbons and heterocyclic compounds. In: IARC Mongr. on the Evaluation of Carcinogenic Risk of Chemicals to Man, Vol. 3. Int. Agency for Cancer Research, Lyon, 1973.

2. Baum, E. J. Occurrence and surveillance of polycyclic aromatic hydrocarbons. In: H. V. Gelboin and P. O. P. Ts'o (eds.), Polycyclic Hydrocarbons and Cancer, Vol. 1. pp 45-70, New York, Academic Press Inc., 1978.

3. Pelkonen, O. and Nebert, D. W. Metabolism of polycyclic aromatic hydrocarbons: Etiological role in carcinogenesis. Pharmacol. Rev., 34:189-222, 1982.

4. Rovet, P., Alexandrov, K., Markovits, P., Frayssinet, C., and Dansette, P. M. Metabolism of benzo(a)pyrene by brain microsomes of fetal and adult rats and mice. Induction by 5,6 benzoflavone, comparison with liver and lung microsomal activity. Carcinogenesis, 2:919-926, 1981.

5. Keller, G. M. and Jefcoate, C. R. Benzo(a)pyrene activation to 7,8-dihydrodiol-9,10-oxide by rat liver microsomes. J. Biol. Chem., 259:13770-13776, 1984.

6. Gozukara, E. M., Guengerich, F. P., Miller, H., and Gelboin, H. V. Differential patterns of benzo(a)pyrene metabolism of purified cytochrome P-450 from methylcholanthrene, beta-napthoflavone and phenobarbital treated rats. Carcinogenesis, 3:129-133, 1982.

7. Cohen, G. M., and Moore, B. P. Metabolism of [^{3}H]benzo(a)pyrene by different portions of the respiratory tract. Biochem. Pharmacol., 25:1623-1629, 1976.

8. Autrup, H. Separation of water-soluble metabolites of benzo(a)pyrene formed by cultured human colon. Biochem. Pharmacol., 28:1727-1730, 1979.

9. Vahakangas, K. The distribution of benzo(a)pyrene and its metabolites in isolated perfused lung and liver. Toxicol. Letters, 4:413-418, 1979.

10. Smith, B. R., and Bend, J. R. Metabolism and excretion of benzo(a)pyrene 4,5-oxide by the isolated perfused rat liver. Cancer Res., 39:2051-2056, 1979.

11. Wiersma, D. A., and Roth, R. A. Clearance of benzo(a)pyrene by isolated rat liver and lung: Alterations in perfusion and metabolic capacity. J. Pharmacol. Exper. Therap., 225:121-125, 1983.

12. Schlede, E., Kuntzman, R., Haber, S., and Conney, A. H. Effect of enzyme induction on the metabolism and tissue distribution of benzo(a)pyrene. Cancer Res., 30:2893-2897, 1970.

13. Reeve, W. E., and Gallagher, C. H. Metabolism of [^{14}C]benzo(a)pyrene in vivo in the rat. Cancer Letters, 13:79-86, 1981.

14. Wiersma, D. A., and Roth, R. A. Total body clearance of circulating benzo(a)pyrene in conscious rats: Effect of pretreatment with 3-methylcholanthrene and the role of liver and lung. J. Pharmacol. Exper. Therap., 226:661-667, 1983.

15. Chang, L. H. The fecal excretion of polycyclic hydrocarbons following their administration to the rat. J. Biol. Chem., 151:93-99, 1943.

16. Ho, W. Distribution and turnover of benzo(a)pyrene instilled into mouse lungs. Proc. West. Pharmacol. Soc., 18:302-305, 1975.

17. Kotin, P., Falk, H. L., and Busser, R. Distribution, retention, and elimination of ^{14}C-3,4-benzo(a)pyrene after administration to mice and rats. J. Nat. Cancer Inst., 23:541-555, 1959.

18. Mitchell, C. E. Distribution and retention of benzo(a)pyrene in rats after inhalation. Toxicol. Letters, 11:35-42, 1982.

19. Mitchell, C. E. The metabolic fate of benzo(a)pyrene in rats after inhalation. Toxicology, 28:65-73, 1983.

20. Morse, M., and Carlson, G. P. Distribution and macromolecular binding of benzo(a)pyrene in sencar and BALB/c mice following topical and oral administration. J. Toxicol. Environ. Hlth., 16:263-276, 1985.

21. Foth, H., Molliere, M., Kahl, R., Jahnchen, E., and Kahl, G. F. Covalent binding of benzo(a)pyrene in perfused rat lung following systemic and intratracheal administration. Drug Metab. Disp., 12:760-766, 1984.

22. Kuroki, T., and Heidelberger, C. The binding of polycyclic aromatic hydrocarbons to the DNA, RNA, and proteins of transformable cells in culture. Cancer Res., 31:2168-2176, 1971.

23. Kahl, G. F., Klaus, E., Legraverend, G., Nebert, D. W., and Pelkonen, O. Formation of benzo(a)pyrene metabolite-nucleoside adducts in isolated perfused rat and mouse liver and in mouse lung slices. Biochem. Pharmacol., 28:1051-1056, 1979.

24. Smolarek, T. A. and Baird, W. M. Benzo(e)pyrene-induced alterations in the binding of benzo(a)pyrene to DNA in hamster embryo cell cultures. Carcinogenesis, 5:1065-1069, 1984.

25. DiGiovanni, J., Sina, J. F., Ashust, S. W., Singer, J. M., and Diamond L. Benzo(a)pyrene and 7,12-dimethylbenz(a)anthracene metabolism and DNA adduct formation in primary cultures of hamster epidermal cells. Cancer Res., 43:163-170, 1983.

26. Eastman, A., Sweetenham, J., and Bresnick, E. Comparison of in vivo and in vitro binding of polycyclic hydrocarbons to DNA. Chem.-Biol. Interact., 23:345-353, 1978.

27. Nakayama, J., Yuspa, S. H., and Poirier, M. C. Benzo(a)pyrene-DNA adduct formation and removal in mouse epidermis in vivo and in vitro: Relationship of DNA binding to initiation of skin carcinogenesis. Cancer Res., 44:4087-4095, 1984.

28. Boroujerdi, M. Kung, H. C., Wilson, A. E. G., and Anderson, M. W. Metabolism and DNA binding of benzo(a)pyrene in vivo in the rat. Cancer Res., 41:951-957, 1981.

29. Van Cantfort, J., DeGraeve, J., and Gielen, J. E. Radioactive assay for aryl hydrocarbon hydroxylase. Improved method and biological importance. Biochem. Biophys. Res. Commun., 79:505-512, 1977.

30. Shanker, L. S. Drug absorptiom from the lung. Biochem. Pharmacol., 27:381-385, 1978.

31. Selkirk, J. K. High-pressure liquid chromatography: A new technique for studying metabolism and activation of chemical carcinogens. In: H. F. Kraybill, and M. A. Mehlman (eds.), Advances in Modern Toxicology. Environmental Cancer, Vol. 3, pp 1-25, New York, Hemisphere Publ., 1976.

32. MacLeod, M. C., Moore, C. J., and Selkirk, J. K. Analysis of water soluble conjugates produced by hamster embryo cells exposed to polynuclear aromatic hydrocarbons. In: B. Bjorseth and A. J. Dennis (eds.), Polynuclear Aromatic Hydrocarbons: Chemistry and Biological Effects, pp 9-23, Columbus, Battelle Press, 1979.

33. SAAM User's Guide. DHEW Publication No. (NIH) 78-180, 1978.

34. Wagner, J. G. Linear pharmacokinetic equations allowing direct calculation of many needed pharmacokinetic parameters from the coefficients and exponents of polyexponential equations which have been fitted to the data. J. Pharmacokin. Biopharm., 4:443-467, 1976.

35. Diamond, L., Defendi, V., and Brookes, P. The interaction of 7,12-dimethylbenz(a)anthracene with cells sensitive and resistant to toxicity induced by this carcinogen. Cancer Res., 27:890-897, 1967.

36. Labarca, C., and Paigen, K. A simple, rapid, and sensitive DNA assay procedure. Anal. Biochem., 102:344-352, 1980.

37. Ceriotti, G. Determination of nucleic acids in animal tissues. J. Biol. Chem., 214:59-70, 1955.

38. Lowry, O. H., Rosebrough, N. J., Farr, A. L., and Randall, R. J. Protein measurement with folin reagent. J. Biol. Chem., 193:265-271, 1951.

39. Baird, W. M., and Brookes, P. Isolation of the hydrocarbon-deoxyribonucleoside products from the DNA of mouse embryo cells treated in culture with 7-methylbenz(a)anthracene-^{3}H. Cancer Res., 33:2378-2385, 1973.

40. Pylev, L. N., Roe, J. C., and Warwick, G. P. Elimination of radioactivity after intratracheal instillation of tritiated 3,4-benzopyrene in hamster. Br. J. Cancer, 23:103-115, 1969.

41. Pelfrene, A. F. Experimental evaluation of the clearance of 3,4-benzo(a)pyrene in association with talc from hamster lungs. Am. Ind. Hyg. Assoc. J., 37:706-710, 1976.

42. Feron, V. J., Van Den Hevvel, P. D., Koeter, H. B. W. M., and Beems, R. B. Significance of particle size of benzo(a)pyrene for the induction of respiratory tract tumors in hamsters. Int. J. Cancer, 25:301-307, 1980.

43. Dehnen, W., and Verbucheln, J. Studies on the induction of extracts from airborne particulates of benzo(a)pyrene hydroxylase and the binding of benzo(a)pyrene to DNA in rat lung in vivo after pertracheal administration. Zbl. Bakt. Hyg., I. Abt. Orig., 13:260-273, 1981.

44. Medinsky, M. A., and Kampcik, S. J. Pulmonary retention of [^{14}C]benzo(a)pyrene in rats as influenced by the amount instilled. Toxicology, 35:327-336, 1985.

45. Sun, J. O., Wolff, R. K., Kanapily, G. M., and McClellan, R. O. Lung retention and metabolic fate of inhaled benzo(a)pyrene associated with diesel exhaust particles. Toxicol. Appl. Pharmacol., 73:48-59, 1984.

46. Sun, J. D., Wolff, R. K., Aberman, H. M., and McClellan, R. O. Inhalation of 1-nitropyrene associated with ultrafine insoluble particles or as a pure aerosol: A comparison of deposition and biological fate. Toxicol. Appl. Pharmacol., 69:185-198, 1983.

47. Mitchell, C. E., Henderson, R. F., and McClellan, R. O. Distribution, retention, and fate of 2-aminoanthracene in rats after inhalation. Toxicol. Appl. Pharmacol., 75:52-59, 1984.

48. Bond, J. A., Baker, S. M., and Bechtold, W. E. Correlation of the octanol/water partition coefficient with clearance halftimes of intratracheally instilled aromatic hydrocarbons in rats. Toxicology, 36:285-295, 1985.

49. Wiersma, D. A., and Roth, R. A. The prediction of benzo[a]pyrene clearance by rat liver and lung from enzyme kinetic data. Mol. Pharmacol., 24:300-308, 1983.

50. Kari, F. W., Kauffman, F. C., and Thurman, R. G. Effect of bile salts on rates of formation, accumulation, and export of mutagenic metabolites from benzo(a)pyrene produced by the perfused rat liver. Cancer Res., 45:1621-1627, 1985.

51. Chipman, J. K., Hirom, P. C., Frost, G. S., and Millburn, P. The biliary excretion and enterohepatic circulation of benzo(a)pyrene and its metabolites in the rat. Biochem. Pharmacol., 30:937-944, 1981.

52. Dutton, G. J. Metabolic pathways immediately preceding and succeeding glucuronidation-anabolic pathways. In: G. J. Dutton (ed.), Glucuronidation of Drugs and Other Compounds. pp. 83-96, Boca Raton, FL., CRC Press Inc., 1980.

53. Levy, G. A., and Conchie, J. Beta-glucuronidase and the hydrolysis of glucuronides. In: G. J. Dutton (ed.), Glucuronic Acid Free and Combined, pp. 301-357, New York and London, Academic Press Inc., 1966.

54. Suzuki, S., Tomisawa, H., Ichihara, S., Fukazawa, H., and Tateishi, M. A C-S bond cleavage enzyme of cysteine conjugates in intestinal microorganisms. Biochem. Pharmacol., 31:2137-2140, 1982.

55. Tomisawa, H., Suzuki, S., Ichihara, S., Fukazawa, H., and Tateishi, M. Purification and characterization of C-S lyase from fusobacterium varium. J. Biol. Chem., 259:2588-2593, 1984.

56. Elmhirst, T. R. D., Chipman, J. K., Ribeiro, O., Hirom, P. C., and Millburn, P. Metabolism and enterohepatic circulation of benzo(a)pyrene-4,5-epoxide in the rat. Xenobiotica, 15:899-906, 1985.

57. Adriaenssens, P. I., Sivarajah, K., Boorman, G. A., Eling, T. E., and Anderson, M. W. Effect of aspirin and indomethacin on the formation of benzo(a)pyrene-induced pulmonary adenomas and DNA Adducts in A/HeJ mice. Cancer Res., 43:4762-4767, 1983.

Chapter 3

Species Differences in Biliary Excretion of Benzo[a]pyrene

Introduction

Susceptibility of different animal species to chemical carcinogenesis is known to vary widely. For example, benzo[a]pyrene (B[a]P) is a more potent inducer of lung tumors in hamsters than in various strains of rats and mice (1). On the other hand, 2-naphthylamine is a potent carcinogen in mice and hamsters but less potent in most strains of rats (2,3). Interspecies differences in responsiveness to chemical carcinogens may result from qualitative and quantitative differences in absorption, distribution, metabolism, and excretion of carcinogens. Studies investigating carcinogen disposition and metabolism among several species should help to elucidate interspecies differences in molecular events leading to chemical carcinogenesis.

Differences in absorption and tissue disposition of drugs and xenobiotics have been demonstrated among species (4,5). Schanker et al. (6) reported species differences in

the absorption of lipid soluble and lipid insoluble drugs following intratracheal and inhalation exposures. Studies have also investigated tissue disposition of B[a]P under different experimental conditions in a variety of species including mice (7), rats (8,9), hamsters (10), chickens (11) and dogs (7).

Interspecies comparisons of cytochrome P-450 dependent monooxygenase systems and/or conjugation systems have been reported using microsomes (12,13,14,15) and cell culture (16,17). Gregus et al. (18) compared oxidation and conjugation systems in avian and aquatic species to other species more commonly used in the laboratory such as mouse, rat, hamster, and guinea pig. Enzyme activities were quantitatively different among species for several substrates examined. However, a study by Ioannides et al. (19) compared B[a]P metabolism in rat, hamster, and guinea pig microsomes and found that each was similar in the formation of mutagenic metabolites.

Species comparisons in B[a]P covalent binding to DNA have also been reported primarily in cell culture systems (20,21) and to a lesser extent in vivo (21). Sebti et al. (22) noted variations in the types of B[a]P:DNA adducts formed in early-passage embryo cells from mice, rats, and hamsters.

Early studies established that B[a]P is excreted primarily via the feces (23,24). More recent studies have investigated B[a]P biliary excretion to characterize excretion in more detail (25,26,27). These studies have examined the effect of pretreatment with modifiers of metabolism along with effect of dose administered. However, in these studies, only a single species, in most cases the Sprague-Dawley rat, was used.

The purpose of this study was to characterize tissue disposition and biliary excretion of B[a]P and/or its metabolites in several species. The animals used were Sprague-Dawley rats, Gunn rats, Syrian hamsters, and Dunkin-Hartley guinea pigs. These animals were selected because of their common use in the laboratory and/or unique metabolism characteristics which have been well documented (28,29,30). That is, Gunn rats were chosen because of their inability to conjugate bilirubin to glucuronic acid for subsequent excretion (31). Guinea pigs were chosen because of their low activity in N-acetylation of cysteine conjugates and hamsters were chosen because of their common use in carcinogenesis studies and particular susceptibility to lung tumorigenesis by B[a]P (32,33). Finally, Sprague-Dawley rats were chosen because of their extensive use in drug and xenobiotic metabolism studies.

In this study we have investigated biliary excretion of radioactivity following intratracheal administration of [^{3}H]-B[a]P. Effect of dose on excretion was examined by administering several concentrations of B[a]P to Sprague-Dawley rats and two very different concentrations to Gunn rats, hamsters, and guinea pigs. In addition the types of conjugates of B[a]P metabolites excreted in bile were characterized and disposition of radioactivity in organs determined in each species. We also investigated the effect of glutathione depletion on biliary excretion of B[a]P.

Materials and Methods

Chemicals

[G-^{3}H]-B[a]P (specific activity of 50.5 Curies/mmole) was obtained from Amersham Corp. (Arlington Heights, Ill.) and was purified before use by silica gel chromatography with hexane as the eluent. Unlabeled B[a]P and DL-buthionine-(S,R)-sulfoximine were purchased from Sigma (Sigma Chemical Co., St. Louis, Mo.).

Animal Treatment

Sprague-Dawley rats (SD rat, 200-250g), Gunn rats (200-250g), Syrian Golden hamsters (100-140g), and Dunkin-Hartley guinea pigs (600-850g) were used. Male animals were used exclusively. Animals were housed in a room with 12-hour light-dark cycles and allowed water and food ad libitum. Animals were fasted for 24 hours before each experiment.

Animals were anesthetized with sodium pentobarbital (rat and hamster: 60 mg kg^{-1}, guinea pig: 40 mg kg^{-1}) and anesthesia was maintained by further administration of

pentobarbital as required. Tracheas were cannulated with polyethylene tubing (PE240) according to the method of Shanker (34). Modifications in the length of the cannula were made to accommodate different sizes of species.

In experiments in which bile was collected from rats, bile ducts were cannulated with polyethylene tubing (PE 10). In experiments in which bile was collected from hamsters and guinea pigs, a method different than that used for rats was developed since these animals have a gall bladder. Through an abdominal midline incision, the common bile duct was ligated and the gall bladder exposed. The gall bladder was drained through a small incision made in the wall of the bladder and a section of polyethylene tubing (PE 10 for hamsters and PE 90 for guinea pigs) was inserted into the bladder. Subsequently, the gall bladder was ligated several times along the length of the inserted tubing. The cannula was secured to abdominal muscle by several ligations when suturing the midline incision. The void volume between the liver and PE tubing was minimal and bile flow was continuous throughout the experiments. Body temperatures were monitored and maintained at 37-38°C and saline equal to the amount of bile excreted was administered hourly by subcutaneous injection. Before [^{3}H]-B[a]P administration, bile flow was monitored for 30 min to confirm that bile

flow was continuous.

[^{3}H]-B[a]P was dissolved in triethylene glycol and administered at the bronchial bifurcation by injection through the tracheal cannula. Concentrations of [^{3}H]-B[a]P instilled are listed in the text. Animals were maintained on a steep incline for 5-10 min following administration of B[a]P. After instillation, bile was collected at 5 or 10 min intervals over a 6 hr time period.

Total Tissue Radioactivity

Six hrs after [^{3}H]-B[a]P administration, animals were sacrificed by decapitation and organs quickly removed, weighed, and placed on ice. Organs were homogenized in water using a Tekmar tissuemizer at high speed. Carcasses were digested at 50°C in 1.5N NaOH and the digest was stirred vigorously prior to sampling. Duplicate samples of tissue homogenate (0.5 ml) were solubilized in 1.0 ml NCS Solubilizer (Amersham Corp.) by digestion at 45°C for 2 hrs. After solubilization, samples were neutralized with acetic acid, and 15 ml of Ready Solv EP (Beckman) scintillation fluid was added and samples counted. Radioactivity in urine and bile was measured directly, without solubilization, by

liquid scintillation counting. Quench was corrected by the external standardization method and efficiencies ranged from 20-43 percent. Recoveries of radioactivity were 83-100 percent. Data were normalized to recovered doses for all experiments.

Buthionine Sulfoximine Treatment

Buthionine sulfoximine (BSO) was dissolved in distilled water and administered by i.p. injection (8 mmoles kg^{-1} body wt.) to two rats between 0700 and 0830 (35). At the time of BSO treatment glutathione levels in lung and liver of a third animal were determined to estimate control glutathione levels. The method of Brehe et al. (36) was used to quantitate glutathione. One to two hrs after BSO treatment, the two animals were anesthetized and tracheas and bile ducts cannulated as described in a previous section. Two and one-half hours after BSO treatment, [^{3}H]-B[a]P (0.5 μg kg^{-1} body wt.) was administered to one of the BSO-treated rats by injection through the tracheal cannula. At the time of [^{3}H]-B[a]P administration glutathione levels in lung and liver of the other BSO-treated rat were determined to estimate glutathione levels at the time of B[a]P administration. Immediately after B[a]P instillation, bile

was collected at 10 min intervals over 6 hr. After 6 hrs, BSO-treated animals receiving [^{3}H]-B[a]P were sacrificed and glutathione levels in lung and liver were determined. [^{3}H]-radioactivity in tissue and bile was determined as described in the previous section.

Analysis of B[a]P Metabolites

B[a]P metabolites in cumulative 6 hr bile samples were identified using the method of MacLeod et al. (37) as described in Chapter 2.

Statistical Analysis

Data were compared using the SAS System (SAS Institute, Inc., Cary, NC). The General Linear Model (GLM) procedure for analysis of variance was performed, with means being compared by Duncan's multiple range test.

Results

Effect of Dose on Biliary Excretion of B[a]P in Sprague-Dawley Rats

The effect of B[a]P dose (6 ng to 380 μg) on biliary excretion of B[a]P and/or its metabolites was investigated in SD rats (Figure 3.1.). When B[a]P doses in the range of 6 ng to 5 μg were intratracheally instilled, little variation in the rate of biliary excretion was detected, with 70% of the dose being excreted in bile within 6 hrs. At doses of B[a]P ranging from 44 to 140 ug, the rate of excretion generally declined as the dose increased. At doses in excess of 240 μg, rates of excretion of radioactivity were similar, with only 54% of the dose being excreted in 6 hrs.

Species Variation in B[a]P Biliary Excretion

Biliary excretion of B[a]P was investigated in Gunn rats, hamsters and guinea pigs at two concentrations of B[a]P. The low concentration (0.16 μg) was well below that

Figure 3.1. Effect of B[a]P dose on biliary excretion of [^{3}H]-radioactivity in Sprague-Dawley rats. [^{3}H]-B[a]P over 6 ng to 380 μg range was administered to rats by intratracheal instillation and the amount of [^{3}H]-radioactivity in bile determined over a 6 hr time period. The rate of excretion (% dose/fraction) for 2 doses is depicted in the upper part of the Fig. Cumulative excretion is shown in the lower part of the Fig. Each value represents the percent of dose, mean ± S.E., for 7, 5 and 4 rats for 6 ng-5 μg, 44-140 μg and 240-380 μg B[a]P, respectively.

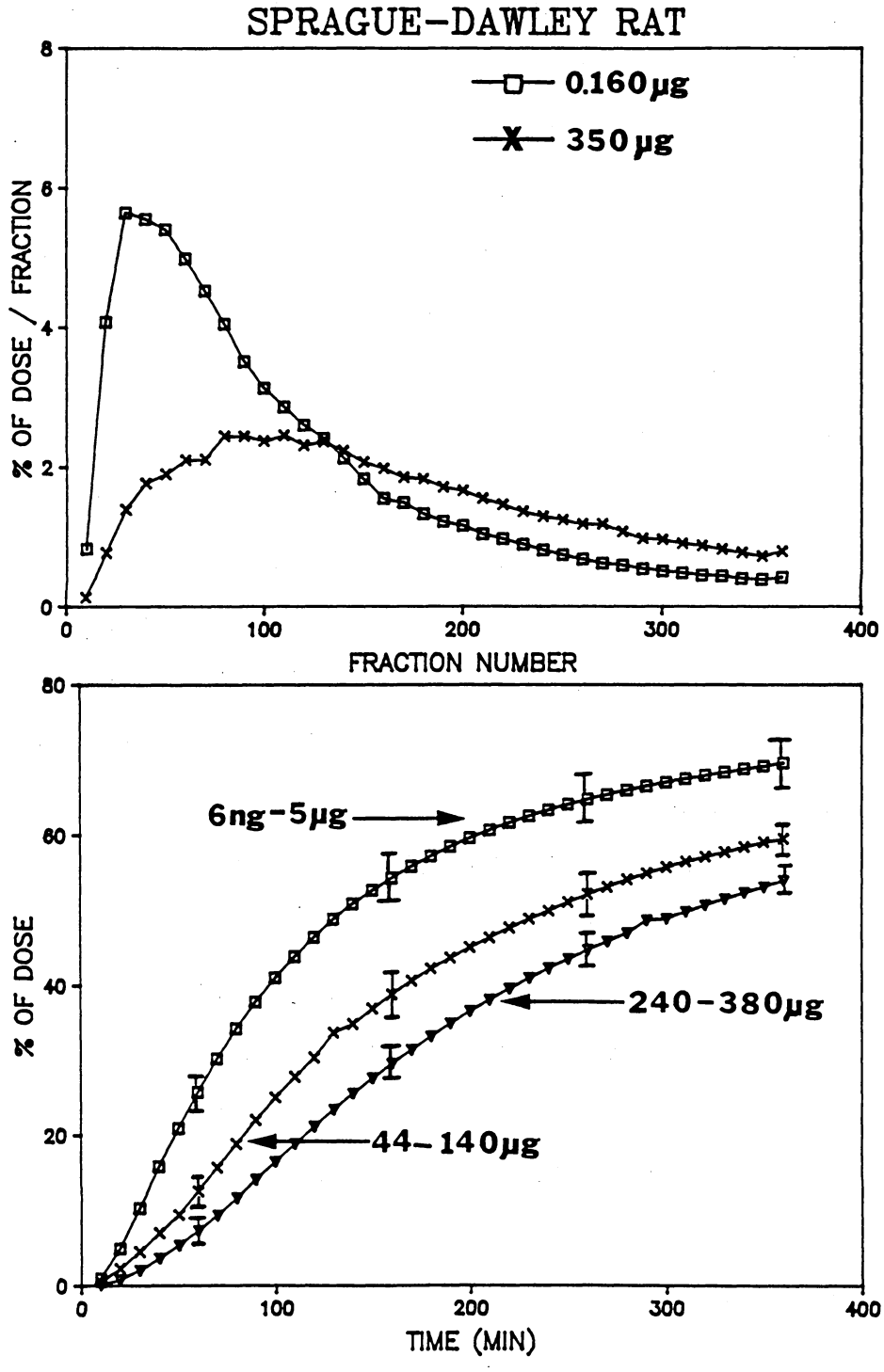
SPRAGUE-DAWLEY RAT
0.160µg
350µg
% OF DOSE / FRACTION
FRACTION NUMBER
6ng-5µg
240-380µg
44-140µg
% OF DOSE
TIME (MIN)

at which metabolic processes appeared to be saturated in Sprague-Dawley rats, and the high concentration (350 μg), well above. Excretion profiles for Gunn rats and guinea pigs were qualitatively similar to those determined for SD rats (Figures 3.2. and 3.3.). A 0.16 μg dose was excreted faster (% of dose/fraction) and to a greater extent (% of dose/time) than a 350 μg dose. However, quantitative differences among species in the total percent excreted were observed. At the low dose, 62% was excreted from guinea pigs in 6 hrs and 60%, from Gunn rats, which is significantly less ($p<0.05$) than that excreted from SD rats. At the higher dose guinea pigs excreted 48% in 6 hrs while Gunn rats excreted only 31% of the dose into bile.

Biliary excretion of B[a]P in hamsters was distinctly different than that observed in the other species examined (Figure 3.4.). Amounts of radioactivity excreted at both low and high doses were similar. Although the amount excreted from hamsters in 6 hr after administration of a high dose (53%) was similar to that excreted from SD rats and guinea pigs, the amount excreted from hamsters following administration of a low dose of B[a]P was significantly lower ($p<0.05$) than that excreted from SD rats.

In all species examined the rate of excretion of radioactivity was maximum at 20-30 min after a 0.16 μg B[a]P

dose. Similar profiles were detected in hamsters and guinea pigs following a 360 μg B[a]P dose. However, in SD rats and Gunn rats the amount of radioactivity in bile fractions was much lower with a maximum being reached 100 min after a 360 μg B[a]P dose.

Figure 3.2. Effect of dose of B[a]P on biliary excretion of [^{3}H]-radioactivity in Gunn rats. [^{3}H]-B[a]P in amounts of either 0.16 μg or 350 μg was administered to rats by intratracheal instillation and the amount of [^{3}H]-radioactivity in bile was determined over a 6 hr time period. The rate of excretion (% dose/fraction) is shown in the upper part of the Fig. and cumulative excretion, in the lower part. Each value represents the percent of dose, mean ± S.E., for 3 rats.

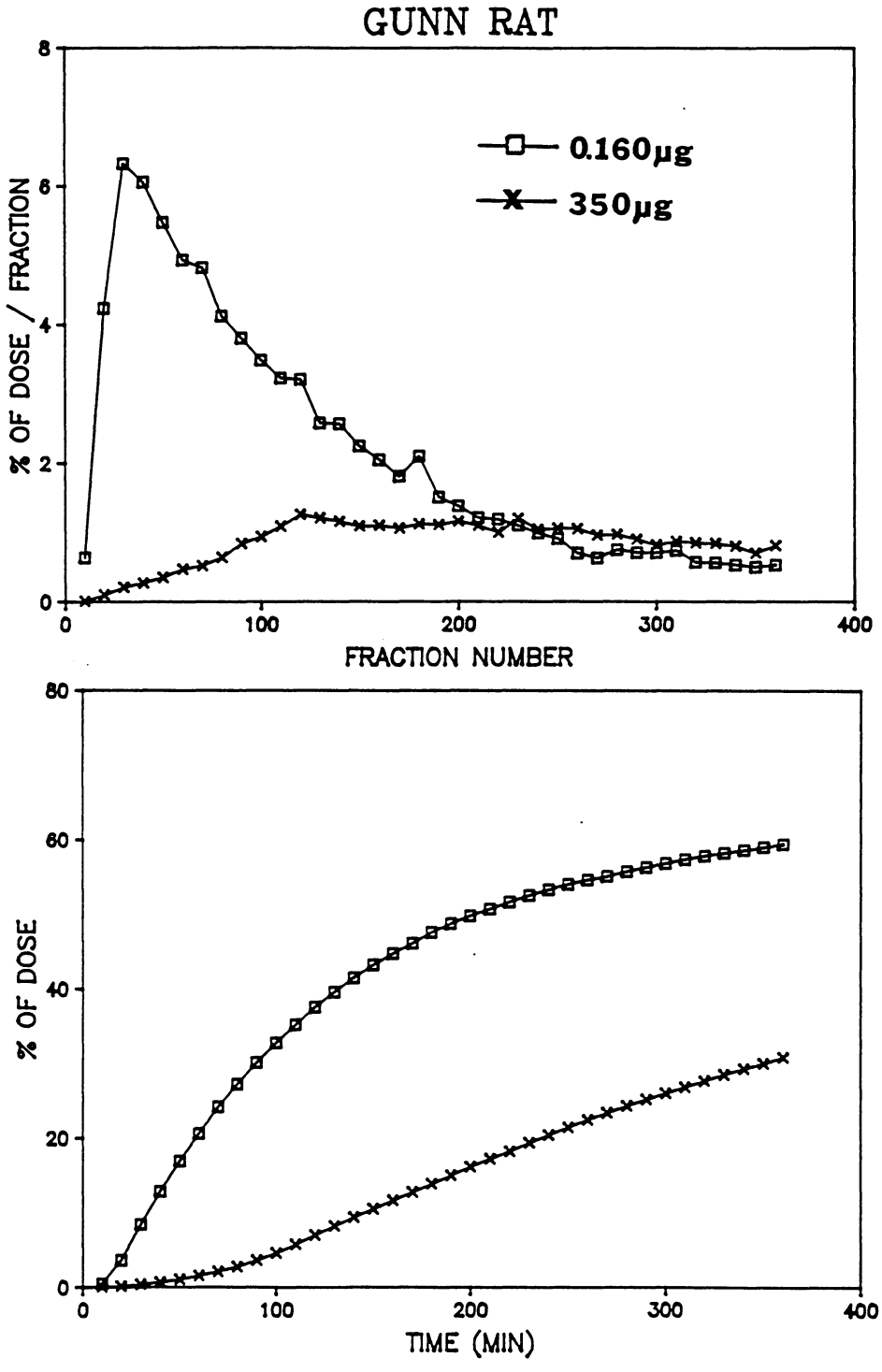
GUNN RAT
0.160µg
350µg
% OF DOSE / FRACTION
FRACTION NUMBER
% OF DOSE
TIME (MIN)

Figure 3.3. Effect of dose of B[a]P on biliary excretion of [^{3}H]-radioactivity in Dunkin-Hartley guinea pigs. [^{3}H]-B[a]P in amounts of 0.16 μg or 350 μg was administered by intratracheal instillation and the amount of [^{3}H]-radioactivity in bile determined over a 6 hr time period. The rate of excretion (% dose/fraction) is shown in the upper part of the Fig. and cumulative excretion, in the lower part. Each value represents the percent of dose, mean ± S.E., for 3 guinea pigs.

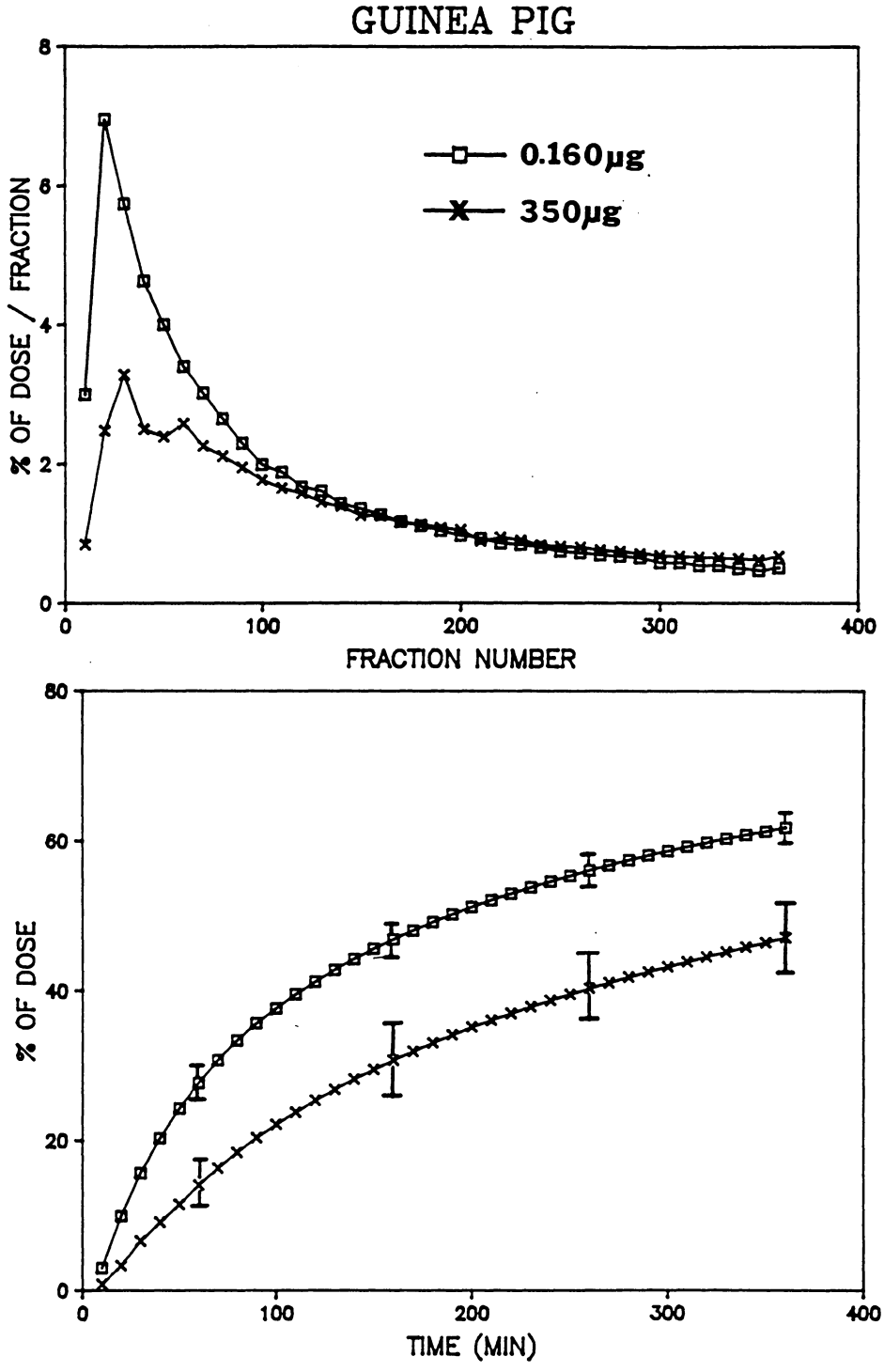
GUINEA PIG
0.160µg
350µg
% OF DOSE / FRACTION
FRACTION NUMBER
% OF DOSE
TIME (MIN)

Figure 3.4. Effect of dose of B[a]P on biliary excretion of [^{3}H]-radioactivity in Syrian Golden hamsters. [^{3}H]-B[a]P in amounts of either 0.16 μg or 350 μg was administered to rats by intratracheal instillation and the amount of [^{3}H]-radioactivity in bile determined over a 6 hr time period. The rate of excretion (% dose/fraction) is shown in the upper part of the Fig. and cumulative excretion, in the lower part. Each value represents the percent of dose, mean ± S.E., for 3 hamsters.

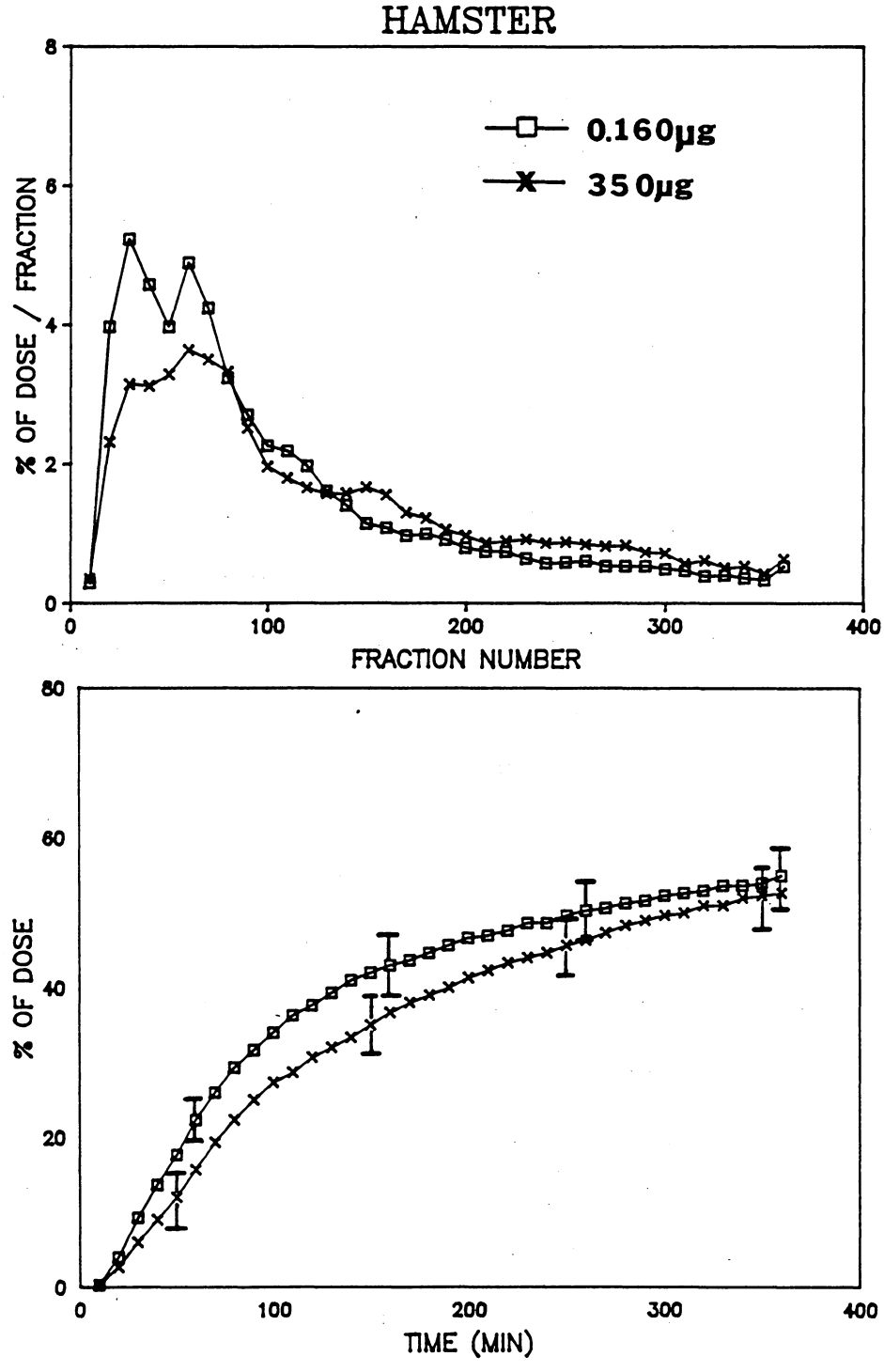
HAMSTER
0.160µg
350µg
% OF DOSE / FRACTION
FRACTION NUMBER
% OF DOSE
TIME (MIN)

Tissue Disposition of [^{3}H]-Radioactivity

Tissue disposition of [^{3}H]-radioactivity 6 hr after administration of a low dose of [^{3}H]-B[a]P to each of the species under investigation is listed in Table 3.1. Tissue disposition in hamsters was different than that observed in SD rats, Gunn rats or guinea pigs. Higher amounts of radioactivity were observed in all tissues of hamsters as compared to the other species, as would be expected due to the slower rate of excretion of B[a]P and metabolites from hamsters and smaller size of hamsters. Most, but not all, of the differences were statistically significant. Of particular interest, however, is the much higher amount of radioactivity remaining in lungs of hamsters, an amount which is about 5-fold greater than that remaining in lungs of the other species.

Tissue disposition of [^{3}H]-radioactivity following a high dose of [^{3}H]-B[a]P is listed in Table 3.2. As mentioned above, total amounts of radioactivity excreted into bile of SD rats, hamsters, and guinea pigs were similar. However, decreased amounts of radioactivity were excreted into bile of SD rats, guinea pigs, and Gunn rats following the higher dose in comparison to the lower dose. In Sprague-Dawley and Gunn rats, these differences between

doses were statistically significant ($p<0.05$) though in guinea pigs they were not.

Table 3.1.

Disposition of [^{3}H]-radioactivity in SD rat, hamster, guinea pig, and Gunn rat following a 0.16 μg dose of B[a]P

[^{3}H]-B[a]P (0.16 μg/animal) was administered intratracheally to animals in which cannulas were implanted in the bile duct. Tissue and excreta levels of [^{3}H]-radioactivity were determined 6 hours after [^{3}H]-B[a]P administration as detailed in "Materials and Methods". Results are expressed as percent of dose (mean ± S.E., for 3 animals/experiment, except Gunn rat data which represent the mean ± range for two animals).

	SPECIES			
	Sprague-Dawley rat	Hamster	Guinea pig	Gunn rat
% dose/g tissue				
Lung	1.70 ± 0.42^{b}	7.97 ± 1.16^{a}	1.40 ± 0.084^{b}	2.07 ± 0.03^{b}
Liver	0.67 ± 0.11^{b,c}	2.16 ± 0.24^{a}	0.35 ± 0.053^{c}	1.02 ± 0.18^{b}
GI tract	0.19 ± 0.01^{b,c}	0.59 ± 0.09^{a}	0.033 ± 0.012^{c}	0.40 ± 0.22^{a,b}
Kidney	0.76 ± 0.02^{b}	2.19 ± 0.57^{a}	1.21 ± 0.13^{a,b}	1.31 ± 0.08^{a,b}
Stomach	0.13 ± 0.02^{b}	0.46 ± 0.05^{a}	0.023 ± 0.01^{c}	0.15 ± 0.08^{b}
Testes	0.21 ± 0.02^{b}	0.37 ± 0.05^{a}	0.044 ± 0.013^{c}	0.27 ± 0.01^{a,b}
Spleen	0.21 ± 0.01^{b}	1.17 ± 0.22^{a}	0.083 ± 0.009^{b}	0.35 ± 0.17^{b}
Heart	0.21 ± 0.02^{b,c}	0.64 ± 0.10^{a}	0.049 ± 0.001^{c}	0.34 ± 0.01^{b}
Carcass	0.071 ± 0.004^{b,c}	0.18 ± 0.03^{a}	0.018 ± 0.001^{c}	0.084 ± 0.01^{b}
% of dose				
Urine	2.21 ± 1.1^{a}	3.74 ± 1.2^{a}	2.22 ± 1.2^{a}	0.98 ± 0.16^{a}
Blood	0.83 ± 0.2^{a,b}	0.27 ± 0.1^{b}	0.59 ± 0.7^{b}	1.44 ± 1.01^{a}
Bile	70.3 ± 2.0^{a}	54.6 ± 3.1^{b}	61.7 ± 1.9^{b}	59.4 ± 1.07^{b}

$^{a-c}$Data for each tissue or for excreta were compared among species. Values with different superscripts are significantly different ($p<0.05$).

Table 3.2.

Disposition of [^{3}H]-radioactivity in SD rat, hamster, guinea pig, and Gunn rat following a 350 μg dose of B[a]P

[^{3}H]-B[a]P (350 μg/animal) was administered intratracheally to animals in which cannulas were implanted in the bile duct. Tissue and excreta levels of [^{3}H]-radioactivity were determined 6 hours after [^{3}H]-B[a]P administration as detailed in "Materials and Methods". Results are expressed as percent of dose (mean ± S.E., for 3 animals/experiment, except Gunn rat data which represent the mean ± range for two animals).

	SPECIES			
	Sprague-Dawley rat	Hamster	Guinea pig	Gunn rat
% dose/g tissue				
Lung	9.01 ± 1.86^{b}	8.04 ± 1.72^{b}	4.48 ± 1.57^{b}	17.4 ± 4.28^{a}
Liver	0.65 ± 0.05^{b,c}	2.46 ± 0.27^{a}	0.33 ± 0.047^{c}	1.10 ± 0.33^{b}
GI tract	0.22 ± 0.03^{b}	0.84 ± 0.22^{a}	0.058 ± 0.032^{b}	0.36 ± 0.07^{b}
Kidney	0.88 ± 0.10^{b}	3.47 ± 0.78^{a}	0.84 ± 0.10^{b}	1.24 ± 0.61^{b}
Stomach	0.14 ± 0.02^{b}	0.64 ± 0.11^{a}	0.040 ± 0.013^{b}	0.21 ± 0.01^{b}
Testes	0.27 ± 0.04^{b}	0.42 ± 0.04^{a}	0.033 ± 0.007^{c}	0.33 ± 0.06^{a,b}
Spleen	0.14 ± 0.01^{b}	0.87 ± 0.29^{a}	0.12 ± 0.04^{b}	0.29 ± 0.15^{b}
Heart	0.18 ± 0.05^{c}	0.78 ± 0.08^{a}	0.058 ± 0.010^{c}	0.35 ± 0.03^{b}
Carcass	0.067 ± 0.005^{b,c}	0.19 ± 0.03^{a}	0.022 ± 0.003^{c}	0.10 ± 0.02^{b}
% of dose				
Urine	1.68 ± 0.6^{a}	2.53 ± 0.4^{a}	1.27 ± 0.4^{a}	1.44 ± 1.82^{a}
Blood	0.70 ± 0.2^{a,b}	0.50 ± 0.2^{b}	0.60 ± 0.1^{a,b}	1.31 ± 0.82^{a}
Bile	55.0 ± 2.0^{a}	52.9 ± 2.7^{a}	47.9 ± 4.9^{a}	30.8 ± 1.51^{b}

$^{a-c}$Data for each tissue or for excreta were compared among species. Values with different superscripts are significantly different ($p<0.05$).

Most of the additional radioactivity remaining in SD rats, Gunn rats, and guinea pigs at 6 hrs after administration of the higher dose of B[a]P was associated with lungs. Because of the smaller size of hamsters as compared to other species in this study, the fraction of dose in tissues when expressed on a per gram tissue basis generally was higher for hamsters than for other species. However, the fraction of dose remaining in lungs of hamsters was essentially the same after administration of a high dose as it was after a low dose.

B[a]P Metabolites In Bile

B[a]P metabolites in a cumulative six hour bile sample were identified for each species investigated following either a 0.16 μg or a 350 μg dose of [^{3}H]-B[a]P. Listed in Table 3.3. are metabolites identified in bile following a 0.16 μg dose. SD rats and hamsters were similar in the types and relative amounts of B[a]P metabolites excreted in bile after 6 hrs. The predominant metabolites were thio-ether conjugates which accounted for 61 and 63% of the material in bile of SD rats and hamsters, respectively. Gunn rats, in comparison to SD rats and hamsters, excreted similar amounts of thio-ether conjugates and significantly

higher amounts of sulfate conjugates and lower amounts of glucuronides. The amount of metabolites in guinea pig bile were significantly different than the amounts determined for all other species. Thio-ether conjugates accounted for 89% of the metabolites in bile while glucuronides, sulfate conjugates and non-conjugated metabolites accounted for a total of 11%.

Types of B[a]P metabolites excreted in bile following a 350 μg dose of [^{3}H]-B[a]P are listed in Table 3.4. As was observed with the lower dose, SD rats and hamsters were similar in types and relative amounts of metabolites excreted in bile following a high dose of [^{3}H]-B[a]P. Relative amounts of glucuronides and sulfate conjugates increased while thio-ether conjugates decreased following a high dose in comparison to a low dose. Once again the relative amounts of metabolites in Gunn rat bile were different from those observed in SD rat and hamster bile with glucuronides being significantly lower and sulfate conjugates being 2.0-2.5-fold higher. Thio-ether conjugates remained the predominant metabolite in guinea pig bile, accounting for 95% of metabolites in bile.

Table 3.3.

B[a]P metabolites in a cumulative 6 hr bile sample following a 0.16 μg dose of B[a]P

Bile was collected for 6 hr following intratracheal administration of 0.16 μg B[a]P and analyzed for thio-ether, glucuronic acid, and sulfate conjugates and non-conjugated metabolites as described in "Materials and Methods". Results are expressed as percent of each metabolite in bile (mean ± S.E., for 3 animals/experiment, except for Gunn rat data which represent the mean ± range for two animals). Numbers in parentheses are amounts of each metabolite as a percent of dose.

	SPECIES			
METABOLITE	Sprague-Dawley rat	Hamster	Guinea pig	Gunn rat
thio-ether conjugates	61.0 ± 1.5^{c} (42.9)	64.6 ± 1.6^{b,c} (33.8)	88.5 ± 0.3^{a} (54.1)	66.6 ± 3.1^{b} (40)
glucuronides	18.4 ± 1.1^{a} (12.9)	21.3 ± 0.7^{a} (11.9)	6.7 ± 0.2^{c} (4.5)	12.3 ± 0.9^{b} (7)
sulfate conjugates	4.27 ± 0.8^{c} (3.0)	7.0 ± 0.1^{b} (3.7)	2.0 ± 0.3^{d} (1.9)	14.0 ± 3.6^{a} (8)
non-conjugated	16.3 ± 1.4^{a} (11.5)	7.1 ± 1.0^{b} (4.1)	2.8 ± 0.2^{c} (1.7)	7.1 ± 1.3^{b} (4)

$^{a-d}$Data for each class of metabolites were compared among species. Values with different superscripts are significantly different ($p<0.05$).

Table 3.4.

B[a]P metabolites in a cumulative 6 hr bile sample following a 350 μg dose of B[a]P

Bile was collected for 6 hr following intratracheal administration of 350 μg B[a]P and analyzed for thio-ether, glucuronic acid, and sulfate conjugates and non-conjugated metabolites as described in "Materials and Methods". Results are expressed as percent of each metabolite in bile (mean ± S.E., for 3 animals/experiment, except for Gunn rat data which represent the mean ± range for two animals). Numbers in parentheses are amounts of each metabolite as a percent of dose.

	SPECIES			
METABOLITE	Sprague-Dawley rat	Hamster	Guinea pig	Gunn rat
thio-ether conjugates	40.2 ± 1.8[b] (22.1)	44.8 ± 4.2[b] (23.7)	94.7 ± 0.3[a] (45.4)	39.8 ± 10.2[b] (12)
glucuronides	34.0 ± 1.6[a] (18.7)	34.2 ± 4.3[a] (18.1)	0.3 ± 0.1[c] (0.2)	27.5 ± 3.5[b] (9)
sulfate conjugates	10.7 ± 1.1[b] (5.9)	13.1 ± 1.9[b] (6.9)	2.3 ± 0.3[c] (1.1)	27.0 ± 5.7[a] (8)
non-conjugated	15.1 ± 1.0[a] (8.3)	7.9 ± 1.0[b] (4.2)	2.6 ± 0.1[c] (1.3)	5.7 ± 1.0[b] (2)

[a-c]Data for each class of metabolites were compared among species. Values with different superscripts are significantly different ($p<0.05$).

Effect of Buthionine Sulfoximine Treatment on Biliary Excretion of B[a]P in Sprague-Dawley Rats

The effect of altered glutathione levels on the metabolic fate of B[a]P *in vivo* was assessed by monitoring tissue disposition and biliary excretion of [^{3}H]-radioactivity and identifying types of B[a]P metabolites excreted in bile following BSO treatment.

BSO treatment was more effective in reducing glutathione levels in rat liver than in rat lung (Table 3.5.). Following BSO treatment but prior to [^{3}H]-B[a]P administration, glutathione levels in lung and liver were 82 and 30% of control values, respectively. Six hrs after [^{3}H]-B[a]P administration, lung levels of glutathione decreased to 72% and liver levels dropped to 19% of control values.

Figure 3.5. depicts the rate and extent at which [^{3}H]-radioactivity was excreted into the bile of BSO-treated rats. A maximum amount of radioactivity per fraction was reached at 30 min. Over a 6 hr time period 66% of the dose was excreted from BSO-treated animals which is not significantly different from the amount excreted from control SD rats (74%). Distribution of radioactivity among

organs and excreta of animals treated with BSO is listed in Table 3.6. Distribution of radioactivity was similar in animals with and without BSO pretreatment (Tables 3.6 and 3.1), with significant differences being observed only in kidneys and carcass.

Conjugates of B[a]P metabolites were identified in a cumulative 6 hr bile sample from animals treated with BSO (Table 3.7.). Thio-ether conjugates were present in greatest amounts, accounting for 57% of the material in bile. Glucuronides and non-conjugated metabolites were similar with each accounting for 12-14%. Small amounts of sulfate conjugates were detected. Amounts of conjugates and non-conjugated metabolites excreted from animals pretreated with BSO were not significantly different ($p<0.05$) from amounts excreted from controls (Tables 3.3. and 3.7.).

Table 3.5.

Effect of buthionine sulfoximine treatment on glutathione levels in SD rat lung and liver

Buthionine sulfoximine was administered by i.p. injection (8 mmoles kg^{-1}) to Sprague-Dawley rats and glutathione levels in lung and liver before and 6 hrs after [^{3}H]-B[a]P administration (0.5 μg kg^{-1}) were determined as described in "Materials and Methods". The results are expressed as μmoles glutathione per gram tissue (mean ± S.E. for 3-4 animals). Numbers in parentheses are percent of control levels prior to buthionine sulfoximine treatment.

Organ	Control	Before B[a]P Administration[A]	Six hours After B[a]P Administration[B]
lung	1.48 ± 0.29 (100)	1.21 ± 0.07 (82)	1.07 ± 0.12 (72)
liver	2.32 ± 0.37 (100)	0.70 ± 0.16 (30)	0.48 ± 0.08 (19)

[A]GSH levels determined 2.5 hrs after BSO treatment.
[B]GSH levels determined 8.5 hrs after BSO treatment and 6 hrs after [^{3}H]-B[a]P administration.

Table 3.6.

Effect of buthionine sulfoximine treatment on [^{3}H]-B[a]P disposition in SD rats

Buthionine sulfoximine was administered by i.p. injection (8 mmoles kg^{-1}) to Sprague-Dawley rats. Tracheal and biliary cannulas were implanted, and 2.5 hrs after BSO treatment, [^{3}H]-B[a]P (0.5 μg kg^{-1}) was intratracheally instilled. Tissue levels of [^{3}H]-radioactivity were determined 6 hrs after [^{3}H]-B[a]P administration as detailed in "Materials and Methods". Results are the mean ± S.E., for 4 animals.

<u>% of dose / g tissue</u>	
lung	2.07 ± 0.04
liver	0.68 ± 0.04
gi tract	0.23 ± 0.02
stomach	0.16 ± 0.02
kidney	0.56 ± 0.04[A]
testes	0.17 ± 0.04
spleen	0.27 ± 0.05
heart	0.25 ± 0.04
carcass	0.10 ± 0.02[A]
<u>% of dose</u>	
urine	0.80 ± 0.192
blood	1.56 ± 0.611
bile	65.5 ± 1.26

[A]Significantly different ($p<0.05$) from control (data for control are in Table 3.1.).

Figure 3.5. Effect of buthionine sulfoximine treatment on biliary excretion of [^{3}H]-radioactivity in Sprague-Dawley rats. Buthionine sulfoximine was administered by i.p. injection (8 mmoles/animal) to Sprague-Dawley rats. Tracheal and biliary cannulas were implanted, and 2.5 hrs after BSO treatment, [^{3}H]-B[a]P (0.5 $\mu g\ kg^{-1}$) was intratracheally instilled. The amount of [^{3}H]-radioactivity in bile was determined over a 6 hr time period. The rate of excretion (% dose/fraction) is shown in the upper part of the Fig. and cumulative excretion is shown in the lower part of the Fig. for BSO-treated animals (□——□) and non-treated animals (●——●). Each value represents the percent of dose, mean ± S.E., for 4 animals.

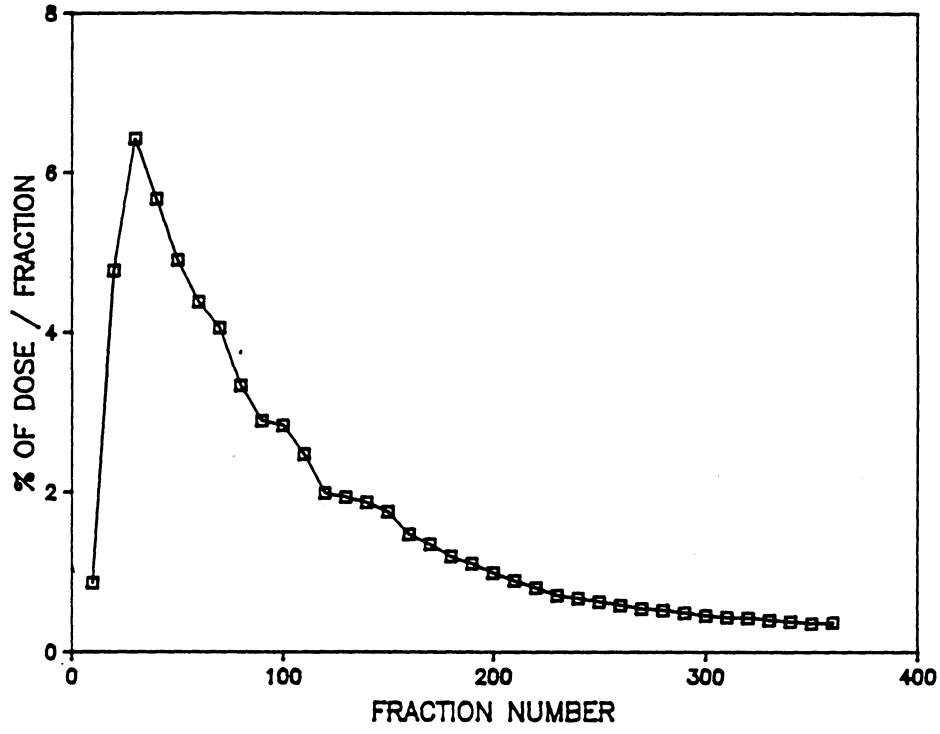
% OF DOSE / FRACTION
0
2
4
6
8
0
100
200
300
400
FRACTION NUMBER

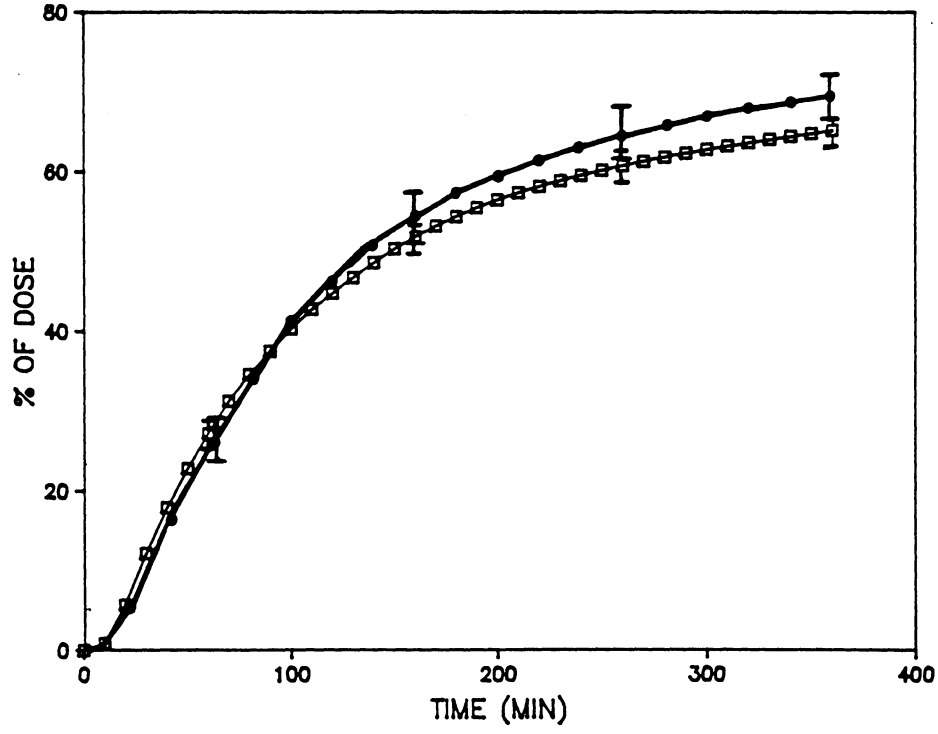
% OF DOSE
0
20
40
60
80
0
100
200
300
400
TIME (MIN)

Table 3.7.

Effect of buthionine sulfoximine treatment on B[a]P metabolites excreted in bile

Aliquots of bile were analyzed for thio-ether, glucuronic acid, and sulfate conjugates and non-conjugated metabolites as described in "Materials and Methods". Results are expressed as percent of dose for each metabolite in bile (mean ± S.E., for 4 animals/experiment). Numbers in parentheses give the amount of each metabolite as a percent of each metabolite in bile.

Metabolite	% of dose	(% in bile)
thio-ether	57.4 ± 2.37	(37.6)
glucuronides	21.7 ± 2.01	(14.3)
sulfate conjugates	2.28 ± 1.45	(1.45)
non-conjugated	18.6 ± 1.79	(12.2)

Discussion

Most studies of biliary excretion of B[a]P have been carried out using rats (24,25). In the present study, SD rats, Gunn rats, hamsters, and guinea pigs were used to facilitate inter-species comparison of biliary excretion and tissue distribution of [^{3}H]-B[a]P. Likewise, differences within species in the amount and types of B[a]P metabolites excreted in bile were also studied.

The observation that low doses of B[a]P are excreted faster and to a greater extent than high doses is consistent with a previous study (26). Boroujerdi et al. (38) reported excretion of 68 and 51% of the dose in bile within 6 hrs after administering 1 and 10 μmol kg^{-1} doses of B[a]P, respectively. Amounts of material that we detected in bile after 6 hrs at similar dose levels are in reasonable agreement. However, differences in the relative amounts of metabolites in bile exist. Boroujerdi et al. reported that 42 and 64% of the material in bile consisted of glucuronides and sulfate conjugates combined, following either a 1 μmol kg^{-1} (63 μg/animal) or 10 μmol kg^{-1} (630 μg/animal) dose of B[a]P. In this study we observed that glucuronides and sulfate conjugates together accounted for 22 and 44% of material in bile following a 0.16 μg or 350 μg B[a]P dose,

respectively. These differences may be due in part to differences in the way B[a]P was administered since we used intratracheal instillation and Boroujerdi et al. used intravenous injection. We observed an increase in amounts of glucuronides and sulfate conjugates as the dose was increased which is similar to the observations of Boroujerdi et al. This suggests a possible saturation of one or more steps involved in B[a]P metabolism.

A comparison of B[a]P biliary excretion in SD rats, Gunn rats, hamsters, and guinea pigs has not been previously reported. The effect of dose on B[a]P biliary excretion was similar in SD rats, Gunn rats, and guinea pigs (Figure 3.1.-3.3.). However, hamsters did not exhibit a dose effect as observed in the other species (Figure 3.4.). Examination of tissue disposition of radioactivity in hamsters revealed that much of the excess radioactivity remaining in hamster following administration was located in lung, liver, and kidneys. We are unaware of any anatomical or physiological characteristics unique to hamsters that may account for this species difference.

Metabolite profiles for SD rat, Gunn rat, and hamster were similar at both doses examined. Glucuronidation in Gunn rats, on a relative scale, was comparable to that determined for SD rats and hamsters. The ability of Gunn

rats to form B[a]P glucuronides is interesting since these animals are unable to conjugate bilirubin to glucuronic acid (30). However, Gunn rats are capable of forming p-nitrophenylglucuronic acid conjugates at half the rate of Wistar rats (30). This suggests that bilirubin glucuronidation probably involves another form of UDP-glucuronyl transferase than that catalyzing p-nitrophenol and B[a]P glucuronidation. A comparative study by Boutin et al. (39) recently provided evidence, based on substrate specificity, that three types of hepatic UDP-glucuronyltransferases exist in several mammalian species. Other studies have isolated and purified at least two forms of liver UDP-glucuronyltransferase from rabbits (40) and rats (41,42).

In our study, Gunn rats formed more sulfate conjugates than any other species. Other studies, using cell culture systems, have reported large amounts of B[a]P sulfate conjugates. Autrup (43) and Mehta et al. (44) using organ cultures of human tissue reported that 30-45% of the water-soluble metabolites were sulfate conjugates. Similarly, other studies have reported that sulfation is a major conjugation pathway in humans as well as in cats (29,31).

The most notable difference among species was in the amount of thio-ether conjugates in guinea pig bile in

comparison to the amount detected in bile of the other species examined. These conjugates accounted for over 90% of the metabolites in bile and over 45% of the instilled dose. Thio-ether conjugates as we have defined them may be conjugates of glutathione, mercapturic acid or derivatives between glutathione and mercapturic acid. It is unlikely that mercapturic acid derivatives are present in any great amount because guinea pigs are deficient in enzymes catalyzing N-acetylation of cysteine conjugates (29,31). A possible metabolite that may be present is the methylthio conjugate. Methylthio metabolites have been identified for bromazepam (45), styrene oxide (46), and naphthalene (47). Bartels et al. (48) recently demonstrated that indene is metabolized in guinea pigs primarily to a methylthio metabolite which probably involves glutathione conjugation. In addition, guinea pigs formed up to 47-times the amount of the indene methylthio metabolite than SD rats (48). Similarly, in the present study thio-ether conjugates of B[a]P are present in greater amounts in guinea pig bile than rat bile (Tables 3.3. and 3.4.).

The role of glutathione in B[a]P metabolism was evaluated in SD rats by lowering glutathione levels with BSO and monitoring biliary excretion. BSO is a specific inhibitor of gamma-glutamylcysteine synthetase which

significantly decreases tissue glutathione content without affecting enzymes involved in phase I and phase II xenobiotic metabolism (36). With hepatic glutathione levels at 30% of control levels, no effect on the rate or extent of biliary excretion was detected in our study. In addition, thio-ether conjugates accounted for 57% of the metabolites in bile which is similar to the amount excreted from animals not previously treated with BSO. A recent study by Meerman et al. (49) reported that pretreatment with diethyl maleate decreased 2-acetylaminofluorene:glutathione conjugates by 60% as compared to control values. However, covalent binding to liver protein and DNA remained the same. A general conclusion from Meerman and coworkers was that glutathione depletion has no major effect on N-hydroxy-2-acetylaminofluorene hepatotoxicity. Similar results have also been reported for carbon tetrachloride (36). Other investigations on acetominophen (50), and chloroform (51) metabolism in animals have demonstrated that lowering hepatic glutathione levels results in severe necrosis which is paralleled by an increase in covalent binding. Although we did not detect any alteration in biliary excretion, it is possible that an increase in covalent binding of B[a]P metabolites to macromolecules may have occurred. Further investigation of B[a]P covalent binding in BSO-treated

animals will help to evaluate better the role of glutathione in carcinogen metabolism.

References

1. Mass, M. J. Species differences in the activation of carcinogen in respiratory epithelium. A possible explanation for the unequal susceptibility of tracheal epithelium of rats and hamsters to carcinogenesis by benzo(a)pyrene. Diss. ads. Int. B., 42:547-B, 1981.

2. Radomski, J. L. Annu. Rev. Pharmacol. Toxicol., 19:129-157, 1979.

3. Hicks, R. M., Wright, R., and Wakefiekd, J. St. J. The induction of rat bladder cancer by 2-napthylamine. Br. J. Cancer, 46:646-661, 1982.

4. Bock, F. G. Species differences in penetration and absorption of chemical carcinogens. NCI Monograph, 10:361-375, 1963.

5. Kao, J., Patterson, F. K., and Hall, H. Skin penetration and metabolism of topically applied chemicals in six mammalian species, including man: An in vitro study with benzo(a)pyrene and testosterone. Toxicol. Appl. Pharmacol., 81:502-516, 1985.

6. Schanker, L. S., Mitchell, E. W., and Brown Jr., R. A. Species comparison of drug absorption from the lung after aerosol inhalation or intratracheal injection. Drug Metab. Dispos., 14:79-88, 1986.

7. Morse, M. A., and Carlson, G. P. Distribution and macromolecular binding of benzo(a)pyrene in sencar and BALB/c mice following topical and oral administration. J. Toxicol. Environ. Hlth., 16:263-276, 1985.

8. Vauhkonen, M., Kuusi, T., and Kinnunen, P. K. J. Serum and tissue distribution of benzo(a)pyrene from intravenously injected chylomicrons in rat in vivo. Cancer Letters, 11:113-119, 1980.

9. Jongeneelen, F. S., Leijdekkers, C. M., and Henderson, P. Urinary excretion of 3-hydroxy-benzo(a)pyrene after percutaneous penetration and oral absorption of benzo(a)pyrene in rats. Cancer

Letters, 25:192-201, 1984.

10. Pylev, L. N., Roe, J. C., and Warwick, G. P. Elimination of radioactivity after intratracheal instillation of tritiated 3,4-benzopyrene in hamsters. Br. J. Cancer, 23:103-115, 1969.

11. Rigdon R. H., and Neal, J. Absorption and excretion of benzpyrene. Observation in the duck, chicken, mouse and dog. Bio. Med. 21:247-261, 1963.

12. Walz Jr., F. G., Vlasuk, G. P., and Steggles, A. W. Species differences in cytochrome P-450 and epoxide hydrolase: Comparisons of xenobiotic-induced hepatic microsomal polypeptides in hamsters and rats. Biochemistry, 22:1547-1563, 1983.

13. Oesch, F., Raphael, D., Schwind, H., and Glatt, H. R. Species differences in activating and inactivating enzymes related to the control of mutagenic metabolites. Arch. Toxicol., 39:97-108, 1977.

14. Hodgson, E. Comparative aspects of the distribution of cytochrome P-450 dependent mono-oxygenase system: An overview. Drug Metab. Rev., 10:15-33, 1979.

15. Souhail-el Amri, H., Batt, A. M., and Siest, G. Comparison of cytochrome P-450 content and activities in liver microsomes of seven animal species, including man. Xenobiotica, 16:351-358, 1986.

16. Holme, J. A. Trygg, B., and Soderlund, E. Species differences in the metabolism of 2-acetylaminofluorene by hepatocytes in primary monolayer culture. Cancer Res., 46:1627-1632, 1986.

17. Autrup, H., Wefald, F. C., Jeffrey, A. M., Tate, H., Schwartz, R. D., Trump, B. F., and Harris, C. C. Metabolism of benzo(a)pyrene by cultured tracheobronchial tissues from mice, rats, hamsters, bovines and humans. Int. J. Cancer, 25:293-300, 1980.

18. Gregus, Z., Wetkins, J. B., Thompson, T. N., Harvey, M. J., Rozman, K., and Klaassen, C. D. Hepatic phase I and phase II biotransformation in quail and trout: Comparison to other species commonly used in toxicity testing. Toxicol. Appl. Pharmacol. 67:430-441, 1983.

19. Ioannides, C. Parkinson, C., and Parke, D. V. Activation of benzo(a)pyrene and 2-acetamidofluorene to mutagens by microsomal preparations from different animal species: Role of cytochrome P-450 and P-448. Xenobiotica, 11:701-708, 1981.

20. Daniel, F. B., Schut, H. A. J., Sandwisch, D. W., Schenck, K. M., Hoffmann, C. O., Patrick, J. R., and Stoner, G. D. Interspecies comparisons of benzo(a)pyrene metabolism and DNA-adduct formation in cultured human and animal bladder and tracheobronchial tissues. Cancer Res., 43:4723-4729, 1983.

21. Stoner, G. D., Schut, H. A. J., Daniel, F. B., and Dixit, R. A comparison of covalent DNA binding of benzo(a)pyrene and 7,12-dimethylbenz[a]anthracene in respiratory tissues from human, rat and mouse. Cancer Letters, 30:231-241, 1986.

22. Sebti, S. M., Pruess-Schwartz, D., and Baird, W. M. Species- and length of exposure-dependent differences in the benzo(a)pyrene:DNA adducts formed in embryo cell cultures from mice, rats, and hamsters. Cancer Res., 45:1594-1600, 1985.

23. Kotin, P., Falk, H. L., and Busser, R. Distribution, retention, and elimination of ^{14}C-3,4-benzopyrene after administration to mice and rats. J. Nat. Cancer Inst., 23:541-555, 1959.

24. Falk, H. L., Kotin, P., Lee, S. S., and Nathan, A. Intermediary metabolism of benz(a)pyrene in the rat. J. Nat. Cancer Inst., 28:699-724, 1962.

25. Schlede, E., Kuntzman, R., and Conney, A. H. Stimulatory effect of benzo(a)pyrene and phenobarbital pretreatment on the biliary excretion of benzo(a)pyrene metabolites in the rat. Cancer Res. 30:2898-2904, 1970.

26. Kari, F. W., Kauffman, F. C., Thurman, R. G. Effect of bile salts on rates of formation, accumulation, and export of mutagenic metabolites from benzo(a)pyrene produced by the perfused rat liver. Cancer Res., 45:1621-1627, 1985.

27. Chipman, J. K., Hirom, P. C., Frost, G. S., and Millburn, P. The biliary excretion and enterohepatic circulation of benzo(a)pyrene and its metabolites in the rat. Biochem. Pharmacol., 30:937-944, 1981.

28. Caldwell, J. The significance of phase II (conjugation) reactions in drug disposition and toxicity. Life Sciences, 24:571-578, 1979.

29. Vainio, H., and Hietanen, E. Drug metabolism in Gunn rats: Inability to increase bilirubin glucuronidation by phenobarbital treatment. Biochem. Pharmacol., 23:3405-3410, 1974.

30. Caldwell, J. The current status of attempts to predict species differences in drug metabolism. Drug Metab. Rev., 12:221-237, 1981.

31. Lester, R., and Schmid, R. Bilirubin metabolism. N. Engl. J. Med., 270:779-786, 1964.

32. Homburger, F., Soto, E., Althoff, J., and Heitz, P. Animal model of human disease, carcinoma of the larynx in hamsters exposed to cigarette smoke. Am. J. Pathol., 95:845-848, 1979.

33. Adams, R. A., DiPaolo, J. A., and Homburger, F. The syrian hamster in toxicology and carcinogenesis research. Cancer Res., 38:2642-2645, 1978.

34. Shanker, L. S. Drug absorption from the lung. Biochem. Pharmacol. 27:381-385, 1978.

35. White, R. D., Norton, R., and Bus, J. S. The effect of buthionine sulfoximine, an inhibitor of glutathione synthesis, on hepatic drug metabolism in the male mouse. Toxicol. Letters, 23:25-32, 1984.

36. Brehe, J. E., and Burch, H. L. Enzymatic assay for glutathione. Anal. Biochem., 74:189-197, 1976.

37. MacLeod, M. C., Moore, C. J., and Selkirk, J. K. Analysis of water-soluble conjugates produced by hamster embryo cells exposed to polynuclear aromatic hydrocarbons. In: B. Bjorseth and A. J. Dennis (eds.), Polynuclear Aromatic Hydrocarbons: Chemistry and Biological Effects, pp 9-23, Columbus, Battelle Press, 1979.

38. Boroujerdi, M., Kung, H. C., Wilson, A. E. G., and Anderson, M. W. Metabolism and DNA binding of benzo(a)pyrene in vivo in the rat. Cancer Res., 41:951-957, 1981.

39. Boutin, J. A., Antoine, B., Batt, A-N., and Siest, G. Heterogeneity of hepatic microsomal UDP-glucuronosyltransferase(s) activities: Comparison between human and mammalian species activities. Chem-Biol. Interact, 52:173-184, 1984.

40. Tukey, R. H., Robinson, R., Holm, B., Falany, C. N., and Tephly, T. R. A procedure for the rapid separation and purification of UDP-glucuronosyltransferases from rabbit liver microsomes. Drug Metab. Dispos., 10:97-101, 1982.

41. Bock, K. W., Josting, D., Lilienblum, W., and Pfeil, H. Purification of rat-liver microsomal UDP-glucuronyltransferase. Separation of two enzyme forms inducible by 3-methylcholanthrene or phenobarbital. Eur. J. Biochem., 98:19-26, 1979.

42. Matsui, M., and Nagai, F. Multiple forms and a deficiency of uridine diphosphate-glucuronosyltransferases in Wistar rats. J. Pharmacobio-Dyn., 8:679-686, 1985.

43. Autrup, H. Separation of water-soluble metabolites of benzo(a)pyrene formed by cultured human colon. Biochem. Pharmacol., 28:1727-1730, 1979.

44. Mehta, R., and Cohen, G. M. Major differences in the extent of conjugation with glucuronic acid and sulphate in human peripheral lung. Biochem.

Pharmacol., 28:2479-2484, 1979.

45. Tateishi, M., Suzuki, S., and Shimizu, H. The metabolism of bromazepam in the rat-identification of mercapturic acid and its conversion in vitro to methylthio-bromazepam. Biochem. Pharmacol., 27:809-810, 1978.

46. Nakatsu, K., Hugenroth, S., Sheng, L-S, Horning, E. C., and Horning, M. G. Metabolism of styrene oxide in the rat and guinea pig. Drug Metab. Dispos., 11:463-470, 1983.

47. Bakke, J., Struble, C., Gustafsson, J-A, and Gustafsson, B. Catabolism of premercapturic acid pathway metabolites of naphthalene to naphthols and methylthio-containing metabolites in rats. Proc. Natl. Acad. Sci., 82:668-671, 1985.

48. Bartels, M. J., Horning, E. C., and Horning, M. M. Formation of methylthio metabolites of indene in the guinea pig and the rat. Drug Metab. Dispos., 14:97-101, 1986.

49. Meerman, J. H. N., and Tijdens, R. B. Effect of glutathione depletion on the hepatotoxicity and covalent binding to rat liver macromolecules of N-hydroxy-2-acetylaminofluorene. Cancer Res., 45:1132-1139, 1985.

50. Gillette, J. A perspective on the role of chemically reactive metabolites of foreign compounds in toxicity-I. Correlation of changes in covalent binding of reactive metabolites with changes in the incidence and severity of toxicity. Biochem. Pharmacol., 23:2785-2794, 1974.

51. Kluwe, W. M., and Hook, J. B. Potentiation of acute chloroform nephrotoxicity by the glutathione depletor diethyl maleate and protection by the microsomal enzyme inhibitor piperonyl butoxide. Toxicol. Appl. Pharmacol., 59:457-466, 1981.

Chapter 4

General Remarks

Benzo[a]pyrene (B[a]P) absorption and distribution in Sprague-Dawley rats following intratracheal instillation was characterized in detail. Interestingly, toxicokinetic parameters which describe B[a]P disposition following intratracheal instillation were similar to those calculated for intravenous injection. The similarity between these parameters probably results from the rapid absorption and clearance of B[a]P from lungs when instilled in a vehicle of triethylene glycol (TEG). B[a]P in TEG is not characteristic of how B[a]P is found in the environment. B[a]P is normally associated with carbonaceous particulates, such as woodstove soot or diesel particulate. Investigations of toxicokinetics of B[a]P associated with such particulates will provide a better assessment of B[a]P bioavailability. One approach that could be used involves monitoring unmetabolized B[a]P blood concentrations as a function of time after exposure. This can be readily accomplished via cannulation of the femoral artery for blood collection. This method would provide the necessary information for calculating toxicokinetic parameters which

describe B[a]P disposition. In addition, these experiments could be done with only three animals per vehicle, thus minimizing the number of animals needed. Comparison of toxicokinetic parameters for soluble vs particulate associated B[a]P would provide novel and potentially significant information.

At 5 min after B[a]P instillation, the majority of the material in lung and liver was ethyl acetate extractable while at later times most of the material was non-extractable. Future characterization of this non-extractable material as conjugates and/or covalently bound material at several times after B[a]P administration will provide an improved assessment of B[a]P activation in specific tissues. Methods described in this study could be used for identifying the types of B[a]P conjugates and the extent of B[a]P metabolite binding to DNA, RNA, and protein. This type of study should establish at what time(s) covalent binding is maximum after B[a]P administration. A detailed investigation into the kinetics of B[a]P covalent binding in organs following intratracheal instillation may provide information on why organs such as lungs are targets for B[a]P carcinogenesis.

That B[a]P and/or B[a]P metabolites undergo extensive enterohepatic circulation was demonstrated directly and

indirectly in the completed experiments. The nature of the material which is undergoing enterohepatic circulation (unmetabolized B[a]P, B[a]P metabolites, conjugated or nonconjugated) remains unknown. A detailed study characterizing the extent to which specific B[a]P metabolites are reabsorbed would provide a good assessment of the significance of enterohepatic circulation in carcinogen metabolism. Most interesting would be delineating the extent to which B[a]P 7,8-dihydrodiol is reabsorbed. Increased availability of this substrate for further metabolism to the ultimate carcinogen by extrahepatic tissues may contribute to organ susceptibility to chemical carcinogenesis. Intraduodenal infusion experiments with B[a]P 7,8-dihydrodiol, as well as the glucuronic acid and/or sulfate conjugates of this metabolite, provides one approach to the delineation of this problem.

The contribution of microbial metabolism to enterohepatic circulation and to activation of carcinogens in vivo is not well understood. The use of antibiotics to eliminate microbial metabolism in whole animal experiments or the use of germ free animals would be one way of assessing the contribution of microbial metabolism in enterohepatic circulation.

Quantitative and qualitative differences were detected in B[a]P biliary excretion among species. Most interesting was the difference in biliary excretion and tissue disposition of B[a]P in hamsters in comparison to SD rats, Gunn rats, and guinea pigs. Further investigation into the types of B[a]P metabolites (Phase I and Phase II) formed and the extent of covalent binding which occurs in lung and liver may provide more definitive evidence as to why the metabolic fate of B[a]P is much different in hamsters in comparison to other species.

B[a]P Phase II metabolites in bile were classified as either glucuronides, sulfate or thio-ether conjugates. This method works well for quantitating glucuronides and sulfate conjugates. However, the classification of thio-ether conjugates by their resistance to enzyme hydrolysis is inadequate. Since all species excrete a large percent of B[a]P as thio-ether conjugates, a better method of characterizing these metabolites is needed. Development of a high performance liquid chromatographic method for analysis of thio-ether conjugates would be useful in studies of carcinogen and drug metabolism. The use of guinea pigs for these experiments would be advantageous since these animals excrete the majority of B[a]P as thio-ether conjugates.

Innate in science are intriguing questions and observations that evolve into further questions. In this study many interesting and novel observations on B[a]P metabolism *in vivo* have been made that have generated new questions. Applying the methods developed and used in this study to the study of other PAHs along with a more detailed investigation into the areas discussed above will ultimately contribute to a better understanding of chemical carcinogenesis.

Appendix A

B[a]P Conjugate Analysis

The method of MacLeod et al. (1) used for quantifying conjugates of B[a]P metabolites was evaluated by synthesizing representative conjugates and assessing their migration patterns on the TLC system which was employed.

Conjugates were synthesized by incubating appropriate substrates with crude enzyme preparations. Cytosolic enzyme fractions and microsomes were obtained from livers of Sprague-Dawley rats. Animals were sacrificed by decapitation and livers were perfused with 0.15 M NaCl and homogenized in 5 volumes of 50 mM HEPES buffer pH 7.5. After a 10 min centrifugation at 10,000 xg, the supernatant was removed and centrifuged at 100,000 xg for 1 hr. Microsomes were obtained by resuspending the pellet in 4-6 mls of 50 mM HEPES buffer pH 7.5 while the 100,000 xg supernatant was retained as the cytosolic enzyme fraction.

The sulfate conjugate of 3-OH B[a]P was synthesized according to the procedure reported by Nemoto et al. (2) with slight modifications. A mixture containing 5 mM ATP, 2 mM Na_2SO_4, 5 mM $MgCl_2$, and 0.05 ml cytosolic protein in 2 ml 40 mM Tris-HCL buffer pH 7.5 was preincubated at 37°C for 10 min before the addition of 60 μM 3-OH B[a]P. This mixture

was incubated for 2 hrs after which the reaction was stopped by addition of 1 volume of cold acetone. Samples were extracted 3 times with 2 volumes of ethyl acetate. Ethyl acetate extracts were combined and evaporated to a small volume under a stream of nitrogen.

Glucuronides of 3-OH B[a]P and 9-OH B[a]P were synthesized according to the procedure reported by Nemoto et al. (3). A mixture containing 6.25 μM 3-OH or 9-OH B[a]P, 1.5 mM uridine diphosphate glucuronic acid, 5 mM $MgCl_2$, and 0.05 ml microsomal protein in 2 ml 50 mM Tris-HCL buffer pH 7.5 was incubated for 2 hrs at 37°C. Samples were combined with 5 vol cold ethanol and placed in the cold for 30 min. Precipitated material was pelleted by centrifugation at 15,000 xg for 20 min. Supernatant fractions were evaporated to dryness under a stream of nitrogen. Residues were redissolved in a small volume of 70% ethanol.

The glutathione conjugate of B[a]P 4,5-oxide was synthesized according to the procedure reported by Hernandez et al. (4). A mixture containing 1 mM B[a]P 4,5-oxide, 5 mM glutathione, and 0.05 ml cytosolic protein in 2.0 ml 20 mM potassium phosphate buffer pH 7.5 was incubated at 37°C for 2 hrs. Samples then were combined with 5 volumes of ethanol and placed in the cold for 30 min. Precipitated material was pelleted by centrifugation at 15,000 xg for 20 min.

Supernatant fractions were evaporated to dryness under a stream of nitrogen. Residues were dissolved in a small volume of 70% ethanol.

Conjugates synthesized as described above were separated by silica gel thin-layer chromatography (TLC) with a solvent of ethyl acetate/methanol/formic acid/water (100:25:20:1). Fluorescent bands with Rf values corresponding to those reported in the literature for these conjugates were scraped from the plates and combined with 2-3 ml 70% ethanol. After 2 hrs samples were centrifuged at 15,000 xg for 30 min and the supernatant removed. Fluorescence spectra of the ethanol phases were obtained with a Perkin-Elmer 650-40 Fluorescence Spectrophotometer.

The sulfate conjugate of 3-OH B[a]P had an Rf value of 0.68. The fluorescence spectrum is depicted in Figure A.1. and is similar to that reported by others (2). This conjugate has an emission maximum at 419 nm. Upon incubation of this compound with aryl sulfatase no fluorescent material could be detected at Rf = 0.68 on TLC.

The glucuronic acid conjugates of 3-OH and 9-OH B[a]P gave Rf values of 0.21 - 0.28. Fluorescence spectra for these conjugates are depicted in Figures A.2. and A.3. The 3-OH B[a]P glucuronide has an emission maximum at 422 nm

Figure A.1. Fluorescence spectra of a sulfate conjugate of 3-OH B[a]P. The spectrum at the left is the emission spectrum recorded using an excitation wavelength of 385 nm; that on the right is the excitation spectrum recorded using an emission wavelength of 415 nm.

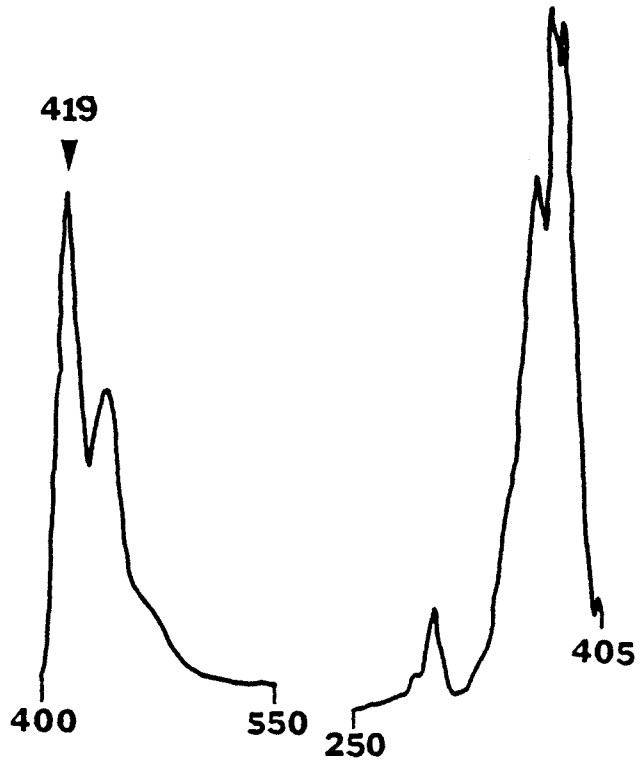
419
400
550
250
405

Figure A.2. Fluorescence spectra of a glucuronic acid conjugate of 3-OH B[a]P. The spectrum at the left is the emission spectrum recorded using an excitation wavelength of 385 nm; that on the right is the excitation spectrum recorded using an emission wavelength of 415 nm.

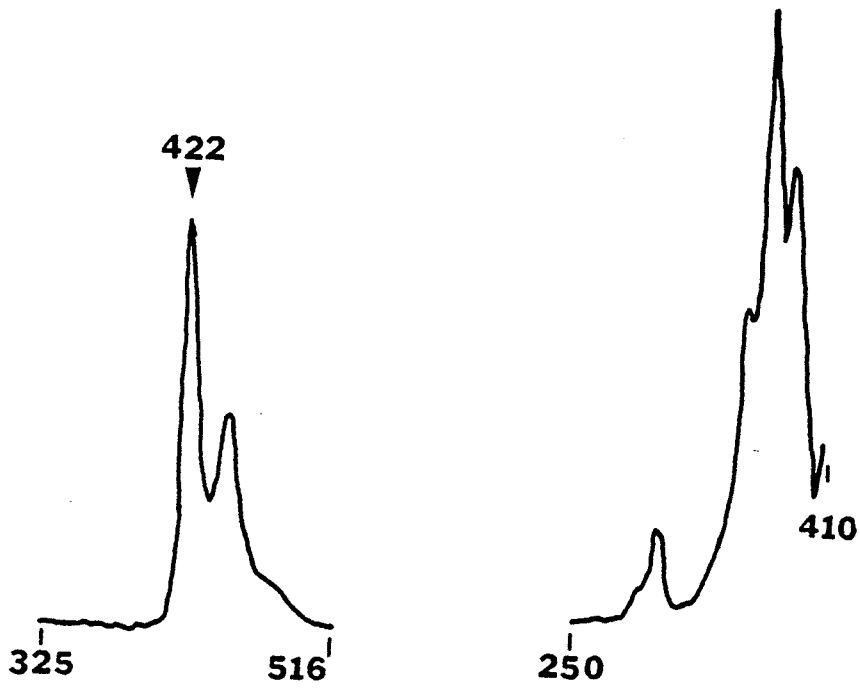
422
325
516
250
410

Figure A.3. Fluorescence spectra of a glucuronic acid conjugate of 9-OH B[a]P. The spectrum at the left is the emission spectrum recorded using an excitation wavelength of 385 nm; that on the right is the excitation spectrum recorded using an emission wavelength of 415 nm.

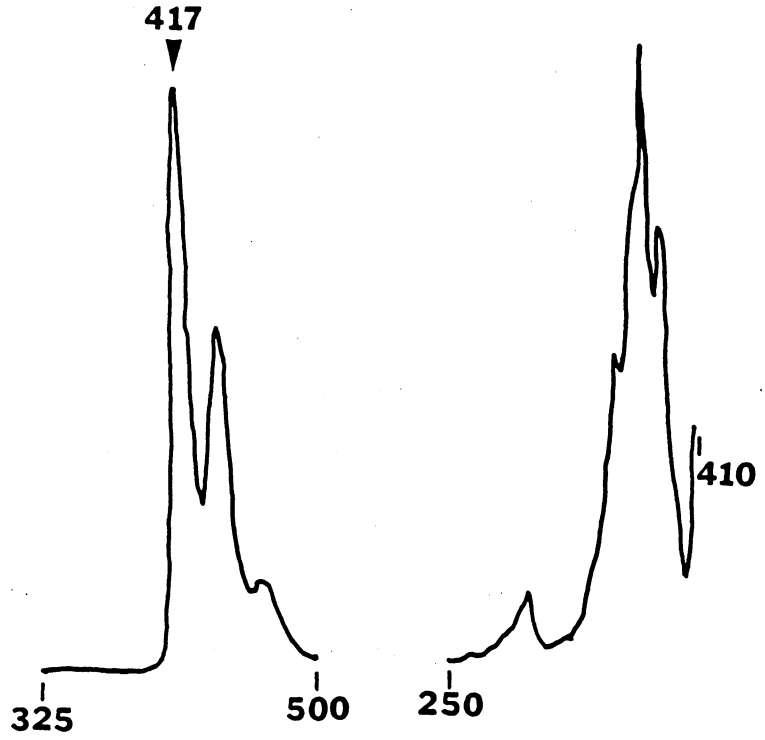
417
325
500
250
410

(Figure A.2.) while the 9-OH B[a]P glucuronide has an emission maximum at 417 nm (Figure A.3.). Upon incubation of these compounds with ß-glucuronidase, no fluorescent material could be detected at Rf = 0.20 - 0.28 on TLC. These conjugates gave a positive reaction (blue color) with napthoresorcinol reagent which indicates the presence of glucuronic acid (5).

The glutathione conjugate of B[a]P 4,5-oxide had an Rf value of 0.19 - 0.24. No distinctive fluorescence spectrum could be detected for this conjugate. However, material at Rf = 0.19 - 0.24 was positive with ninhydrin reagent, indicating the presence of primary amines (5).

A typical thin-layer chromatogram of [^{3}H]-B[a]P biliary metabolites incubated with ß-glucuronidase, aryl sulfatase, or without enzymes is depicted in Figure A.4. Glucuronic acid and sulfate conjugates were quantitated by the increase in radioactivity at the solvent front (fractions above arrow, Figure A.4.) after enzyme hydrolysis in comparison to control samples. The remaining material resistant to enzyme hydrolysis was considered to be thio-ether conjugates. These conjugates represented the percent of material not accounted for as non-conjugated metabolites, glucuronides, or sulfate conjugates.

Figure A.4. Enzymatic hydrolysis of water-soluble metabolites in bile. A typical TLC profile of radioactivity following treatment (A) without enzymes, (B) with β-glucuronidase, and (C) with aryl sulfatase. Unmetabolized B[a]P and non-conjugated B[a]P metabolites are located in fractions above the arrow (fraction number 12-15).

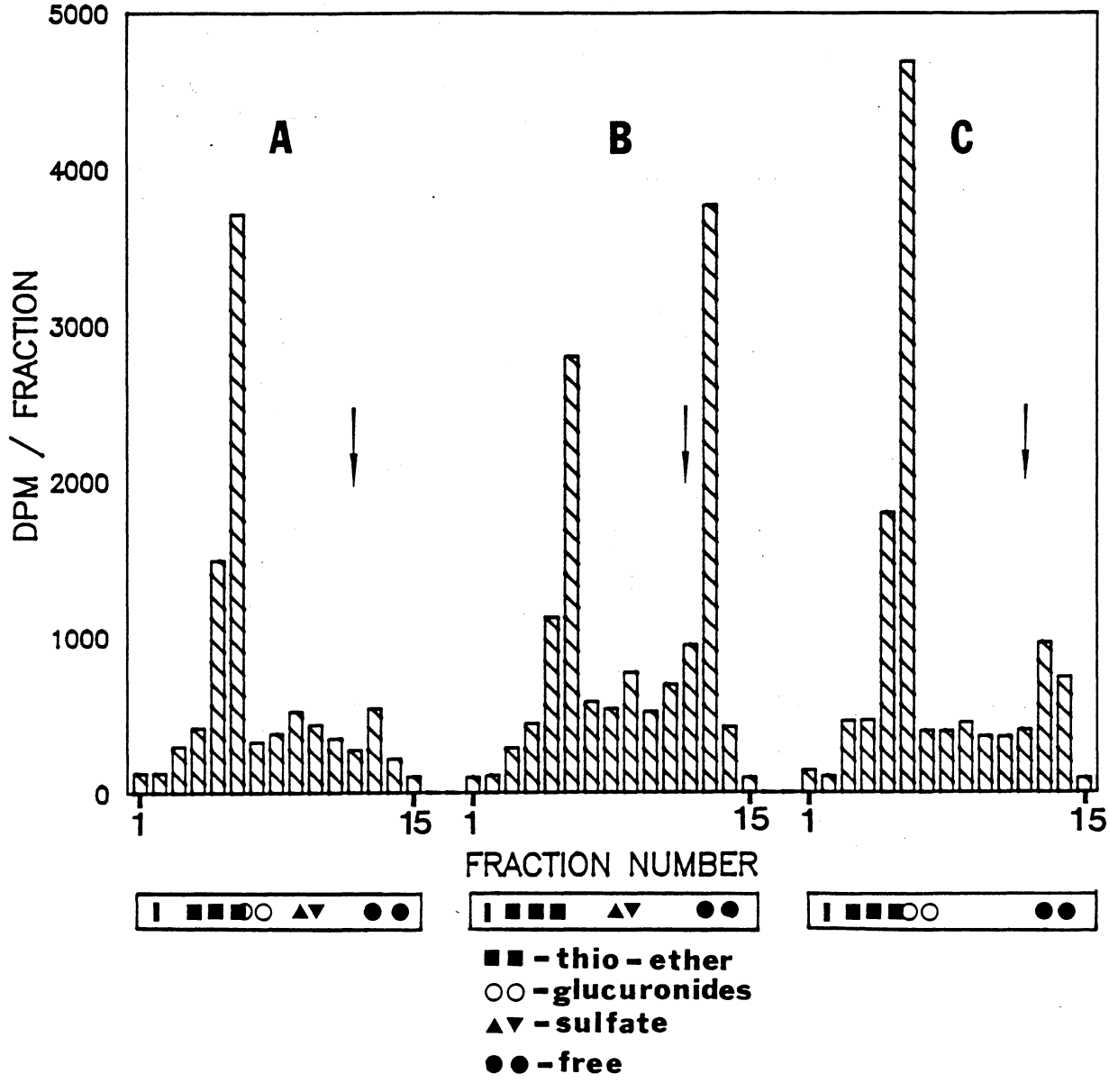
5000
4000
3000
2000
1000
0
DPM / FRACTION
A
B
C
1
15
1
15
1
15
FRACTION NUMBER
■■ - thio - ether
○○ - glucuronides
▲▼ - sulfate
●● - free

References

1. MacLeod, M. C., Moore, C. J., and Selkirk, J. K. Analysis of water soluble conjugates produced by hamster embryo cells exposed to polynuclear aromatic hydrocarbons. In: B. Bjorseth and A. J. Dennis (eds.), Polynuclear Aromatic Hydrocarbons: Chemistry and Biological Effects, pp 9-23, Columbus, Battelle Press, 1979.

2. Nemoto, N., Takayama, S., and Gelboin, H. V. Sulfate conjugation of benzo[a]pyrene metabolites and derivatives. Chem-Biol. Interact., 23:19-30, 1978.

3. Nemoto, N., and Gelboin, H. V. Enzymatic conjugation of benzo[a]pyrene oxides, phenols and dihydrodiols with UDP-glucuronic acid. Biochem. Pharmocol., 25:1224-1226, 1976.

4. Hernandez, O., Walker, M., Cox, R. H., Foureman, G. L., Smith, B. R., and Bend, J. R. Regiospecificity and stereospecificity in the enzymatic conjugation of glutathione with (±)-benzo(a)pyrene 4,5-oxide. Biochem. Biophy. Res. Comm., 96:1494-1502, 1980.

5. Stahl, E. (ed.) Thin-Layer Chromatography, A Laboratory Handbook. New York, Springer-Verlag Berlin, 1967.

Appendix B

Synthesis and Characterization of Boronate Cellulose Columns

Boronate cellulose columns were prepared following the methods outlined by Weith et al. (1) and Ho et al. (2). The preparation of this column involved the synthesis of (1) m-aminobenzeneboronic acid (free base), (2) N-(m-dihydroxyborylphenyl)succinamic acid, (3) m-[[3-(N-succinimidoxycarbonyl)propanoyl]amino]-benzeneboronic acid 1,3-propanediol cyclic ester, (4) N-succinimidyl acetate, and (5) [[N-[N'-[m-(dihydroxybornyl)phenyl]succinamyl]amino]-ethyl]cellulose.

m-Aminobenzeneboronic acid in the hemisulfate salt form (3 g) was combined with 40 ml water and adjusted to pH 7.0 with NaOH. The solution was taken to dryness under vacuum and extracted 4 times with peroxide-free dioxane. The extracts were combined, filtered, and evaporated to dryness under vacuum. The residue was dissolved and recrystallized from a small volume of water. The product, m-aminobenzeneboronic acid (free base; light brown flaky material) had a melting point of 164-165°C. A 90% (2.7 g) yield was obtained.

m-Aminobenzeneboronic acid (1.37 g) and succinic

anhydride (1.1 g) were dissolved in dry pyridine (5ml) and allowed to stand for 12 hrs. The following day, water (5 ml) was added and after 1 hr the solution was evaporated to dryness under vacuum. The residue (dark amber oily color) was dissolved in 10 ml water and evaporated to dryness under vacuum. The residue was redissolved in 10 ml water, the pH adjusted to 1 with concentrated HCl, and the solution was placed on ice for 2 hrs. The precipitate was collected by filtration and washed 2 times with 5 ml of cold water. The product, N-(m-dihydroxyborylphenyl)succinamic acid (long light brown crystals), was recrystallized from hot water and had a melting point of 173-174°C. An 84% yield (1.98 g) was obtained.

N(m-Dihydroxyborylphenyl)succinamic acid (2.06 g) and 1,3-propanediol (0.66 g) were combined with 15 ml dry dioxane and heated in a boiling water bath for 10 min. The solvent was removed under vacuum and the residue was redissolved in 40 ml dry dioxane and evaporated to dryness 2 more times. Finally, the residue was dissolved in 40 ml of dry dioxane and 0.97 g of N-hydroxy-succinimide and then 1.74 g of dicyclohexylcarbodiimide were added and the solution was allowed to stand overnight. The precipitate (dicyclohexylurea) was removed by filtration and washed three times with 2 volumes of dioxane. The filtrate and

washings were combined and evaporated to dryness. The residue was dissolved in a small volume of warm dioxane. The product, m-[[3-(N-succinimidoxycarbonyl)propanoyl]amino]-benzeneboronic acid 1,3-propanediol cyclic ester crystallized upon addition of ethyl acetate. The product had a melting point of 173-176°C. A 56% yield (1.15 g) was obtained.

N-Hydroxysuccinimide (4.8 g) was dissolved in dry pyridine (10 ml) and 6 ml of acetic anhydride was added dropwise to the solution. The mixture was allowed to stand overnight at room temperature. The solvent was removed under vacuum and the the residue was combined with 10 ml of water and evaporated to dryness. The product, N-succinimidyl acetate was recrystalized from water. A 73% yield (6.6 g) was obtained.

Aminoethyl cellulose (1 g, 0.33 meq/g) was washed 2 times with 20 ml 1 M NaOH. The alkali was removed with 4 washes of water and the cellulose suspended in 20 ml of water. m-[[3-(N-succinimidoxycarbonyl)propanoyl]amino]-benzeneboronic acid 1,3-propanediol cyclic ester (150 mg) suspended in 2 ml warm dioxane was added dropwise over a period of 5 min to the slowly stirring cellulose suspension. The pH was maintained at 9 with dilute NaOH and the suspension was stirred for 2 hrs after all of the ester had

been added. The cellulose was then washed several times with water (washes were saved for further analysis) and resuspended in 20 ml water. N-Succinimidyl acetate (200 mg) in 2 ml warm dioxane was added dropwise over a period of 5 min to the slowly stirring cellulose suspension. The pH was maintained at 9 with dilute NaOH and the suspension stirred for 2 hrs after all of the ester had been added. The suspension was then washed several times with water and the product [[N-[N'-[m-(Dihydroxybornyl)phenyl]succinamyl]amino]-ethyl]cellulose, was suspended in water.

To analyze for the amount of boronic acid incorporated onto the resin, the combined first set of washings was analyzed for the amount of unreacted m-[[3-(N-succinimidoxycarbonyl)propanoyl]amino]-benzeneboronic acid 1,3-propanediol cyclic ester. This was done by reacting the m-[[3-(N-succinimidoxycarbonyl)propanoyl]amino]-benzeneboronic acid 1,3-propanediol cyclic ester with NH_4OH to form the amide of N-[m-(dihydroxyboryl)phenyl]-succinamic acid which can be quantitated by its U.V. absorbance at 250 nm. The combined washings were diluted to 200 ml and a 1.5 ml aliquot was removed and diluted to 25 ml with 1 M NH_4OH. An absorbance of 1.27 at 250 nm was obtained. Using a molar extinction coefficient of 19000 for

the amide, it was calculated that 0.223 mmol of boronic acid was incorporated per gram of cellulose.

A 1 x 10 cm boronate column was tested for its ability to separate nucleosides and to bind B[a]P:DNA adducts containing cis vicinal hydroxyl groups. Cytidine, uridine, guanosine, and adenosine (10-20 µg each) were applied to the column and eluted with 0.1 M sodium phophate pH 7.0 (1). Nucleosides were eluted in three peaks (Figure B.1.). Weith et al. (1) using a 1 x 55 cm boronate column achieved base line separation of cytidine and uridine and marginal separation of guanosine and adenosine. Thus the elution of these four nucleosides in three peaks is resonable separation with a 1 x 10 cm boronate column.

B[a]P:DNA adducts were prepared by reaction of (±)7B,8A-dihydroxy-9A,10A-epoxy-7,8,9,10-tetrahydrobenzo[a]pyrene ((±)-anti-B[a]PDE) with calf thymus DNA as described by Pruess-Schwartz et al. (3). DNA was hydrolyzed according to Baird et al. (4). B[a]P nucleoside adducts were applied to the boronate column and eluted first with 1 M morpholine and then with 1 M morpholine containing 10% sorbitol. As would be expected, since (±)-anti-B[a]PDE was used, no material was observed to elute with 1M morpholine buffer using both UV absorbance and fluorescence to monitor the eluate. However, material was eluted with 1M

morpholine:10% sorbitol buffer (Figure B.2.). The 1M morpholine:10% sorbitol fractions were combined and B[a]P nucleoside adducts were concentrated with C_{18} Sep-pak cartridges (4). Cartridges were washed with 5 mls of methanol followed by 10 mls of water. Samples were than applied and the eluate from the cartridges was reapplied 3 more times. The column was then washed with 20 ml water and 1 ml 40% methanol. B[a]P nucleoside adducts were eluted with 100% methanol (4 X 2 ml washings). The fluorescence spectrum was recorded (Figure B.3.) and was determined to be similar to that of (+)-anti-B[a]PDE:deoxyguanosine (5). In addition, when authentic [^{14}C]-(+)-anti-B[a]PDE:deoxyguanosine adduct (provided by William M. Baird and Donna Pruess-Schwartz, Purdue University) was chromatographed, 83% of the radioactivity was eluted with 1M morpholine:10%sorbitol.

Figure B.1. Elution profile of nucleosides from the boronate column. Cytidine (C), uridine (U), guanosine (G), and adenosine (A) were dissolved in 0.1 M sodium phosphate pH 7.0 buffer at concentrations of 100 μM and applied to the boronate column. Nucleosides were eluted with 0.1 M sodium phosphate pH 7.0 buffer. Fractions of 1.2 ml were collected.

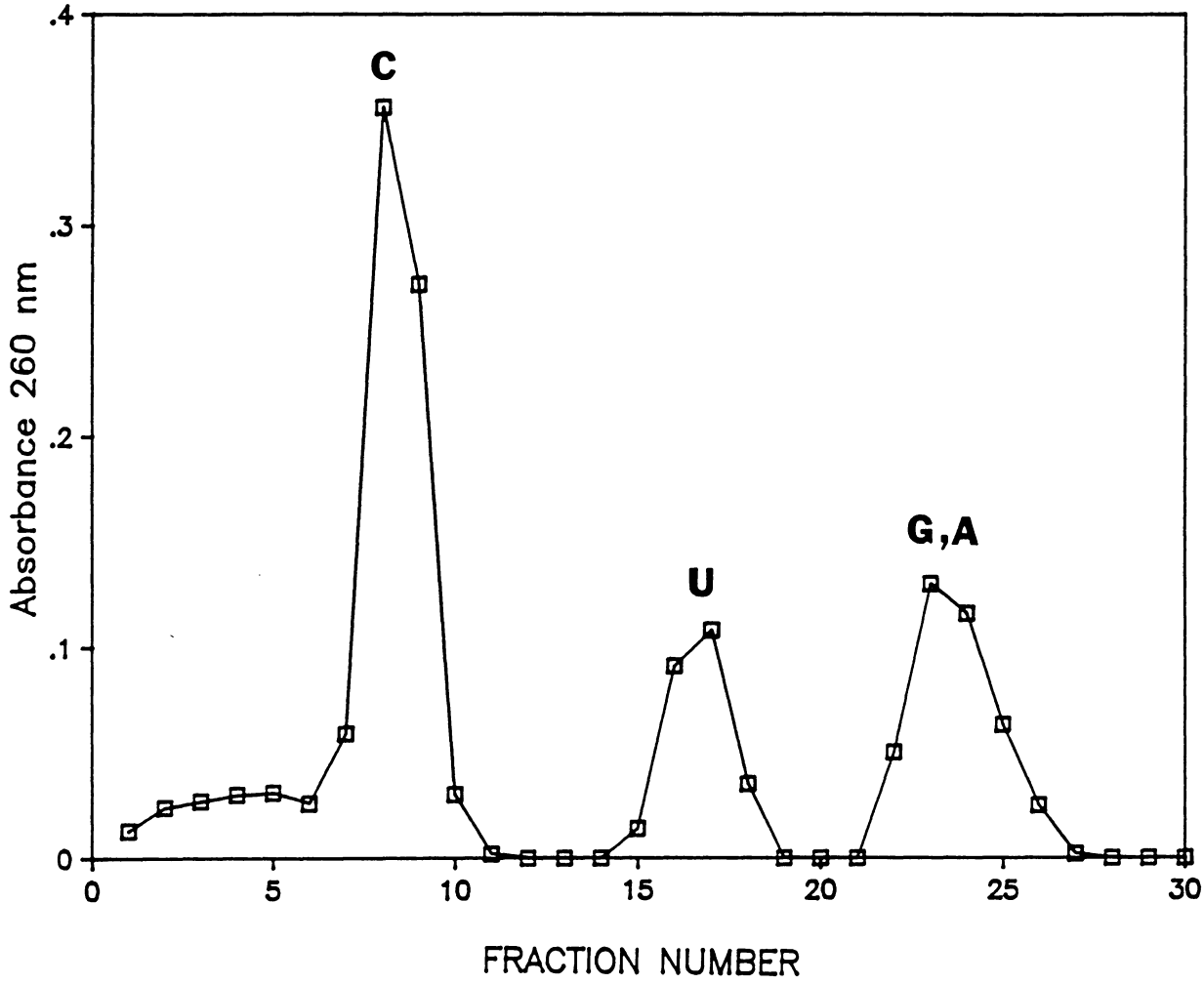
C
U
G,A
Absorbance 260 nm
.4
.3
.2
.1
0
0
5
10
15
20
25
30
FRACTION NUMBER

Figure B.2. Elution profile of B[a]P:DNA adducts from the boronate column. B[a]P:DNA adducts were synthesized by reaction of (±)-anti-B[a]PDE with calf thymus DNA as described in the text. Adducts were applied to the column and the column was washed initially with 1 M morpholine. The arrow indicates the fraction at which elution with 1 M morpholine:10% sorbitol buffer was begun.

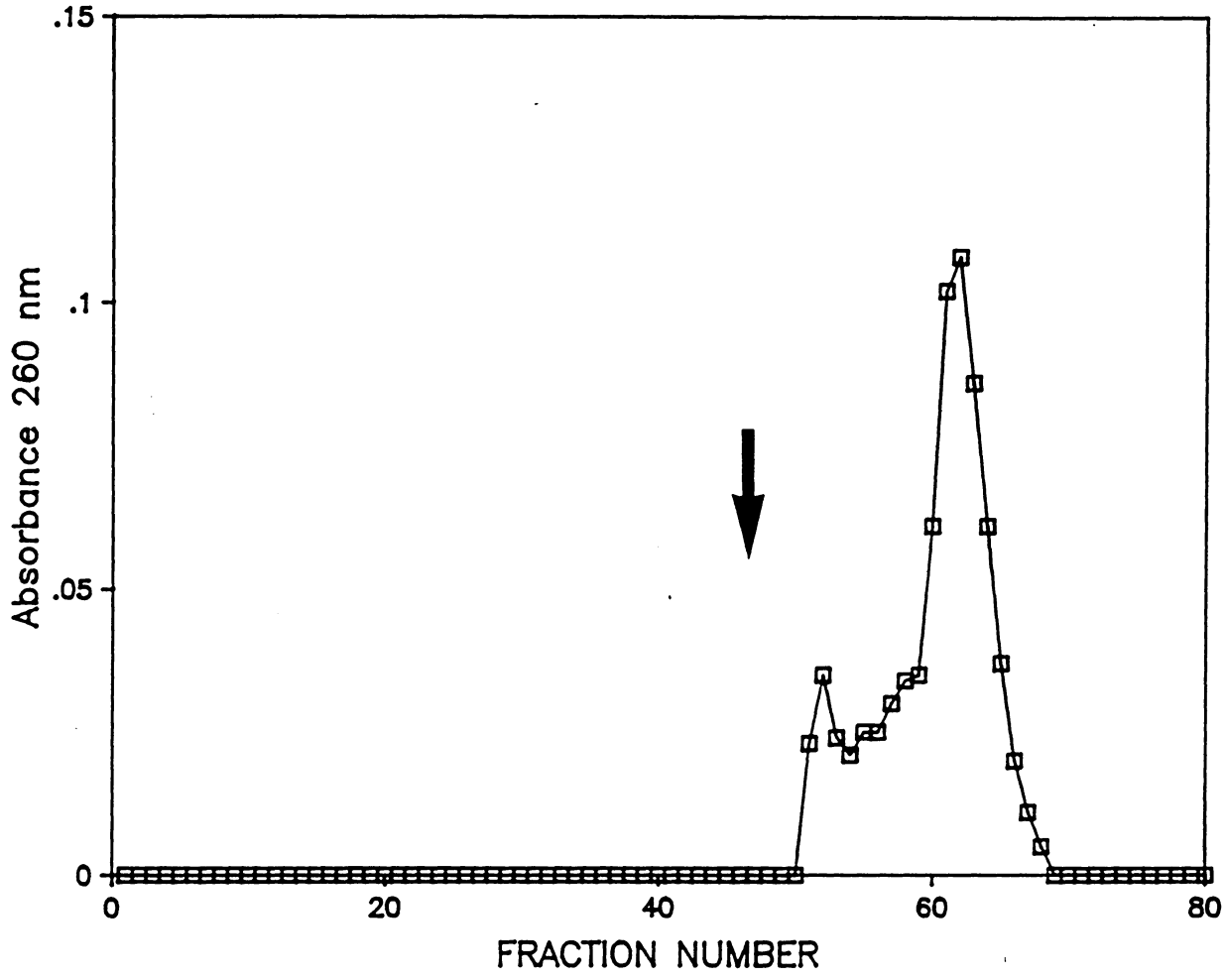
.15
.1
.05
0
Absorbance 260 nm
0
20
40
60
80
FRACTION NUMBER

Figure B.3. Fluorescence spectra of B[a]P:DNA adducts eluted in 1 M morpholine:10% sorbitol buffer. The spectrum on the left is the excitation spectrum recorded using an emission wavelength of 399 nm. The pectrum on thr right is the emission spectrum recorded using an excitation wavelength of 329 nm.

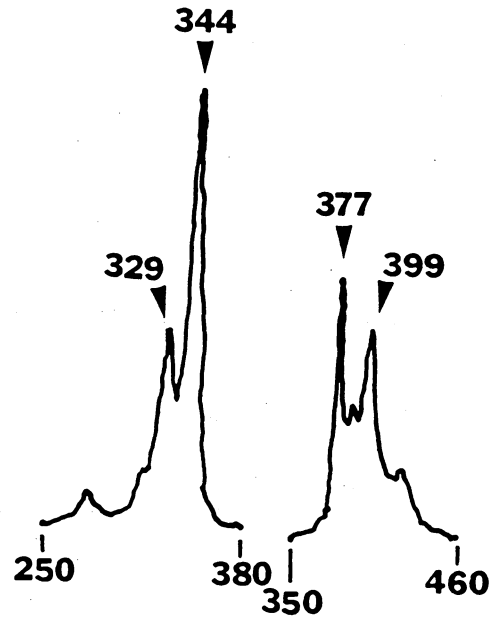
344
377
329
399
250
380
350
460

References

1. Weith, H. L., Wiebers, J. L., and Gilham, P. T. Synthesis of cellulose derivatives containing the dihydroxyboryl group and a study of their capacity to form specific complexes with sugars and nucleic acid components. Biochemisstry, 22:4396-4401, 1970.

2. Ho, N. W. Y., Duncan, R. E., and Gilham, P. T. Esterification of terminal phosphate groups in nucleic acids with sorbitol and its application to the isolation of terminal polynucleotide fragments. Biochemistry, 20:64-67, 1981.

3. Pruess-Schwartz, D., Sebti, S. M., Gilham, P. T., and Baird, W. M. Analysis of benzo[a]pyrene:DNA adducts formed in cells in culture by immobilized boronate chromatography. Cancer Res., 44:4104-4110, 1984.

4. Baird, W. M., and Brookes, P. Isolation of the hydrocarbon-deoxyribonulceoside products from the DNA of mouse embryo cells treated in culture with 7-methylbenz(a)anthracene-3H. Cancer Res., 33:2378-2385, 1973.

5. Jernstrom, B., Lycksell, P-O., Graslund, A., and Norden, B. Spectroscopic studies of DNA complexes formed after reaction with anti-benzo(a)pyrene-7,8-dihydrodiol-9,10-oxide enantiomers of different carcinogenic potency. Carcinogensis, 5:1129-1135, 1984.

The vita has been removed from the scanned document